

Hyperion: The First Global Orbital Spectrometer, Earth Observing-1 (EO-1) Satellite (2000-2017)

Elizabeth M. Middleton
EO-1 Mission Scientist 2007- present

**Biospheric Sciences Laboratory,
NASA GSFC**

July, 2017



IGARSS 2017





Spectroscopy from Space



To Study the Earth

emphasis on land-based observations

General background

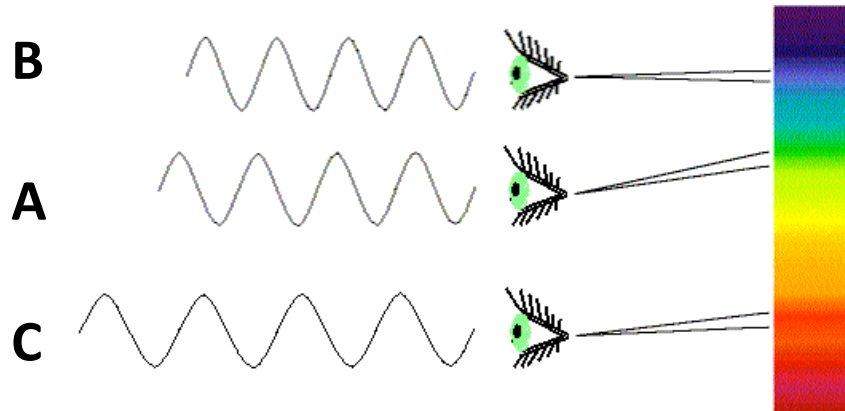
The EO-1 Hyperion spectrometer

What's next?

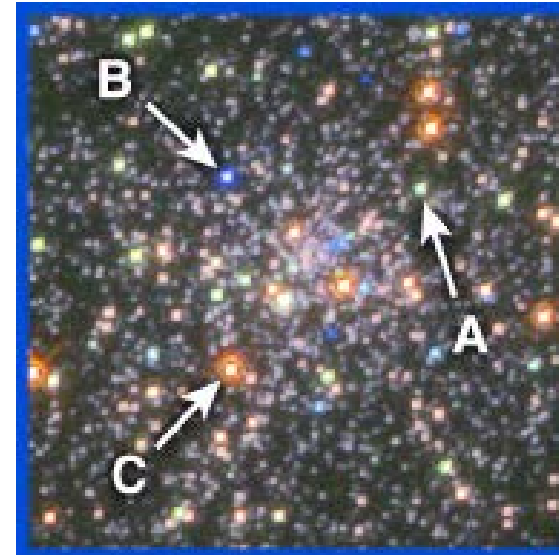


Thanks to the entire
hyperspectral/spectroscopy
community

Special Thanks to Rob Green,
Woody Turner and
HyspIRI Science Team
EARSeL SIG



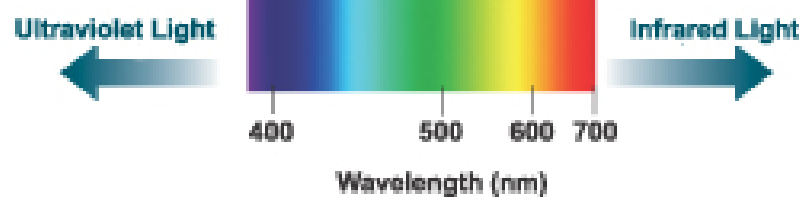
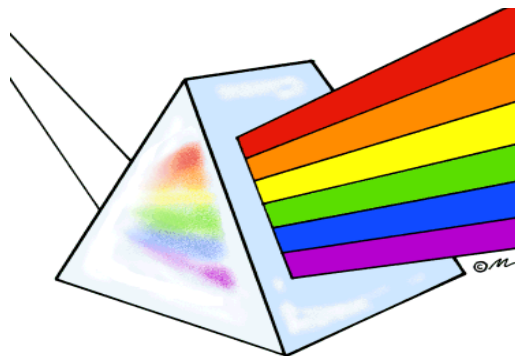
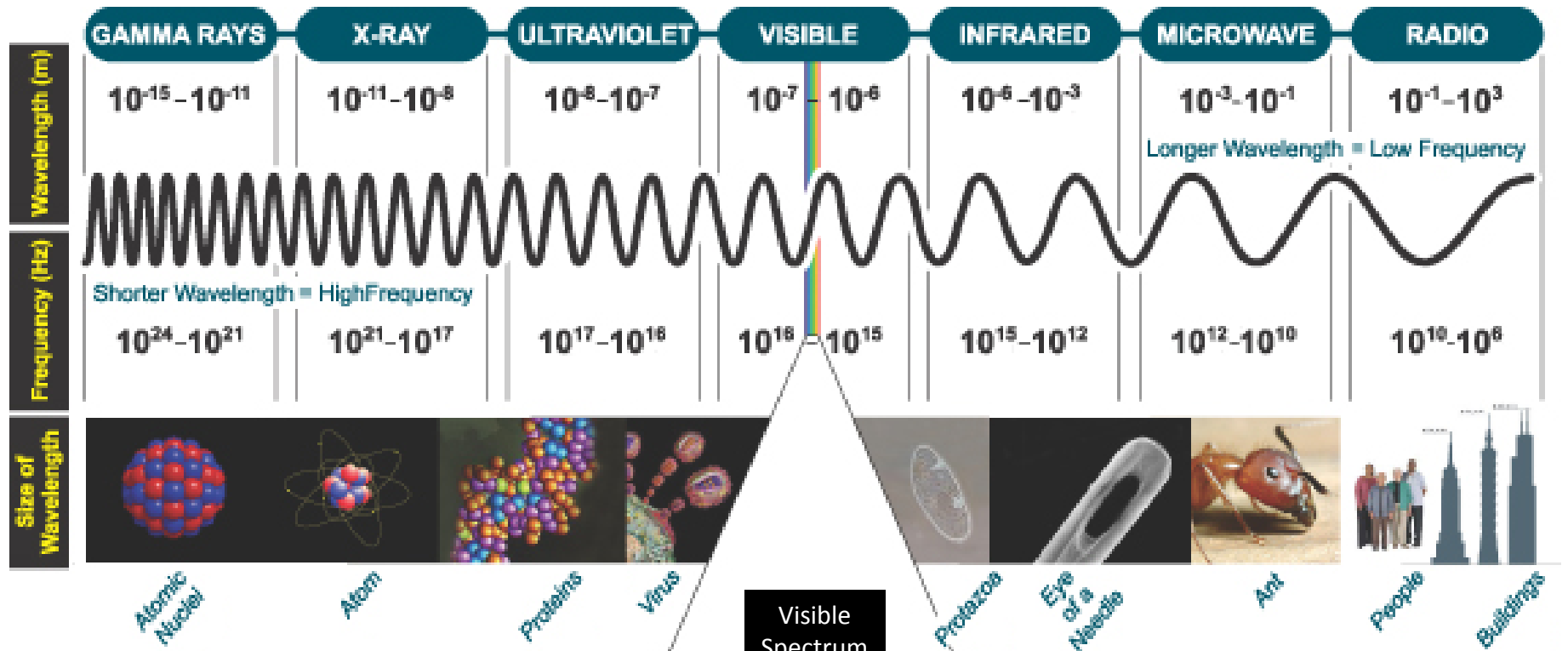
Star A is green, star B is blue, star C is red.
They can be identified by their spectra.



Spectroscopy is one of the most important tools in a scientist's tool-kit – **it is the study of light coming from an object.**

- Spectroscopy is the study of the interaction between radiation and matter ***as a function of wavelength ("λ").***
- A spectrometer is an instrument that can spread light out into its different colors.

The Radiation Spectrum





- **Science Questions**

- How are global ecosystems changing?
- How do ecosystems, land cover, and biogeochemical cycles respond to and affect global environmental change?
- How will carbon cycle dynamics and terrestrial and marine ecosystems change in the future?
- How can Earth system science improve mitigation of, and adaptation to, global change?

Biospheric Sciences Laboratory (Code 618, NASA/GSFC):

Mission Statement

Advance scientific understanding of Earth's terrestrial ecosystems and their responses to natural or human-induced changes and develop applications to benefit humanity.



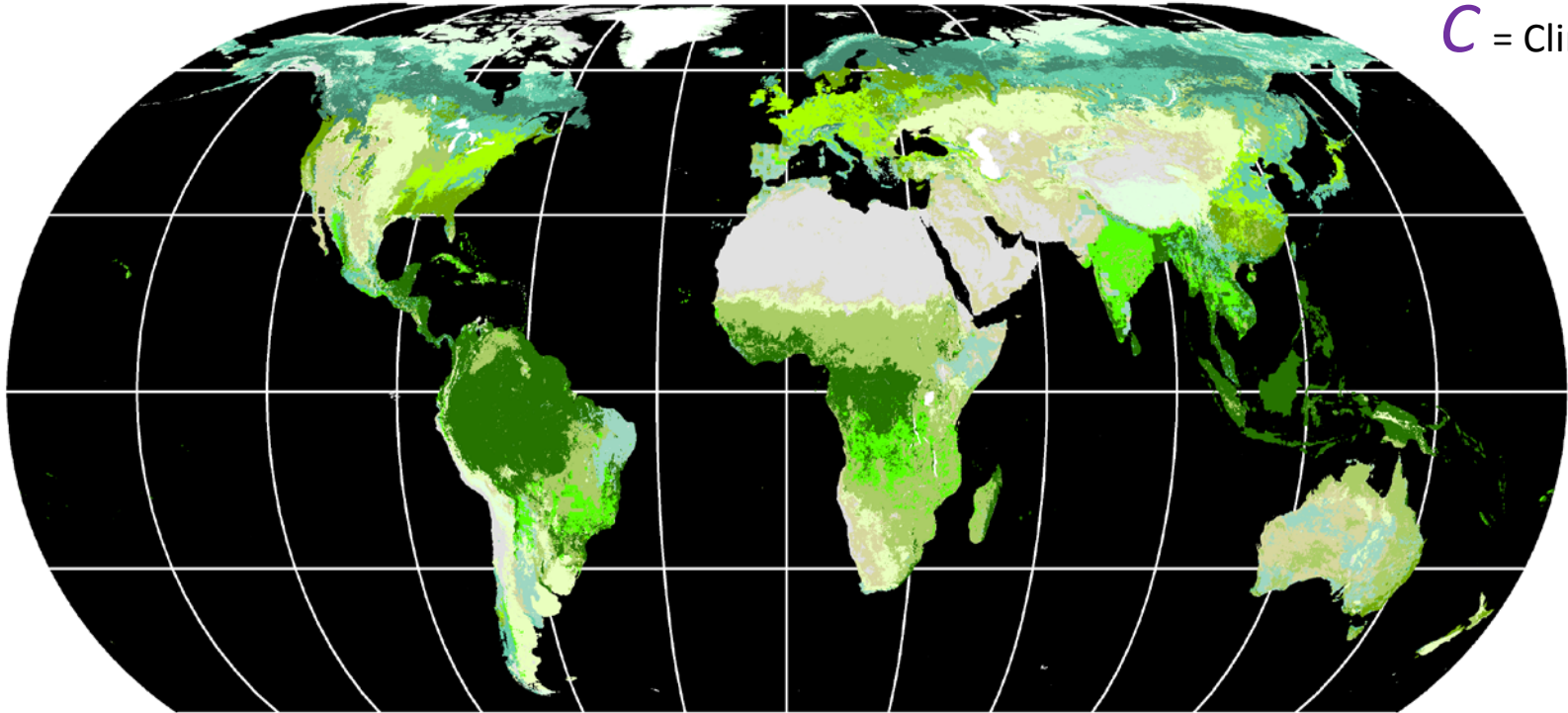
New Directions

- *Detection of biologic groups based on:*
 - * Biodiversity
 - * Functional (spectral) properties
 - * Structure
 - * Vitality, health, persistence
- *Processes*
 - * Seasonal Phenology, Year to Year trends
 - * Diurnal dynamics
- *Data Fusion/Harmonization, Virtual Constellations*

Biomes of the World

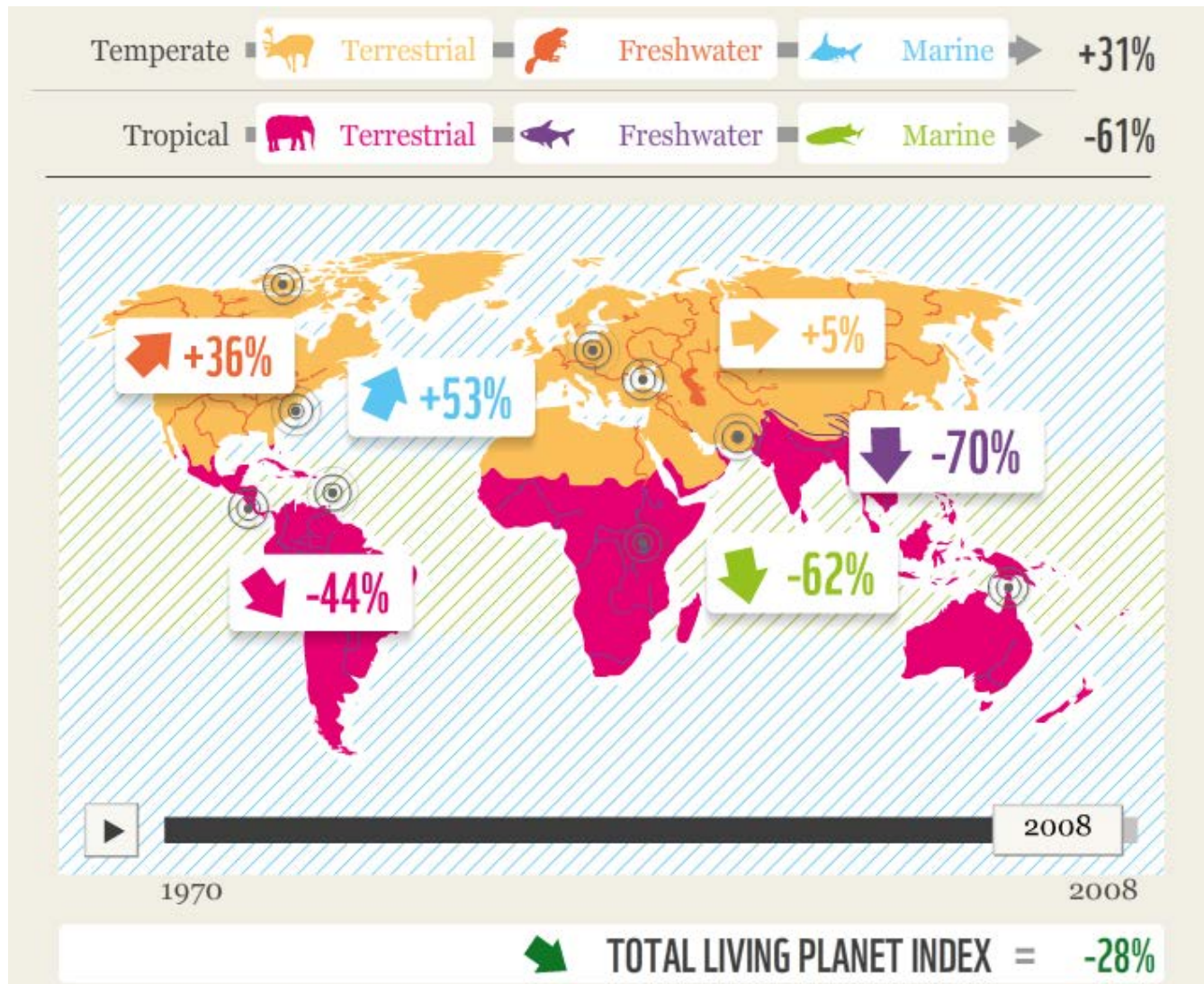
$$\text{Ecosystems} = f(C)$$

C = Climate



	Tropical Evergreen Woodland		Savanna
	Tropical Deciduous Woodland		Dense Shrubland
	Temperate Evergreen Woodland		Grassland & Steppe
	Temperate Deciduous Woodland		Open Shrubland
	Boreal Woodland		Tundra
	Mixed Woodland		Deserts & Barren

Global Diversity of Species

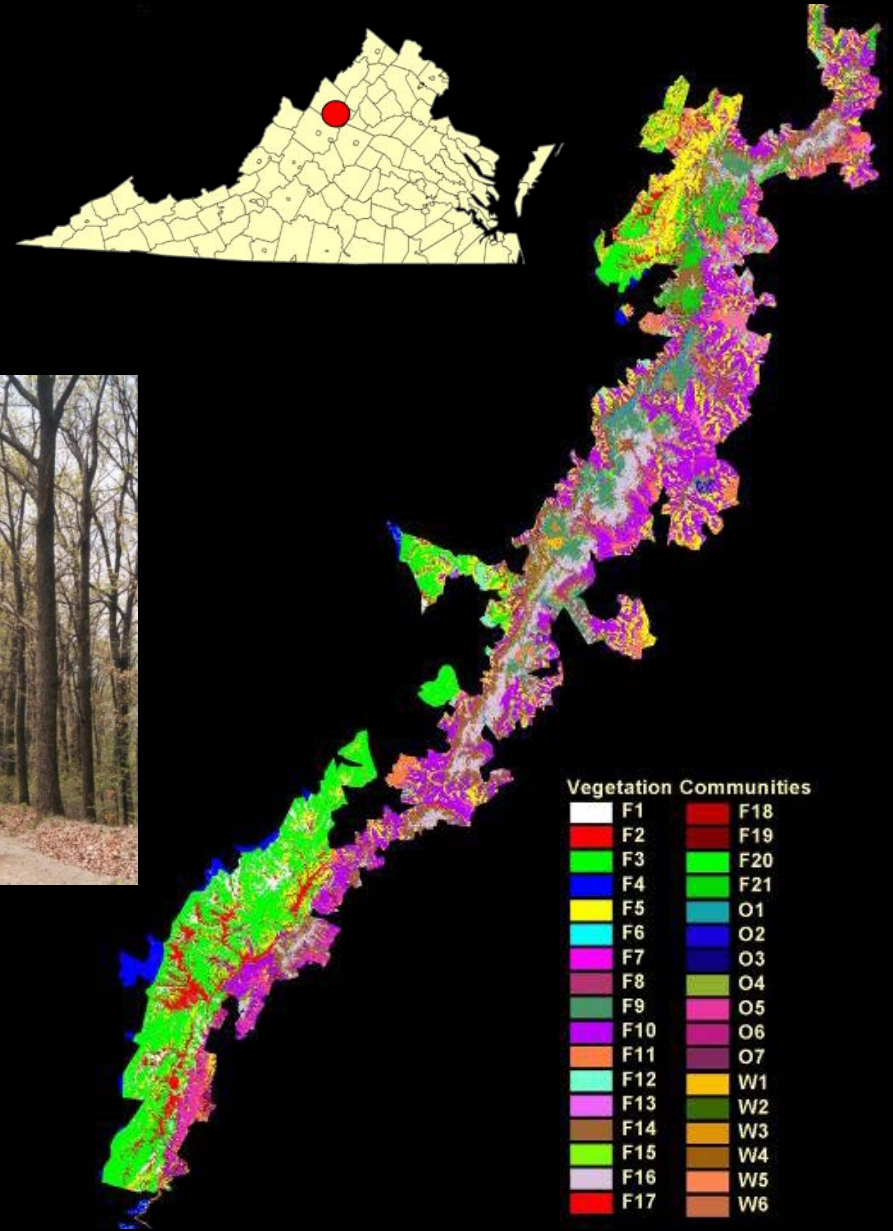


LIVING PLANET REPORT 2012

LIVING PLANET INDEX

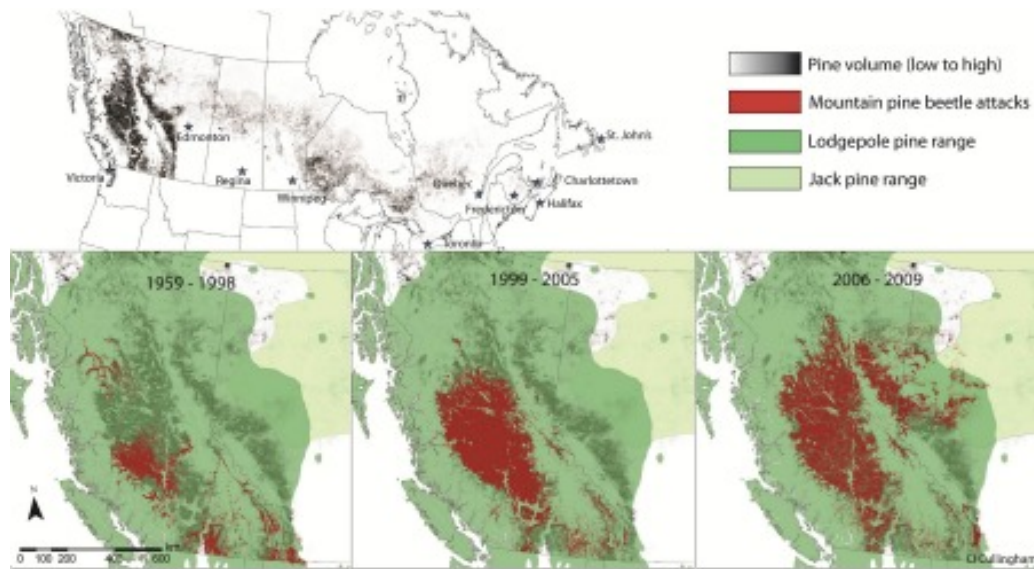
Species Composition and Biodiversity

- Quercus rubra*
- Quercus rubra* - *Quercus* spp. - *Carya*
- Quercus prinus* - *Quercus coccinea*
- Quercus coccinea* / mix
- Quercus velutina* / mix
- Quercus alba*
- Quercus prinus* - *Quercus* spp. / mix
- Quercus prinus* - *Acer rubrum* / mix
- Quercus prinus*
- Carya* sp.
- Pinus virginiana*
- Pinus virginiana* / deciduous mix
- Pinus rigida*
- Pinus strobus*
- Pinus strobus* / *Quercus* mix
- Tsuga canadensis*



- Vegetation Communities
- | | |
|---|---|
| F1 | F18 |
| F2 | F19 |
| F3 | F20 |
| F4 | F21 |
| F5 | O1 |
| F6 | O2 |
| F7 | O3 |
| F8 | O4 |
| F9 | O5 |
| F10 | O6 |
| F11 | O7 |
| F12 | W1 |
| F13 | W2 |
| F14 | W3 |
| F15 | W4 |
| F16 | W5 |
| F17 | W6 |

Recent changes in climate are causing significant and novel changes to arctic/boreal ecosystems over large areas that have widespread impacts on society



Mountain pine beetle outbreaks have accelerated and are spreading (Source: Univ. of Alberta)

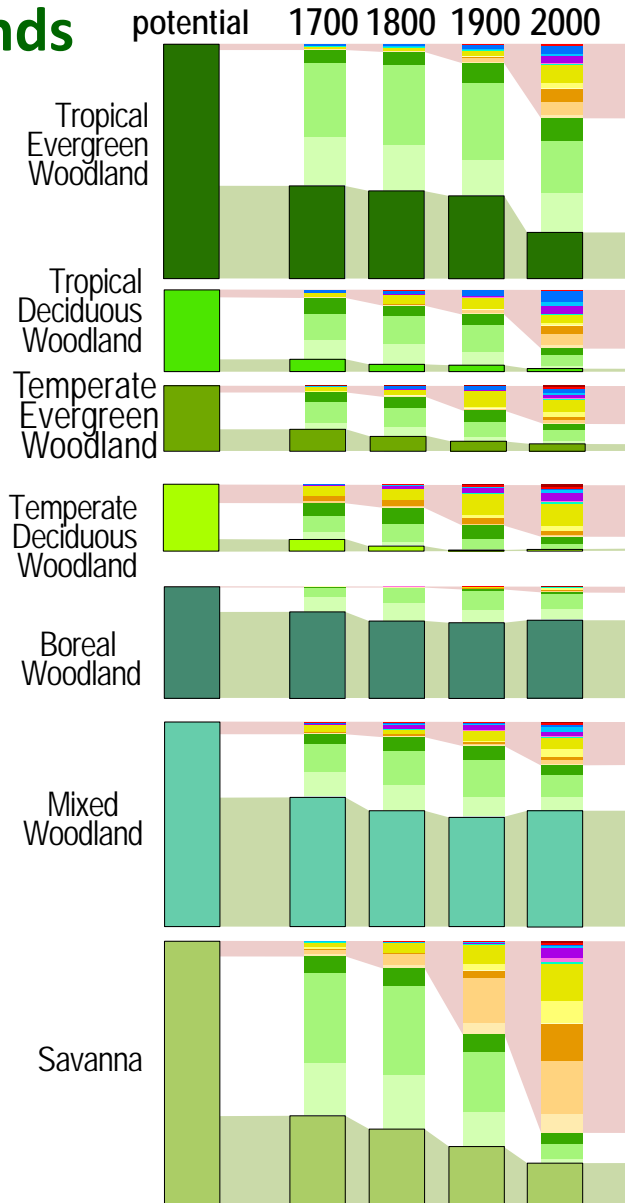


Permafrost thaw is leading to shrinkage of lakes and mobilizing frozen carbon (Photo: G. Grosse)

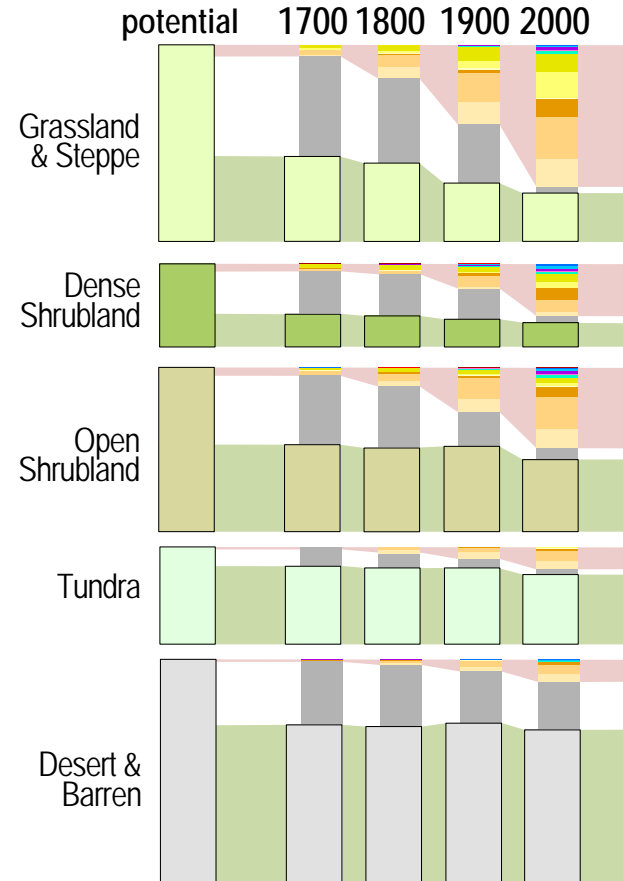


The Slave Lake, Alberta fire in May 2011 was the second largest natural disaster in Canadian history (>\$750 million) (Photo: National Post - news.nationalpost.com)

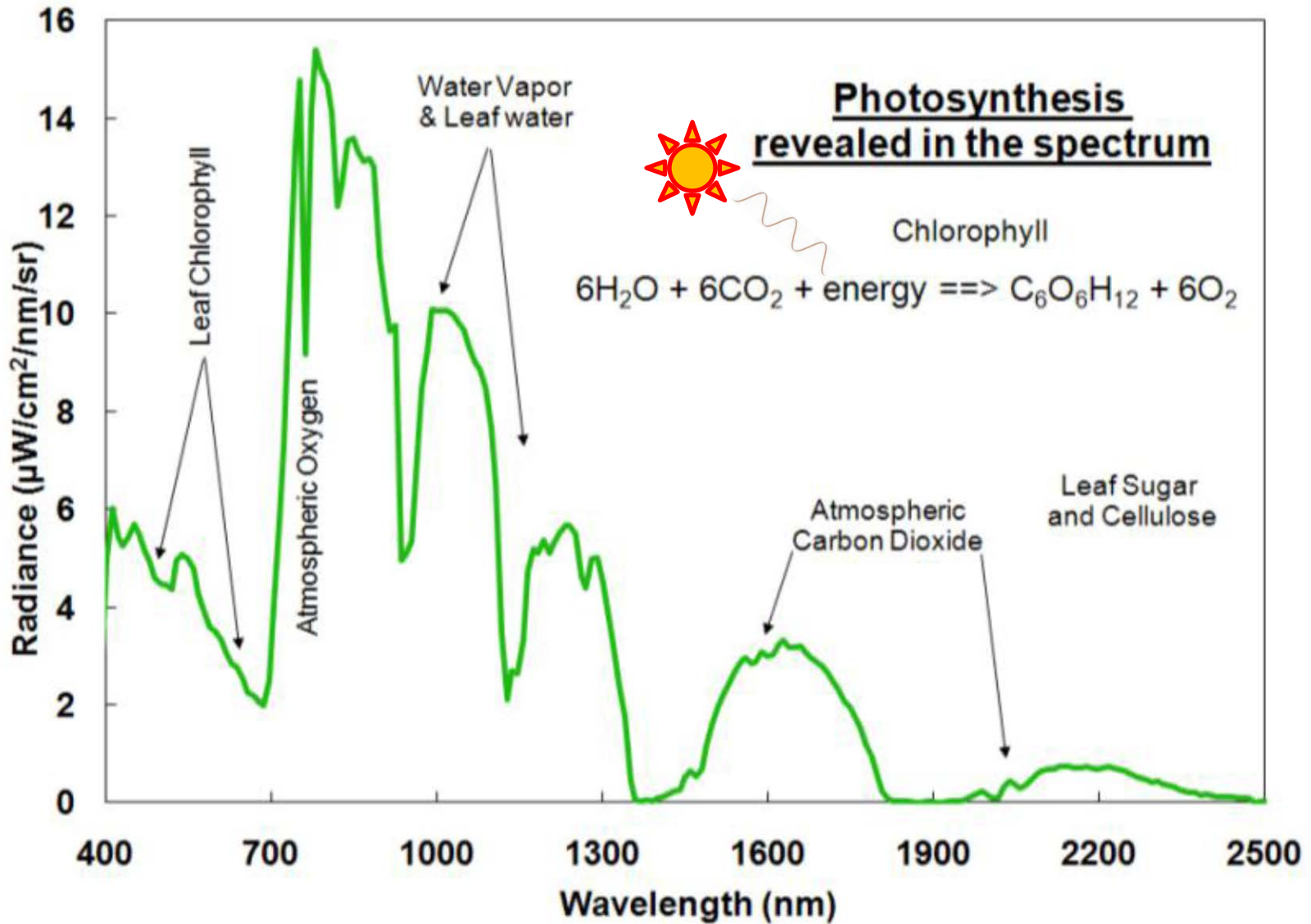
Woodlands



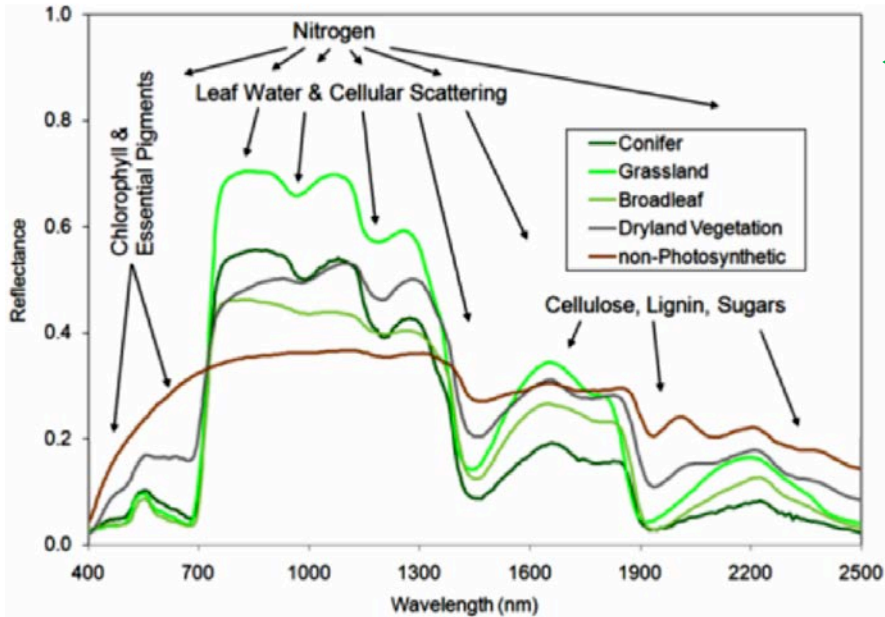
Treeless & Barren Lands



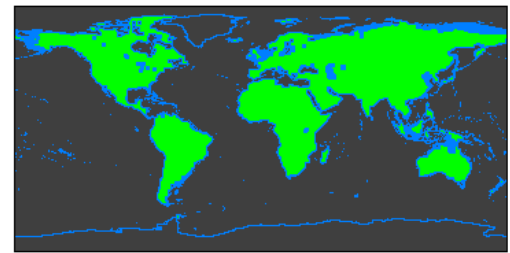
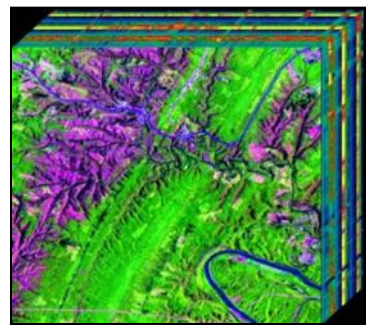
Spectroscopy and Photosynthesis



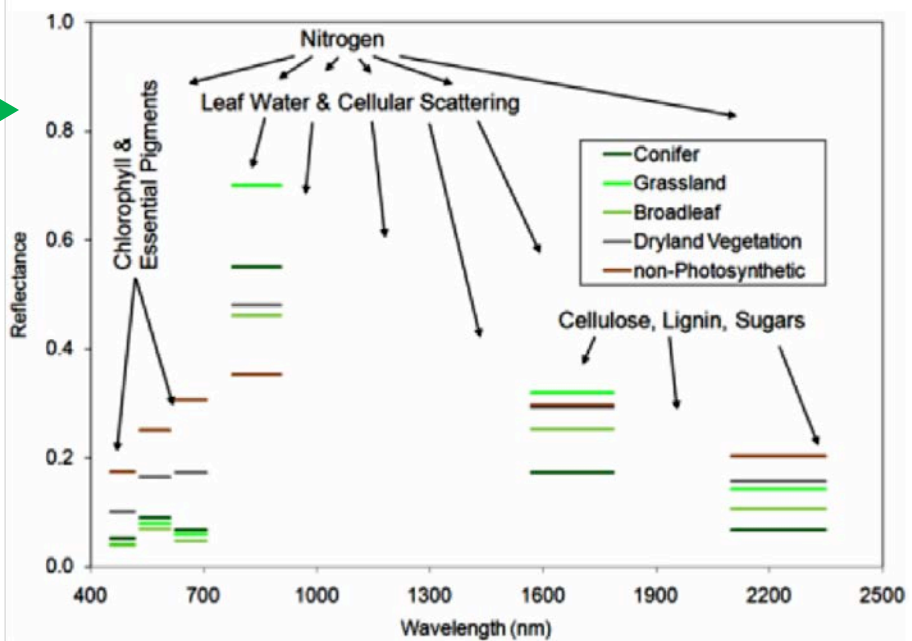
Measuring the Global Terrestrial Biosphere for Ecosystem Composition and Function



← Imaging Spectroscopy is required to measure critical variables of the terrestrial biosphere.



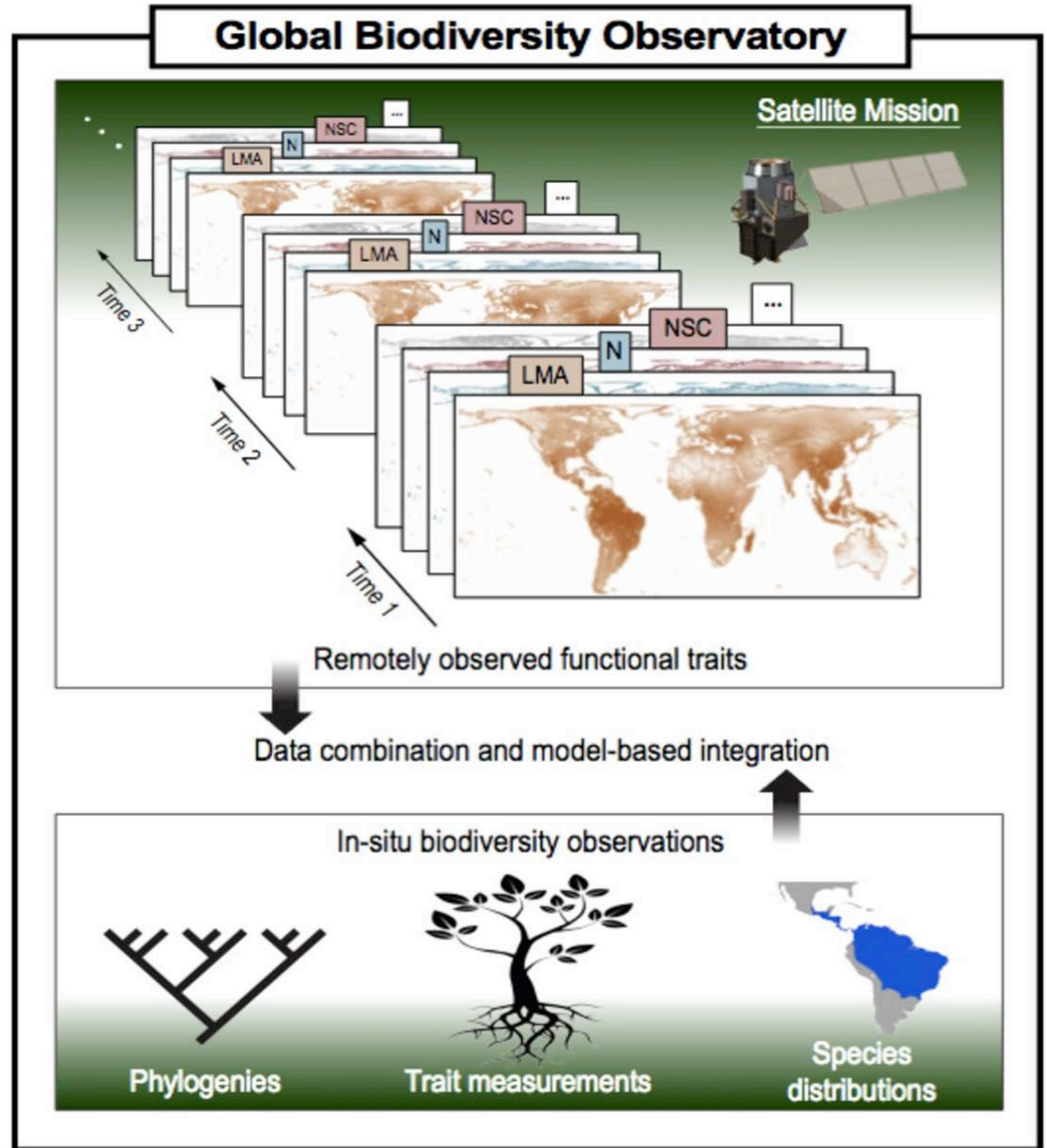
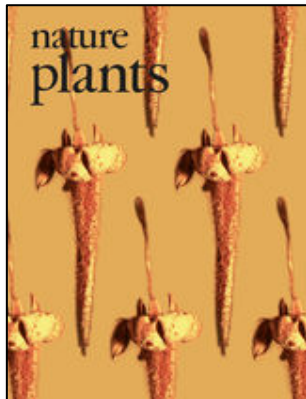
Multi-spectral imaging is insufficient →

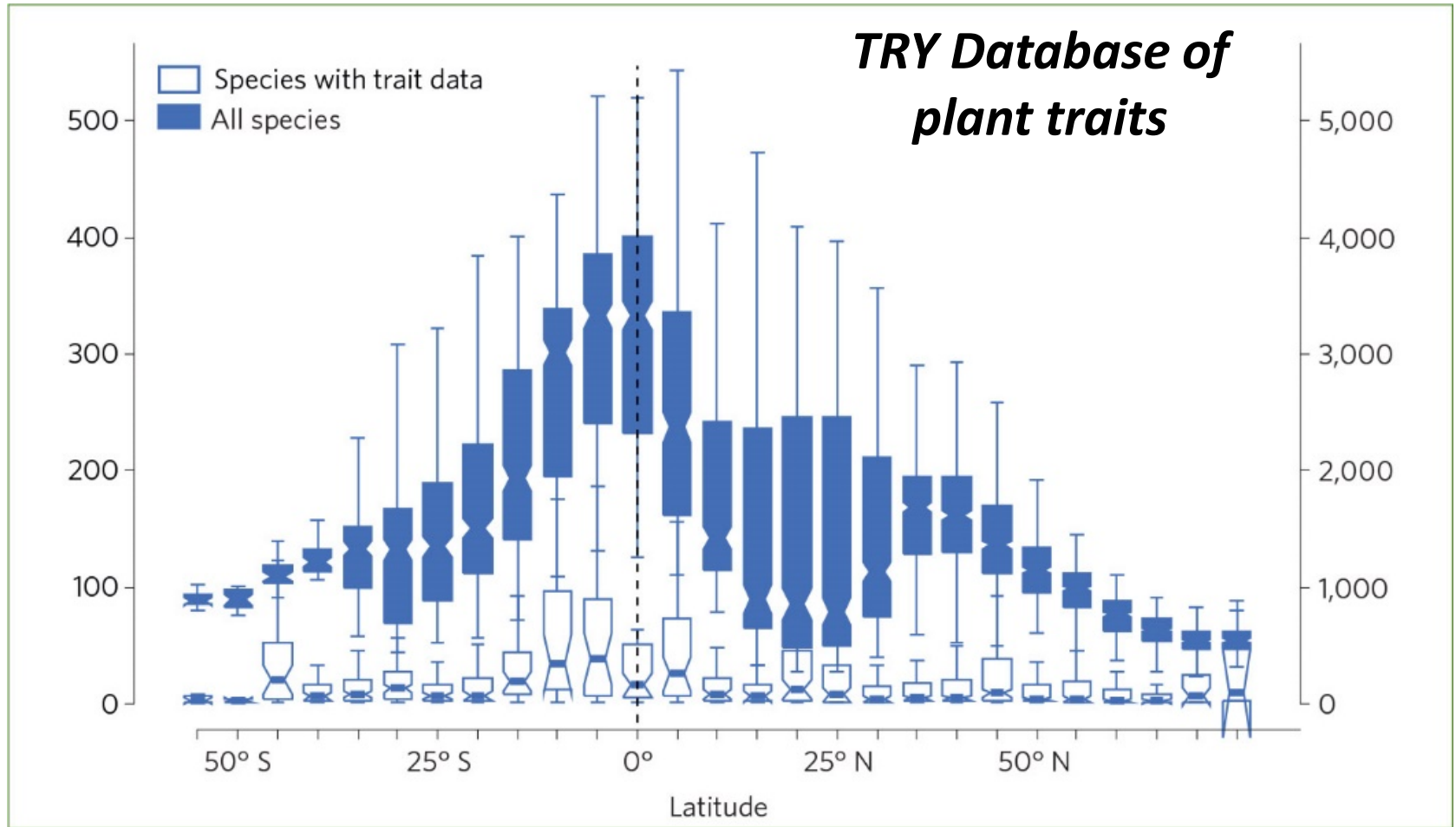


“Monitoring Plant Functional Diversity From Space”

Jetz, W., J. Cavender-Bares, R. Pavlick, D. Schimel, F.W. Davis, G.P. Asner, R. Guralnick, J. Kattge, A.M. Latimer, P. Moorcroft, M.E. Schaepman, M.P. Schildhauer, F.D. Schneider, F. Schrodt, U. Stahl, & S.L. Ustin (2016). Monitoring Plant Functional Diversity From Space, *Nature Plants*, Vol.2(3), Article: 16024, March 2016.

The world's ecosystems are losing biodiversity fast. A satellite mission designed to track changes in plant functional diversity around the globe could deepen our understanding of the pace and consequences of this change, and how to manage it.



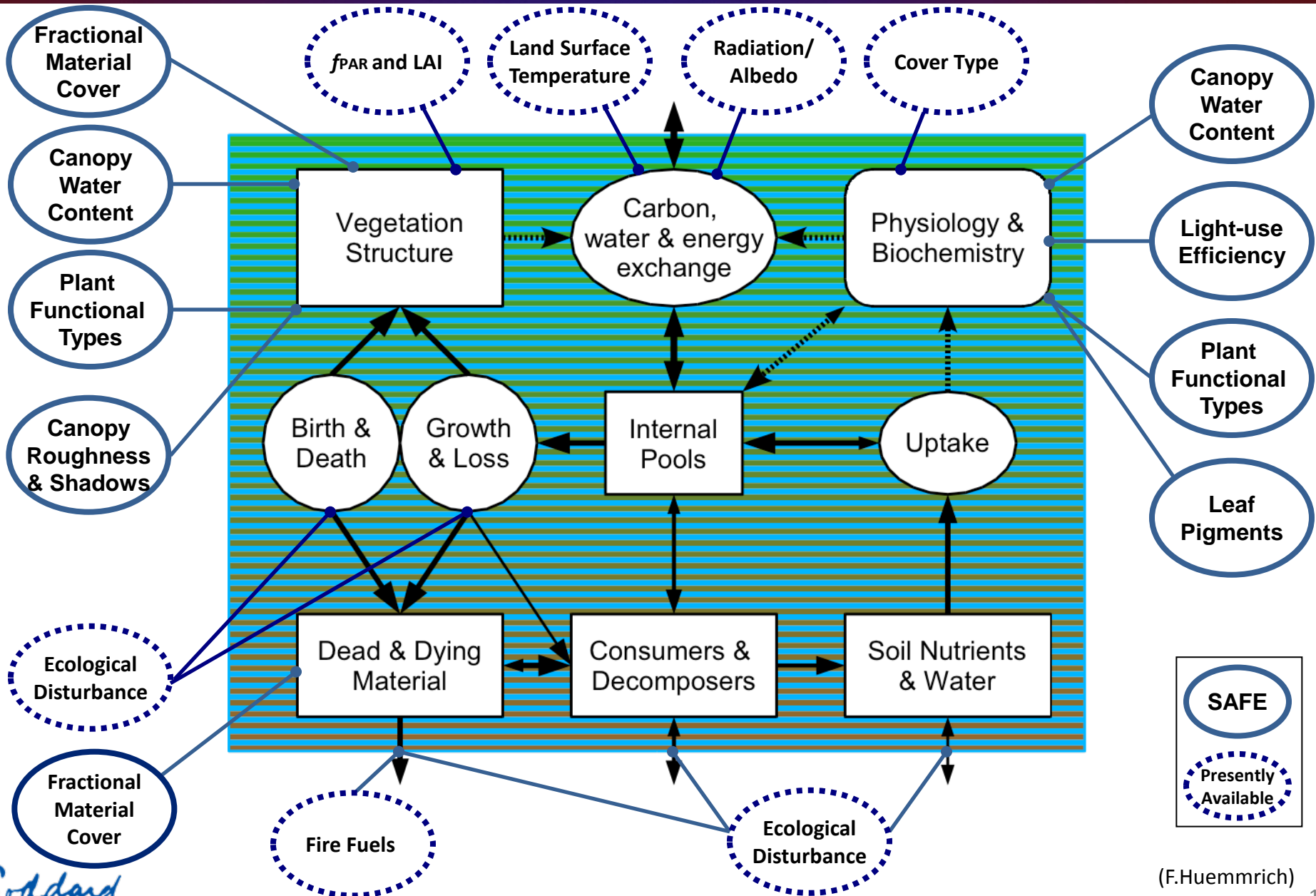
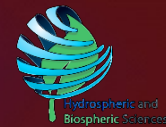


Despite advances in compiling species databases, information from field surveys is insufficient. Latitudinal variation in the richness of all vascular plant species (BLUE; after Kreft & Jetz 2007). Compared to TRY database (WHITE; from TRY, Jun 2015) among 110km grid cells (N = 11,626).

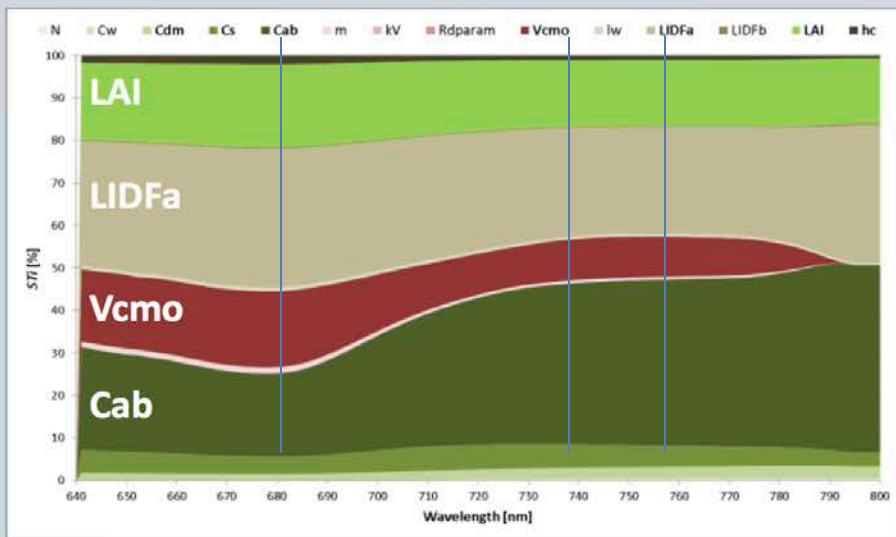
W. Jetz, J. Cavender-Bares, R. Pavlick, D. Schimel et al. 2016. Nature Plants 16024 | DOI:10.1038.Nplants 2016.24



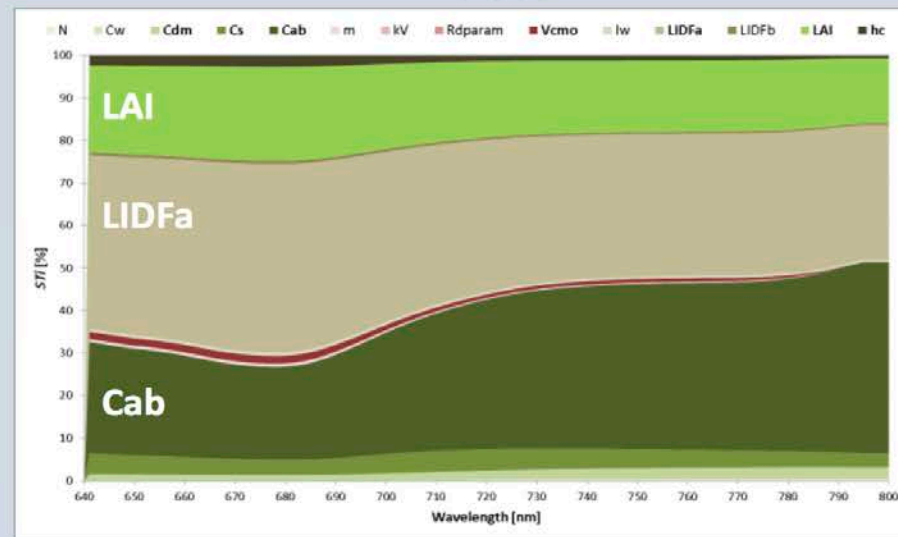
Conceptual Ecosystem Flux Model



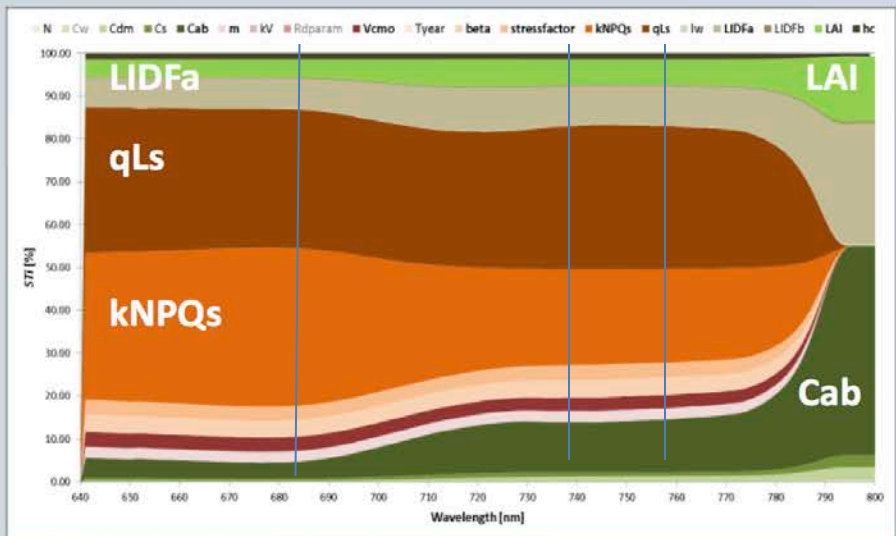
TB12-D



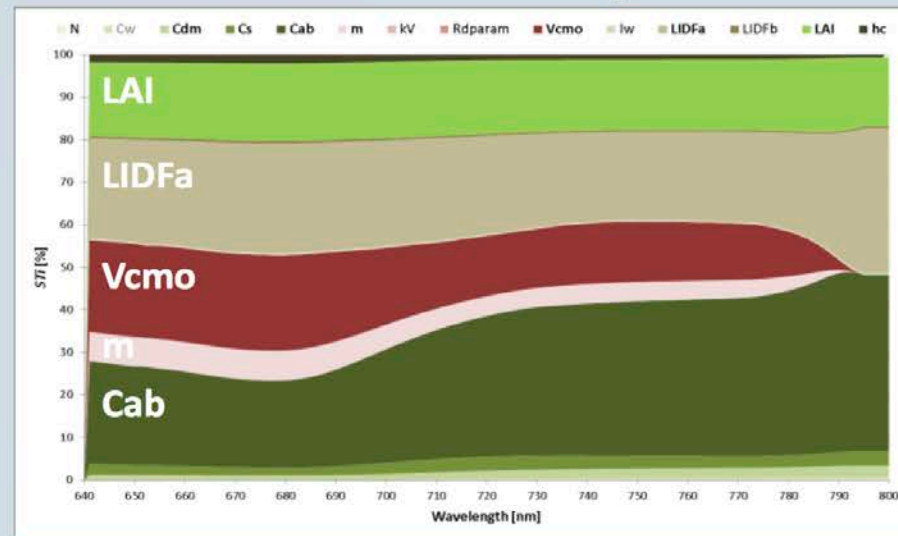
TB12



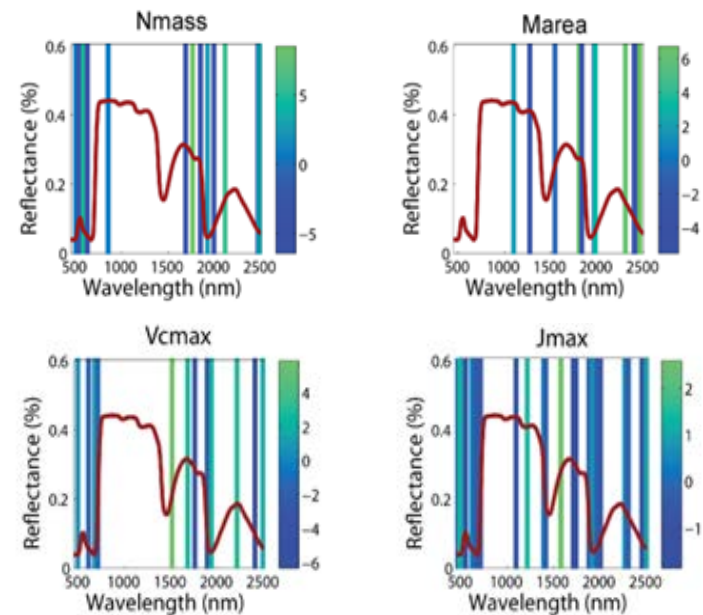
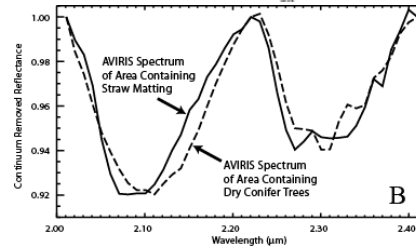
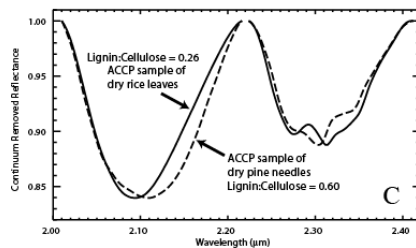
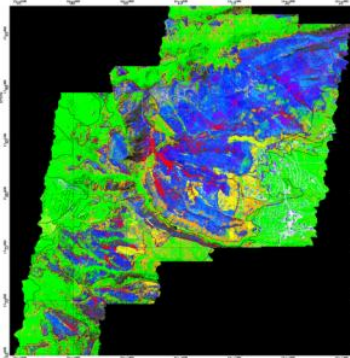
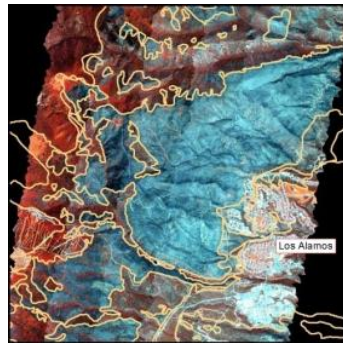
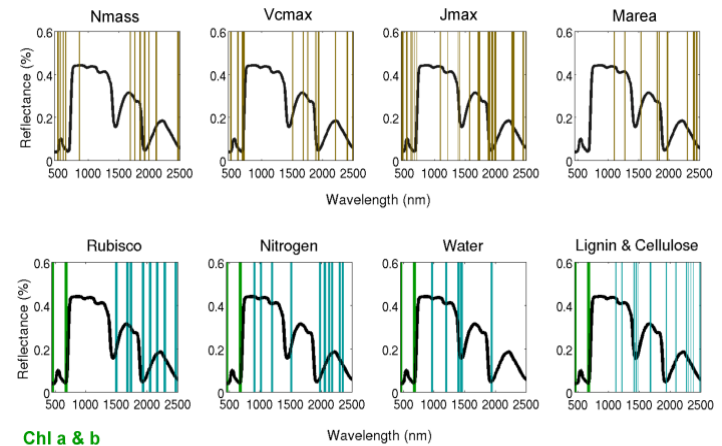
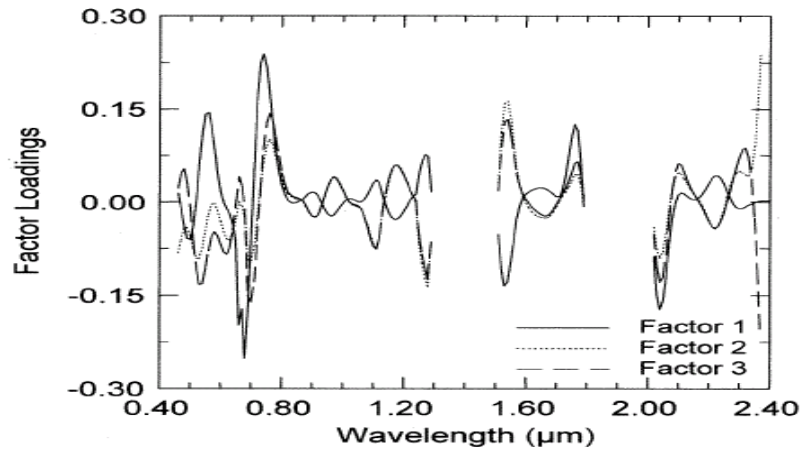
MD12

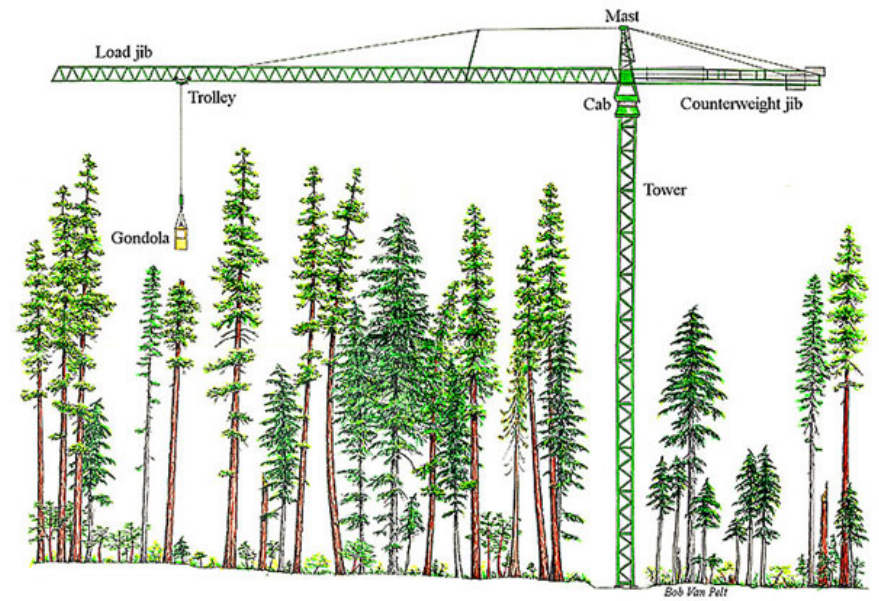
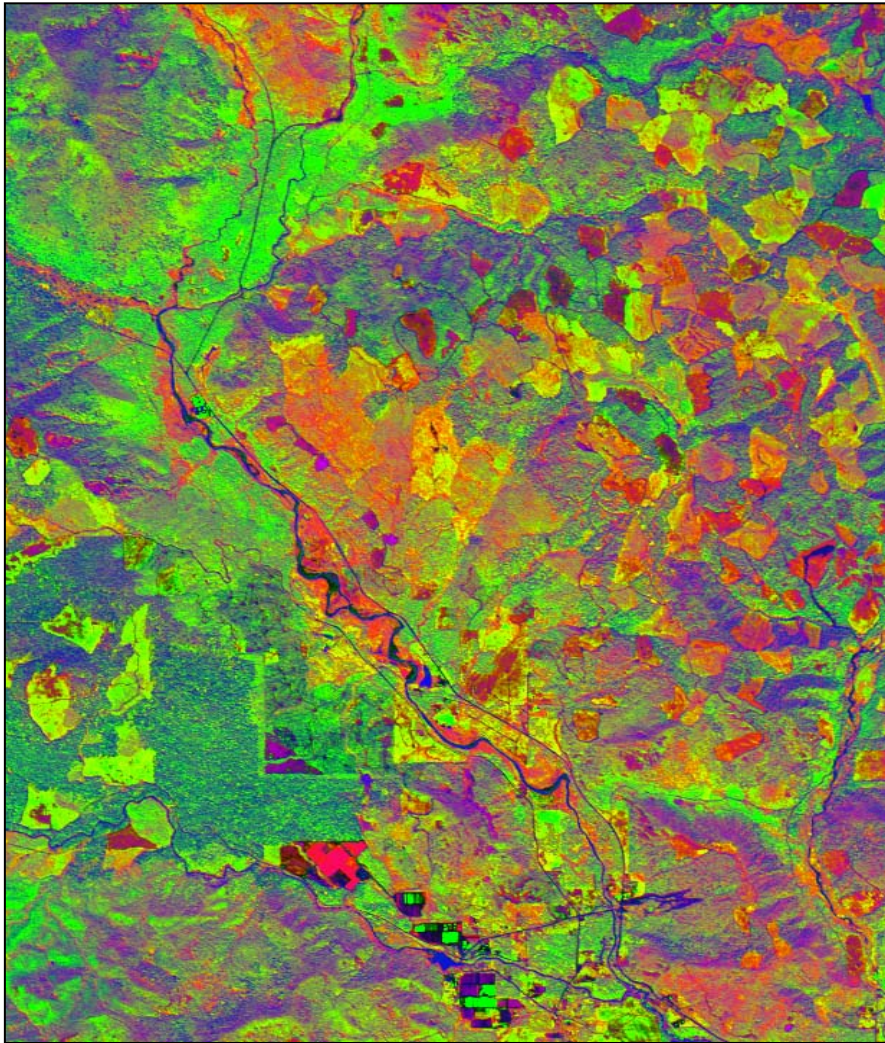


MD12 without MD12-specific vars



Full spectrum is required for species/functional-type, biogeochemistry and physiological condition.



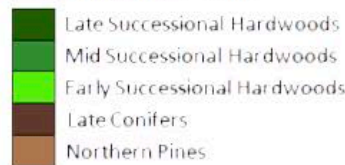


Imaging Spectroscopy Derived Composition

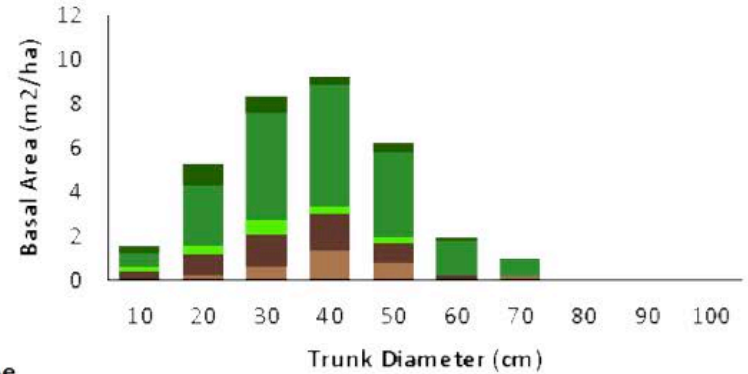
FIELD OBSERVED



Plant Functional Type



Forest Inventory Size Distribution

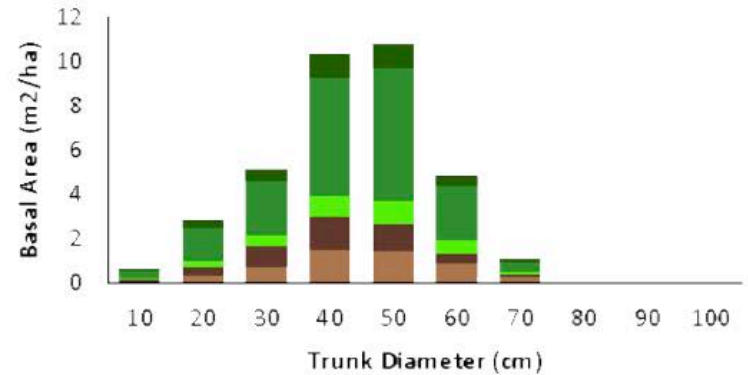


Basal Area = 33.5 m²/ha

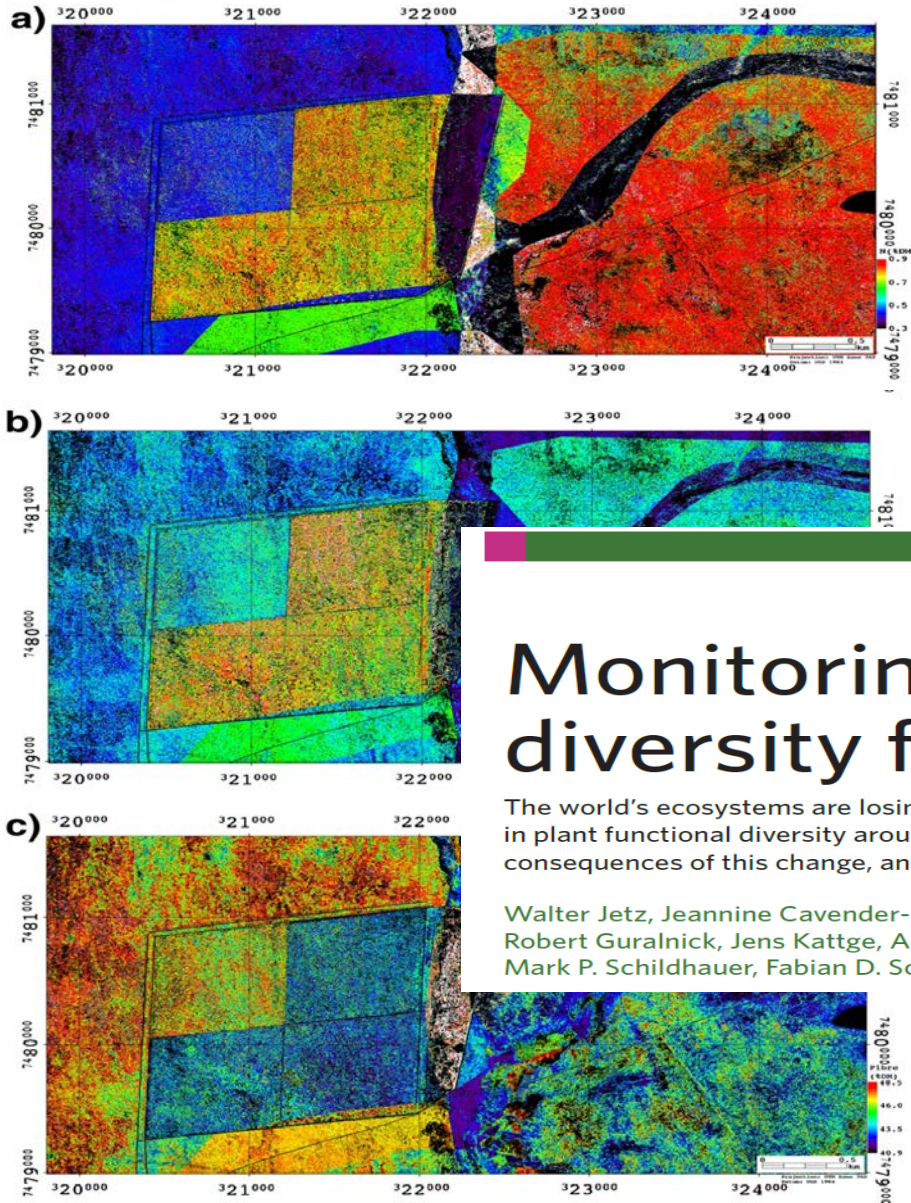
IMAGING SPECTROSCOPY DERIVED



GORT Calculated Size Distribution



Basal Area = 35.6 m²/ha



Contents lists available at ScienceDirect

Remote Sensing of Environment

journal homepage: www.elsevier.com/locate/rse



Dry season mapping of savanna forage quality, using the hyperspectral Carnegie Airborne Observatory sensor

Nichola M. Knox ^{a,*}, Andrew K. Skidmore ^a, Herbert H.T. Prins ^b, Gregory P. Asner ^c, Harald M.A. van der Werff ^a, Willem F. de Boer ^b, Cornelis van der Waal ^{a,2}, Hendrik J. de Knegt ^b, Edward M. Kohi ^{b,f}, Rob Slotow ^d, Rina C. Grant ^e

^a Faculty for Geo-information Science and Earth Observation (ITC), University of Twente, PO Box 6, 7500 AA, Enschede, Netherlands

^b Resource Ecology Group, Wageningen University, Droevendaalsesteeg 3a, 6708 PB, Wageningen, Netherlands

^c Department of Global Ecology, Carnegie Institution of Washington, 260 Panama Street, Stanford, CA 94305, USA

^d Amarula Elephant Research Programme, Biological and Conservation Sciences, Westville Campus, University of KwaZulu-Natal, Private Bag X54001, Durban 4000, South Africa

^e Private Bag X402, Scientific Services, Skukuza, 1350, South Africa

^f Tanzania Wildlife Research Institute, PO Box 661, Arusha, Tanzania

PUBLISHED: 2 MARCH 2016 | ARTICLE NUMBER: 16024 | DOI: 10.1038/NPLANTS.2016.24

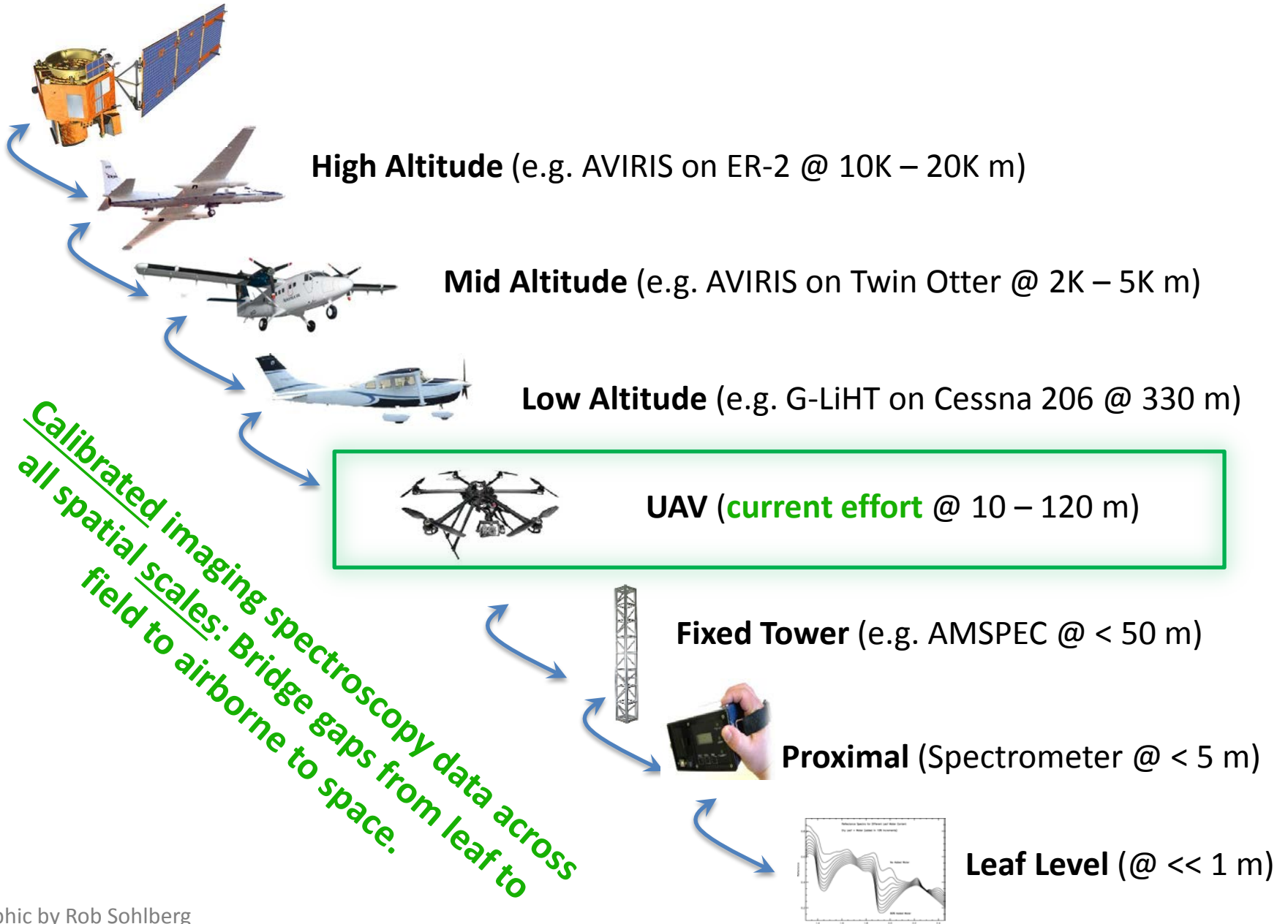
comment

Monitoring plant functional diversity from space

The world's ecosystems are losing biodiversity fast. A satellite mission designed to track changes in plant functional diversity around the globe could deepen our understanding of the pace and consequences of this change, and how to manage it.

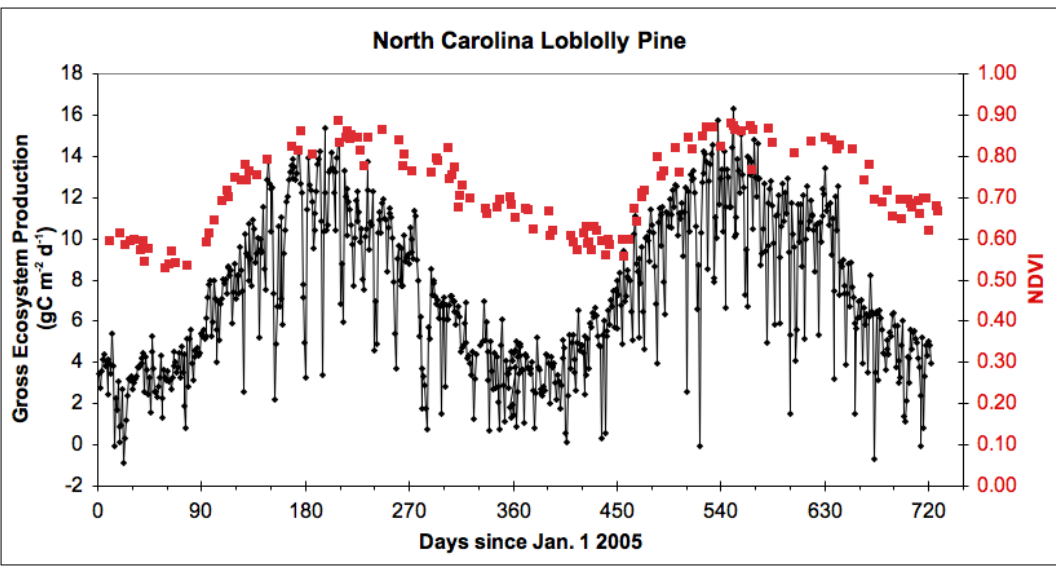
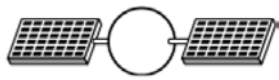
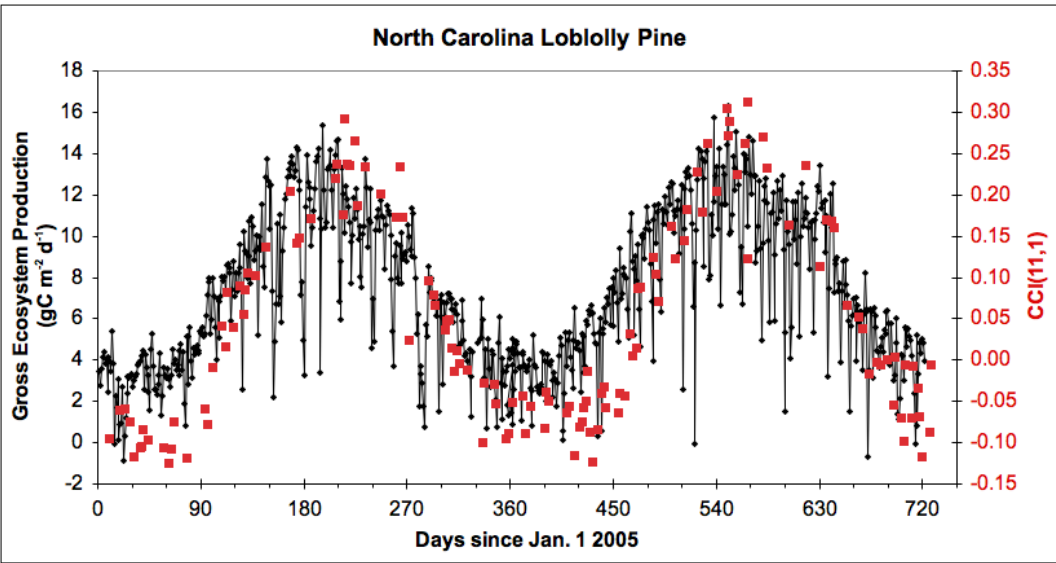
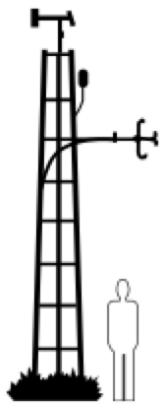
Walter Jetz, Jeannine Cavender-Bares, Ryan Pavlick, David Schimel, Frank W. Davis, Gregory P. Asner, Robert Guralnick, Jens Kattge, Andrew M. Latimer, Paul Moorcroft, Michael E. Schaepman, Mark P. Schildhauer, Fabian D. Schneider, Franziska Schrod, Ulrike Stahl and Susan L. Ustin

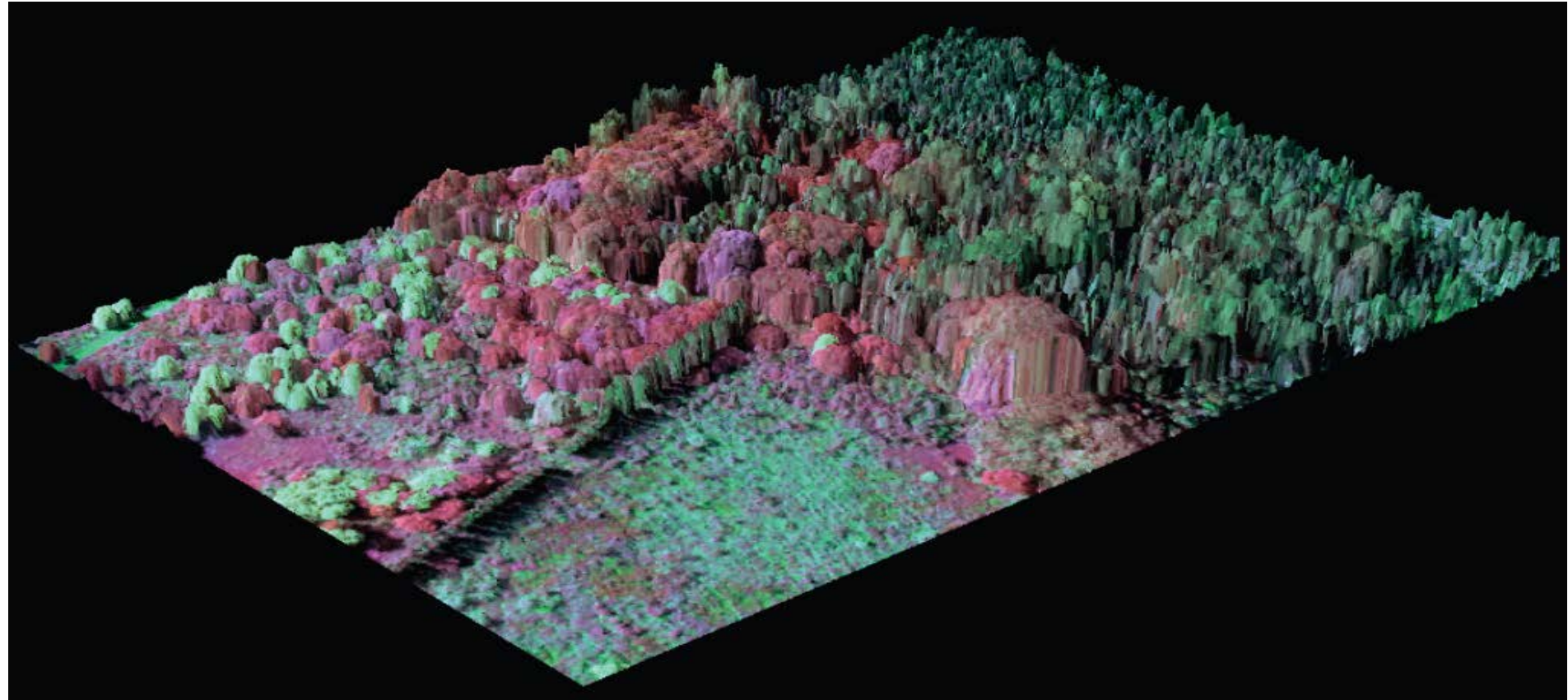
Orbital (e.g. EO-1 / HypsIRI / Landsat @ ~ 700 km)





CCI Does a Better Job of Describing "Invisible" Evergreen Phenology than NDVI

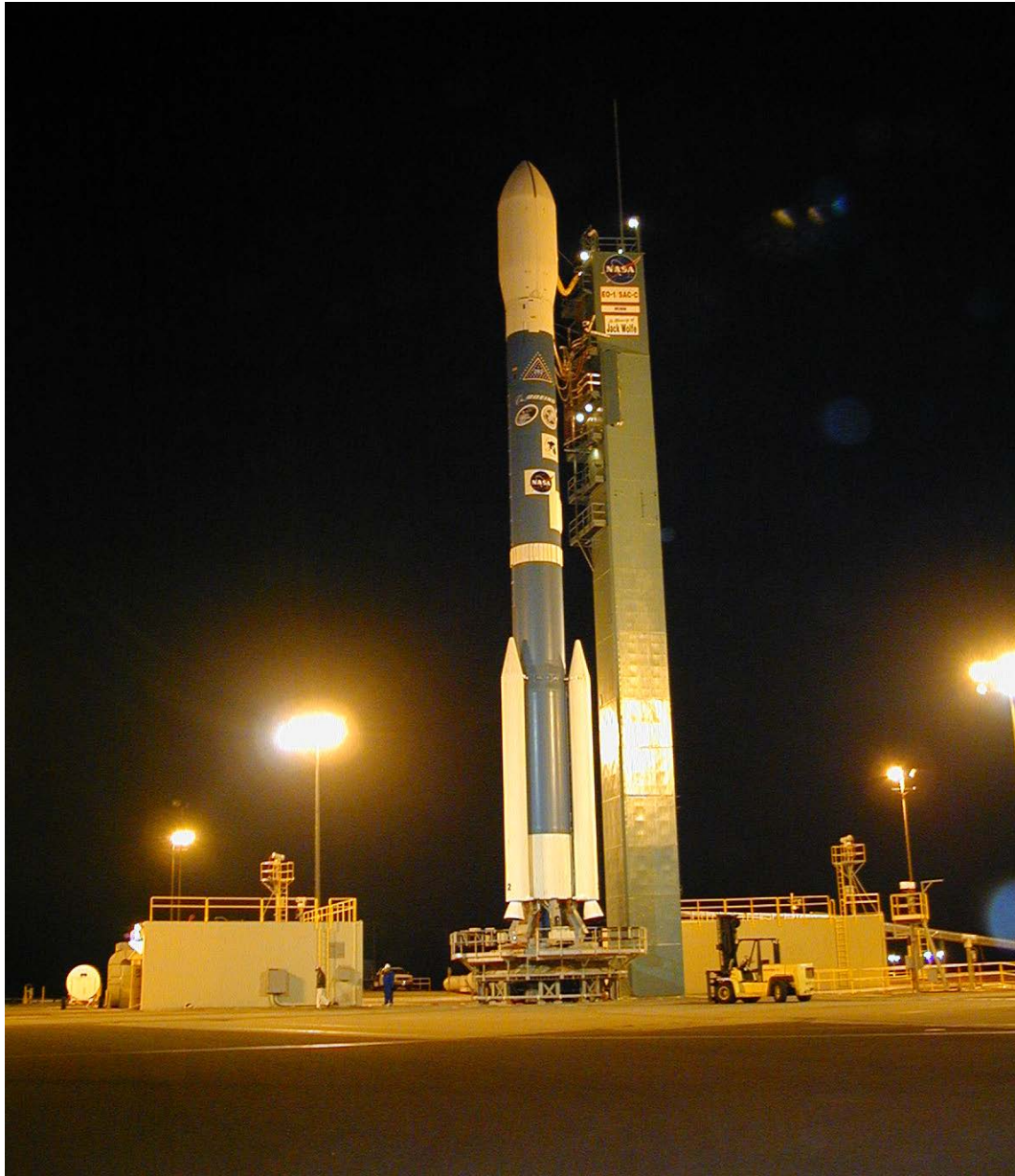




ECOSYSTEM 3-D STRUCTURE & SCALING

EO-1 Overview

EO-1 on the Pad (Nov. 2000)



Earth Observing One (EO-1) Mission

*Mission Scientist: Dr. Elizabeth Middleton 2007-2017; Dr. Stephen Ungar 2000-2007 (NASA/GSFC Code 618)
Mission Manager, Mr. Daniel Mandl (NASA/GSFC Code 581)*

EO-1 was designed to flight validate technologies and operational approaches applicable to future Earth observing missions. Launched on November 21, 2000, it took images of the Earth for over 16 years, with more than 180,000 scenes in archive.



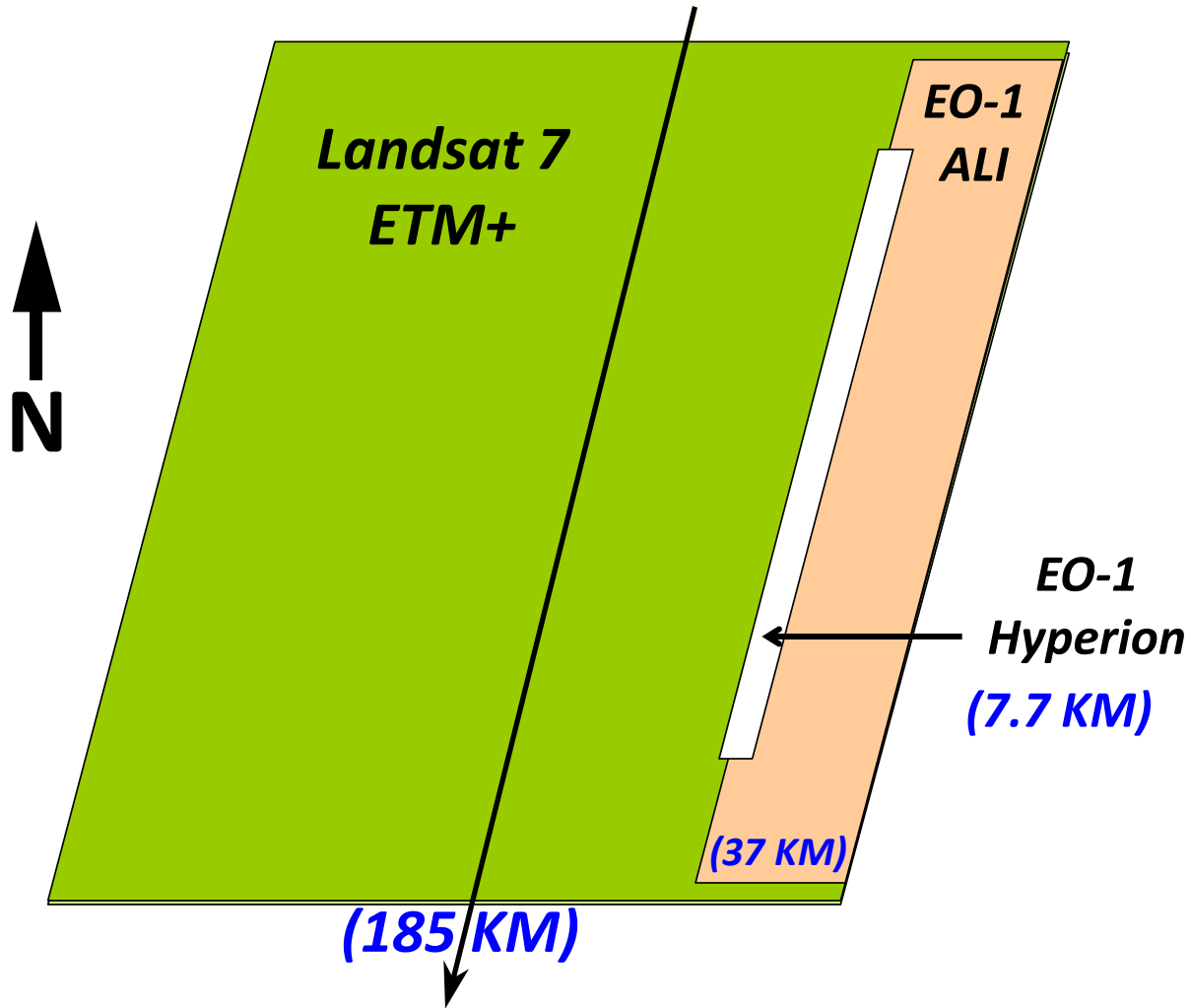
<http://eo1.gsfc.nasa.gov/>

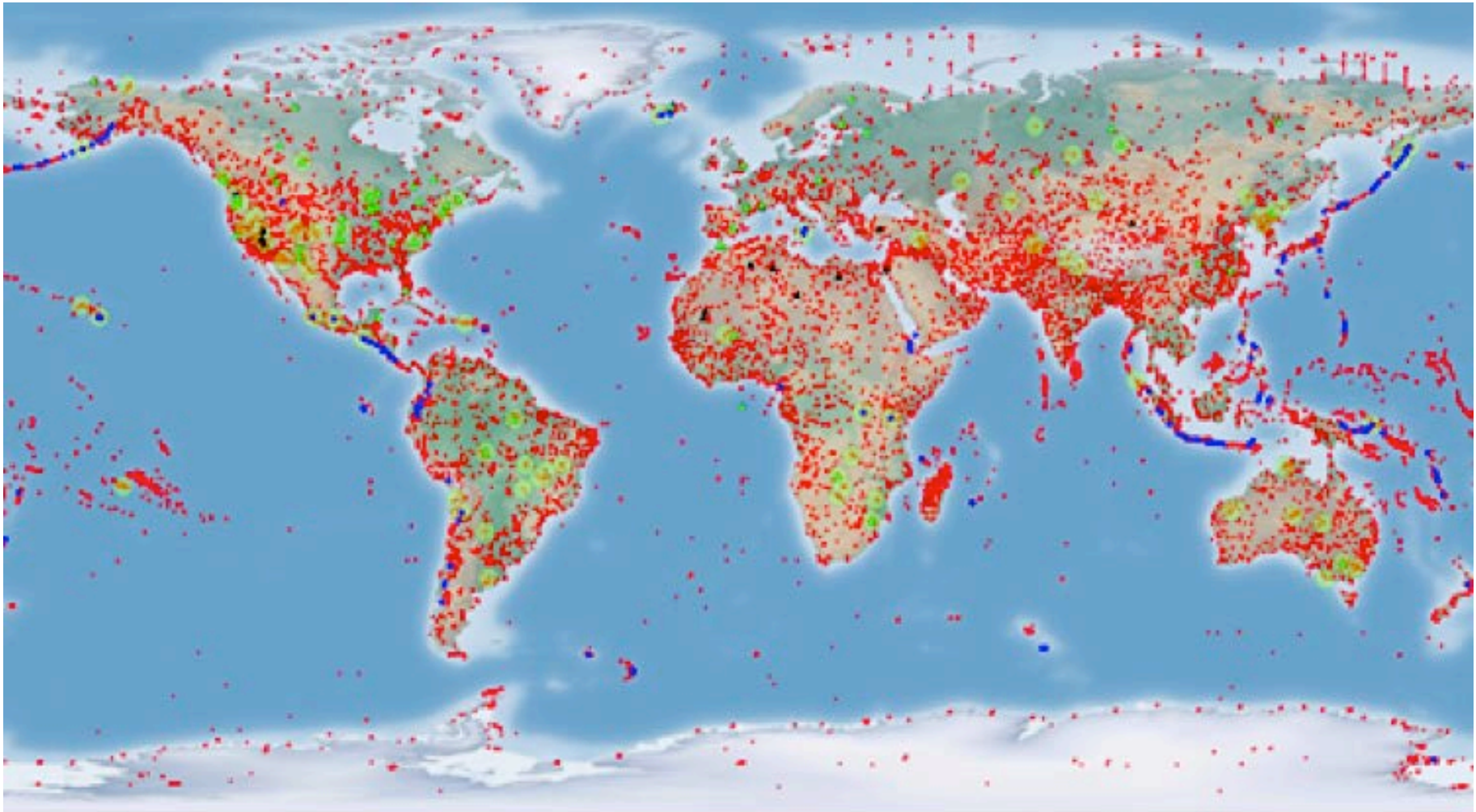
Off-nadir viewing option

ALI		Hyperion
Band Designations	Band Names (wavelength, μm)	
Pan	Pan (0.48 – 0.69)	Continuous Spectra 0.4 – 2.4 μm 242 Bands Bandwidth: 10nm
Blue	MS-1p (0.433 – 0.453)	
	MS-1 (0.450 – 0.515)	
Green	MS-2 (0.525 – 0.605)	
Red	MS-3 (0.633 – 0.690)	
NIR	MS-4 (0.775 – 0.805)	
	MS-4p (0.845 – 0.890)	
SWIR	MS-5p (1.20 – 1.30)	
	MS-5 (1.55 – 1.75)	
	MS-7 (2.08 – 2.35)	
Spatial Resolution	Pan: 10m, MS: 30m	30m
Swath Width	37km	7.7km



EO-1 and Landsat 7 Descending Orbit Ground Tracks





EO-1 Observations

MSO Sites

CEOS Sites

Volcanoes

> 10 Observations

Global map of locations having Hyperion (and ALI) imagery collections. EO-1 collected a total of 91,233 ALI and 90,995 Hyperion images in its 16+ year lifetime.

IEEE JOURNAL OF SELECTED TOPICS IN APPLIED EARTH OBSERVATIONS AND REMOTE SENSING

A PUBLICATION OF THE IEEE GEOSCIENCE AND REMOTE SENSING SOCIETY



APRIL 2013 VOLUME 6 NUMBER 2 IJSTHZ (ISSN 1939-1404)

PART I OF THREE PARTS

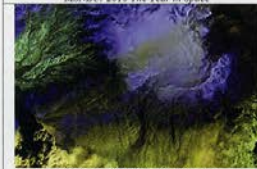
SPECIAL ISSUE ON THE EARTH OBSERVING ONE (EO-1) SATELLITE MISSION: OVER A DECADE IN SPACE



Manam Volcano, New Guinea
MSNBC: 2010 The Year in Space



Gulf Oil Spill (June 2010)
Multiple Web sites and news outlets



Eyjafjallajökull Volcano, Iceland
Back cover of Physics Today (June 2010)



Irrigation Project, Orange River, South Africa
NASA Science Calendar 2011 (one of twelve selected)



Toxic Sludge Flood in Hungary (Oct. 2010)
CNN, MSNBC, Huffington Post Web Site, many other Web sites and news outlets



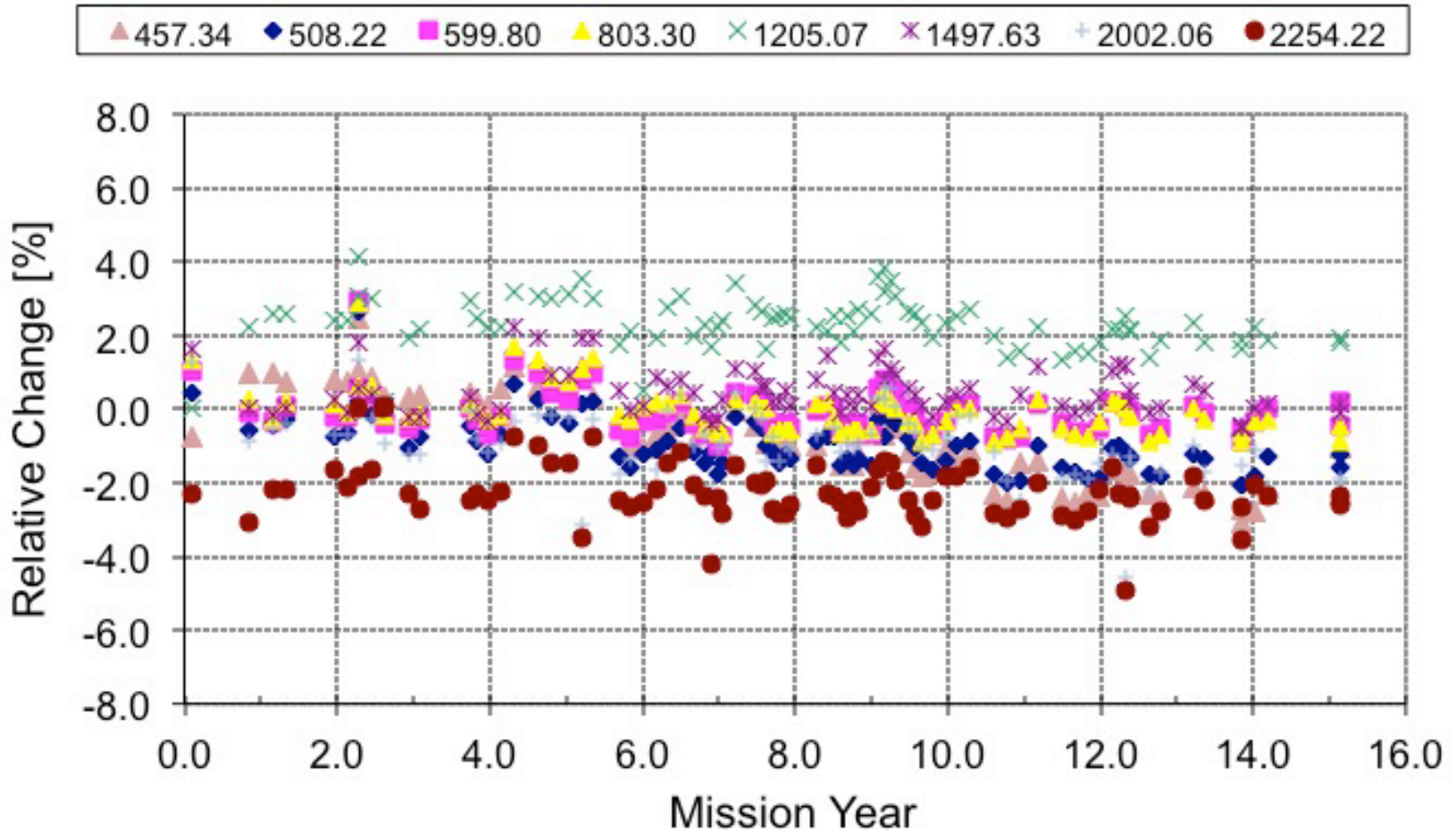
Ice Island Calved off Petermann Glacier, Greenland
NatureNews Web Site: 2010 Images of the Year

Examples of ALI images posted by NASA's Earth Observatory. (See Middleton *et al.*, pp. 243-256.)



Guest Editor,
Elizabeth Middleton

Hyperion Lunar Cal. Trends for Selected Bands

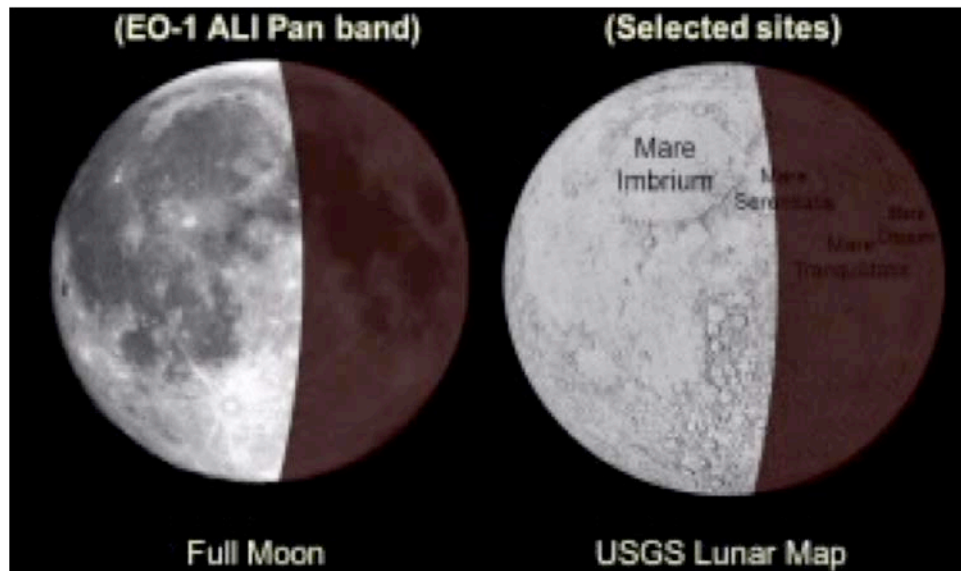


EO-1 Hyperion lunar calibration trends. A comparison of integrated radiance values of Hyperion bands and those from the Robotic Lunar Observatory (ROLO) model, shows that the sensor's performance is within ± 1.0 - 1.5% . Hyperion has remained stable over the last fifteen years.

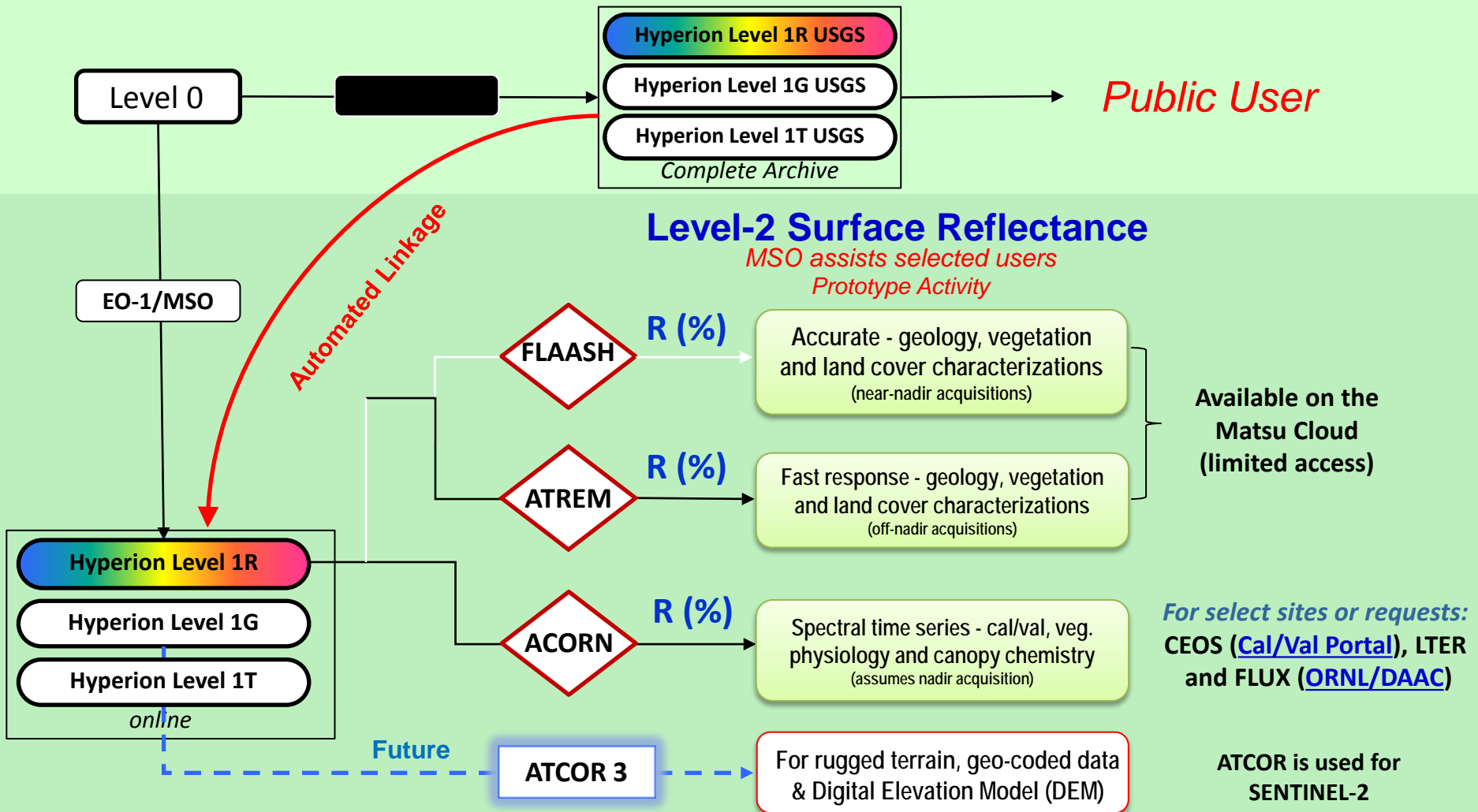
The new lunar acquisition strategy enables high quality Hyperion observations of radiometrically stable features at multiple phase angles.

This new capability is realized through a significant increase in effective SNR engendered by a slow scan of the lunar surface resulting in a 32X oversampling.

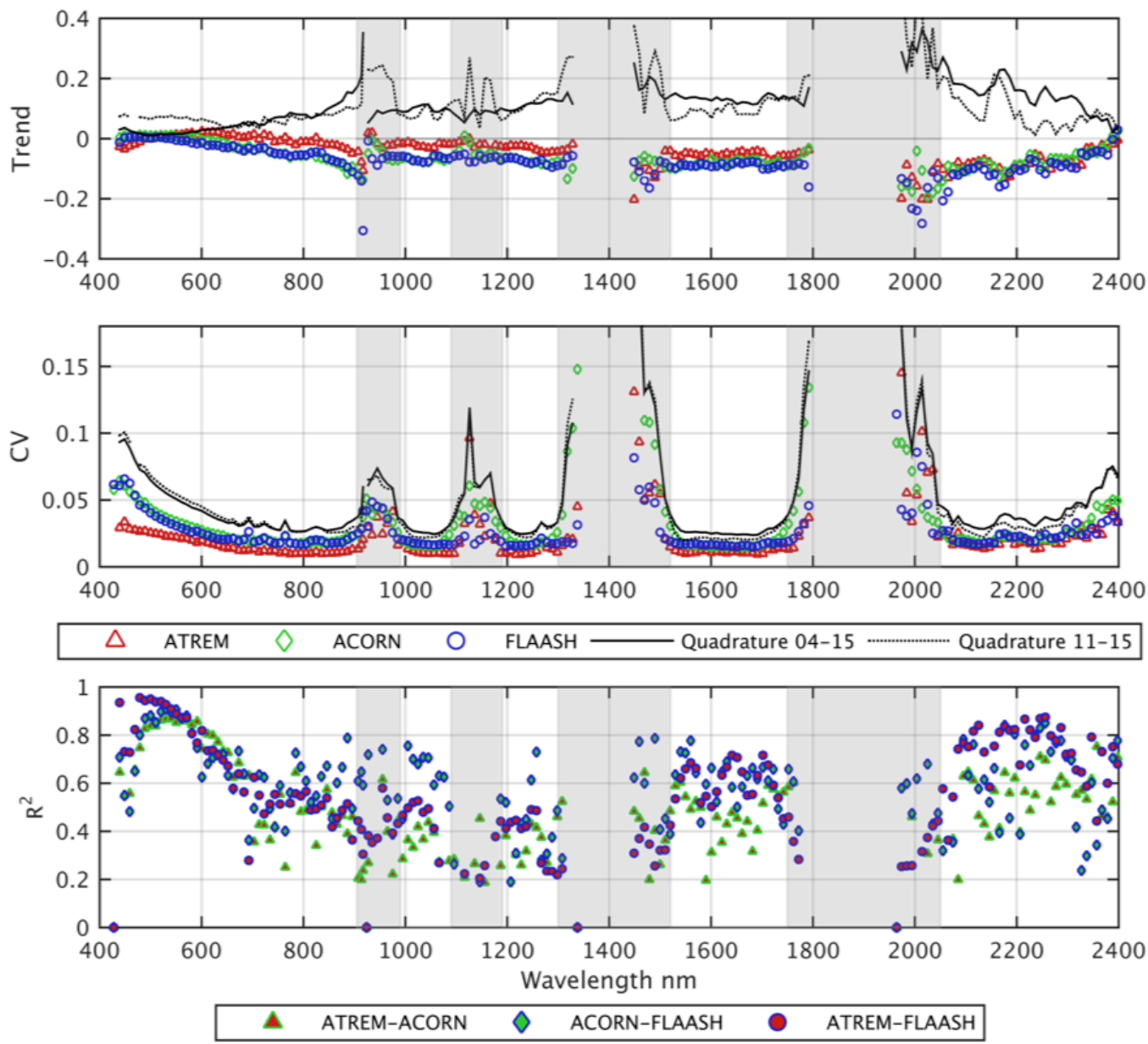
We continue monthly comparisons of Hyperion integrated lunar responses with the USGS Robotic Lunar Observatory (ROLO) Lunar model at near full moon to maintain the EO-1 lifetime trends.



Current Hyperion Products



Hyperion VSWIR Over Libya-4

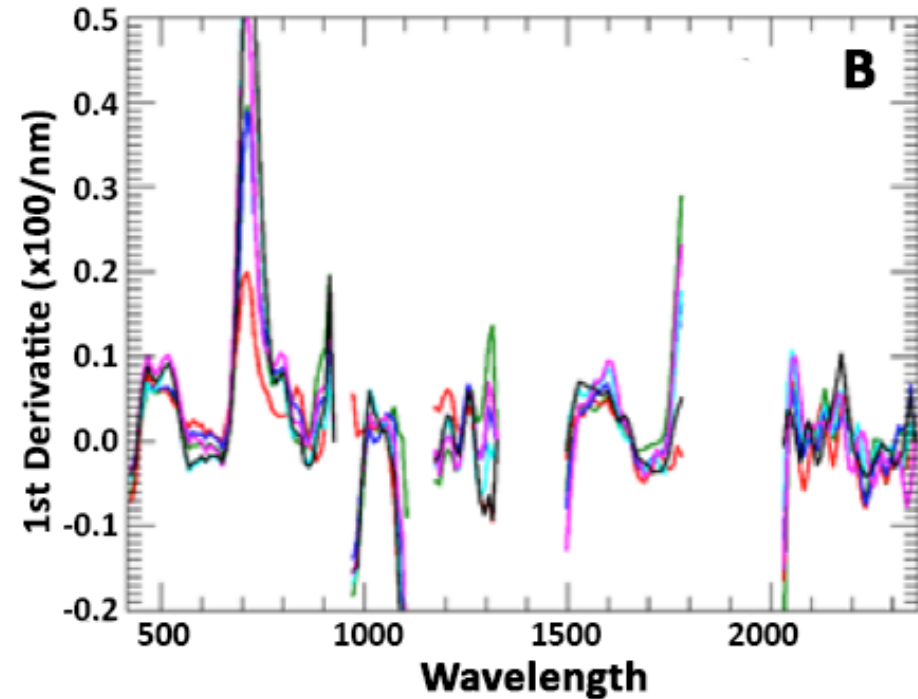
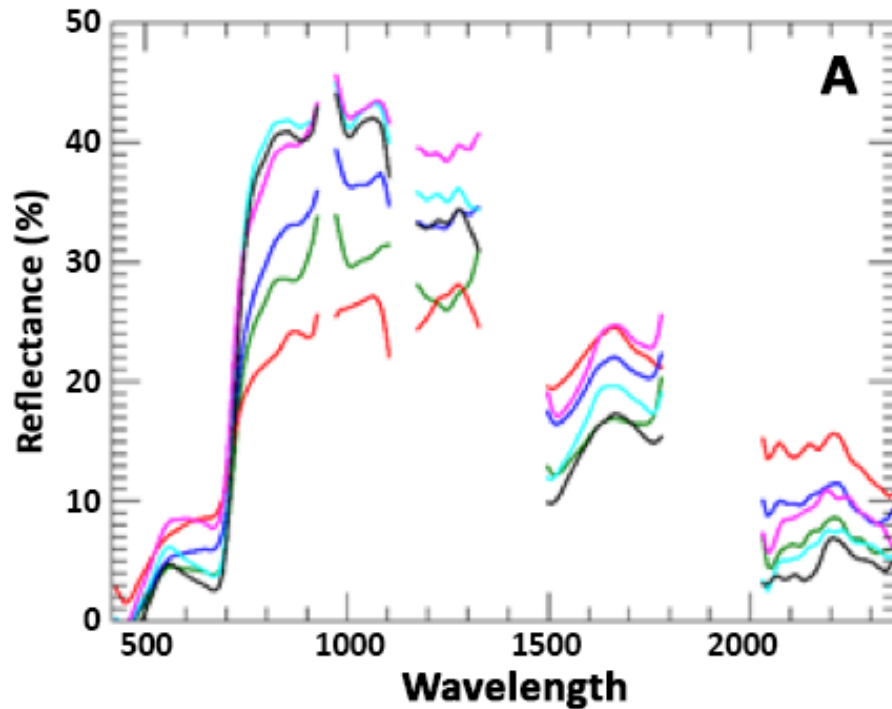


Top: Hyperion VSWIR surface reflectance of 35 images of Libya-4 acquired 2004-2015. Mean lifetime trends were determined with 3 atmospheric correction (AC) models; ATREM, ACORN, and FLAASH.

Middle: Temporal trend means across the spectrum, with the Q uncertainty estimate. Coefficient of variation trend for temporal trend, with Q.

Bottom: Coefficient of determination (R^2) between pairs of AC models, $p < 0.01$.

Neigh et al. 2016



Date	Acq-Time	Off-Nadir
10/01/2005	15:30	-7.74
10/05/2008	15:36	8.05
09/24/2012	15:21	-0.16
09/28/2014	14:34	-13.3
07/26/2015	14:15	-2.81
08/24/2016	14:33	-7.10

Hyperion spectra collected over a cornfield on six dates between 2005 and 2016, representing typical monthly data between July and October in any year: **[A]** original reflectance spectra; and **[B]** first derivative spectra of reflectance.

Frank et al. 2017

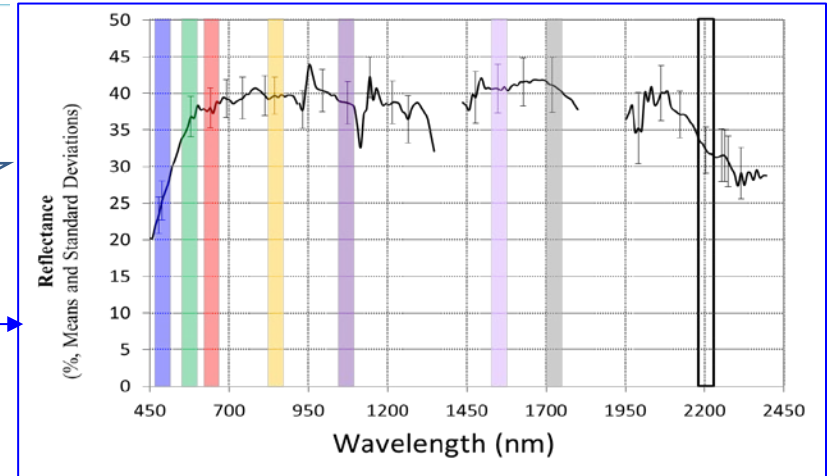
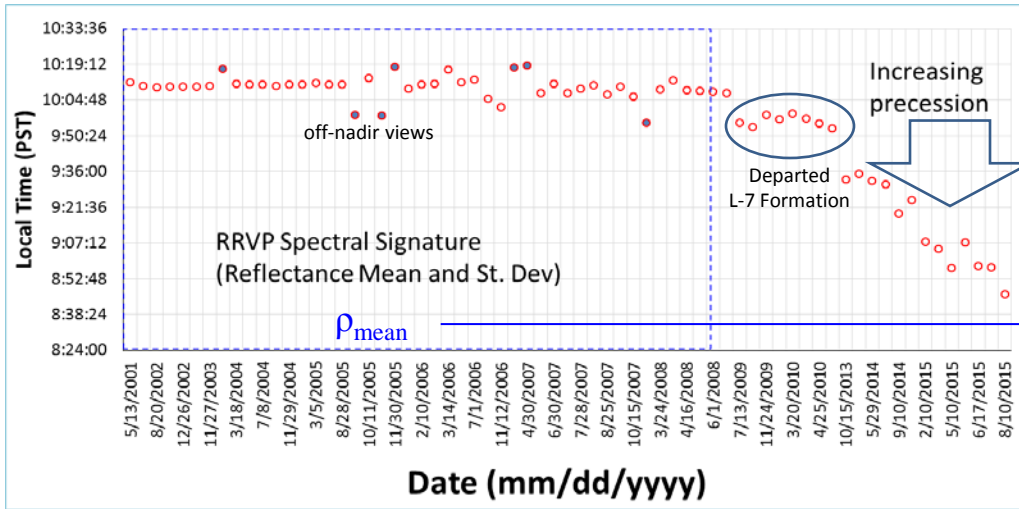


EO-1 Hyperion Reflectance Stability During Increased Precession at Railroad Valley Playa (RRVP)

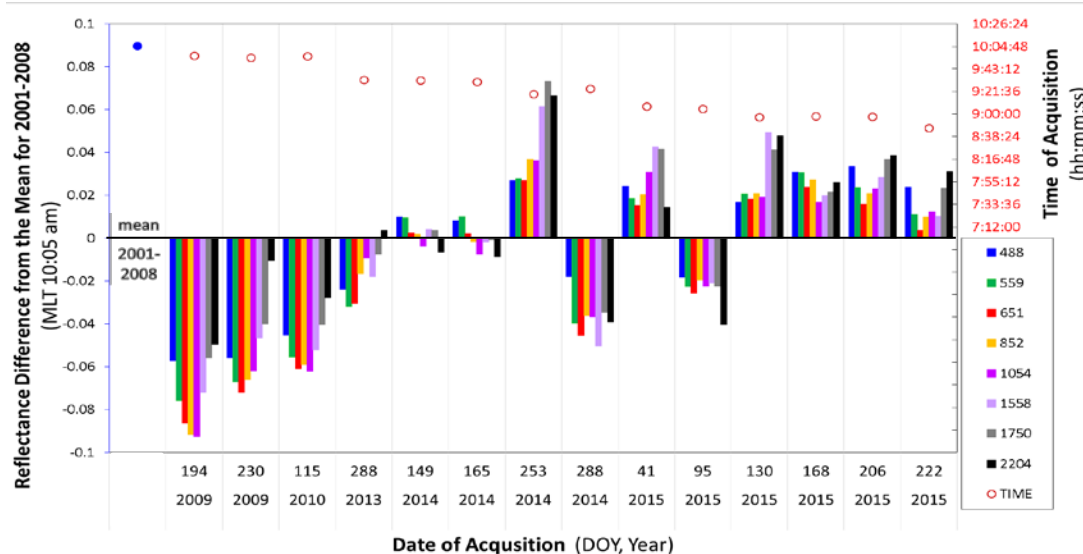


EO-1 increased precession started in 2011. Acquisition time at RRVP declined from 10:05 to 8:40, approximately.

Mean reflectance and standard deviation for RRVP (2001-2008 data, n=15, ~10:05 am MLT acquisition)



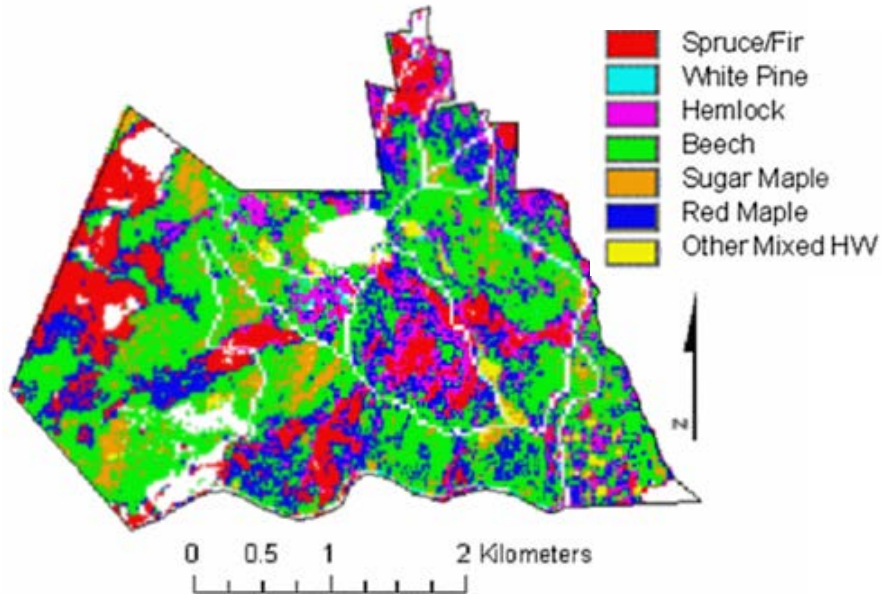
Change in reflectance anomaly ($\Delta\rho$) at select wavelengths at RRVP



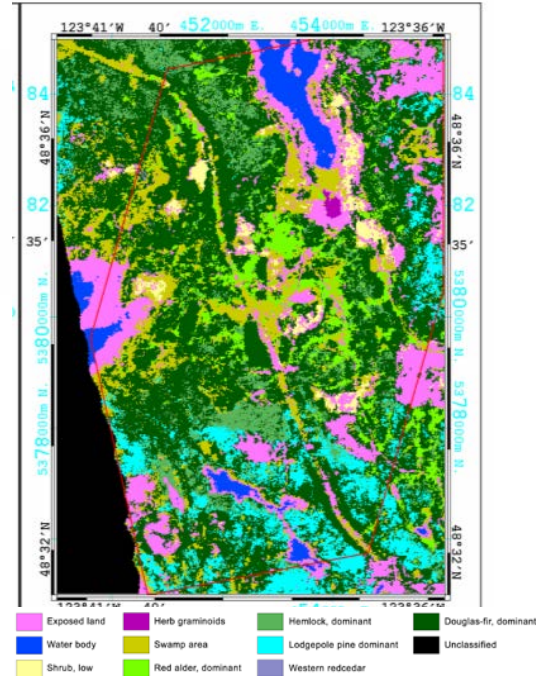
The difference in reflectance continues to be within $\pm 5-9\%$ of the mean prior to Δ precession.

The regions of highest spectral stability (e.g. green, red edge, NIR) remain the same.

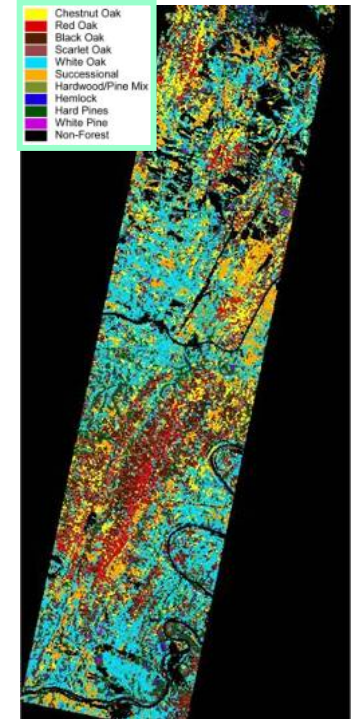
New England, USA



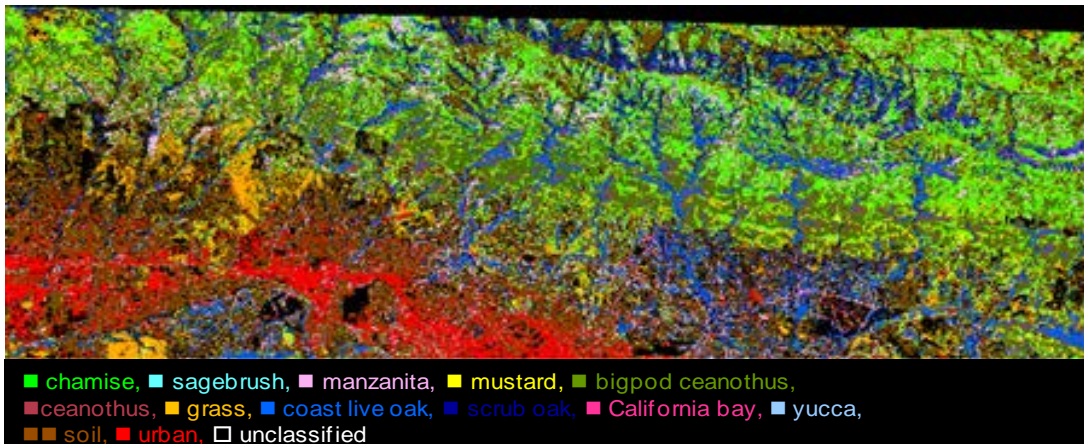
British Columbia, Canada



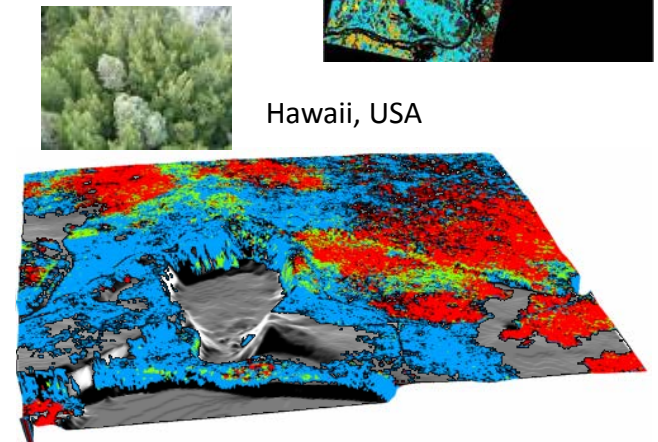
Shenandoah National Park, USA

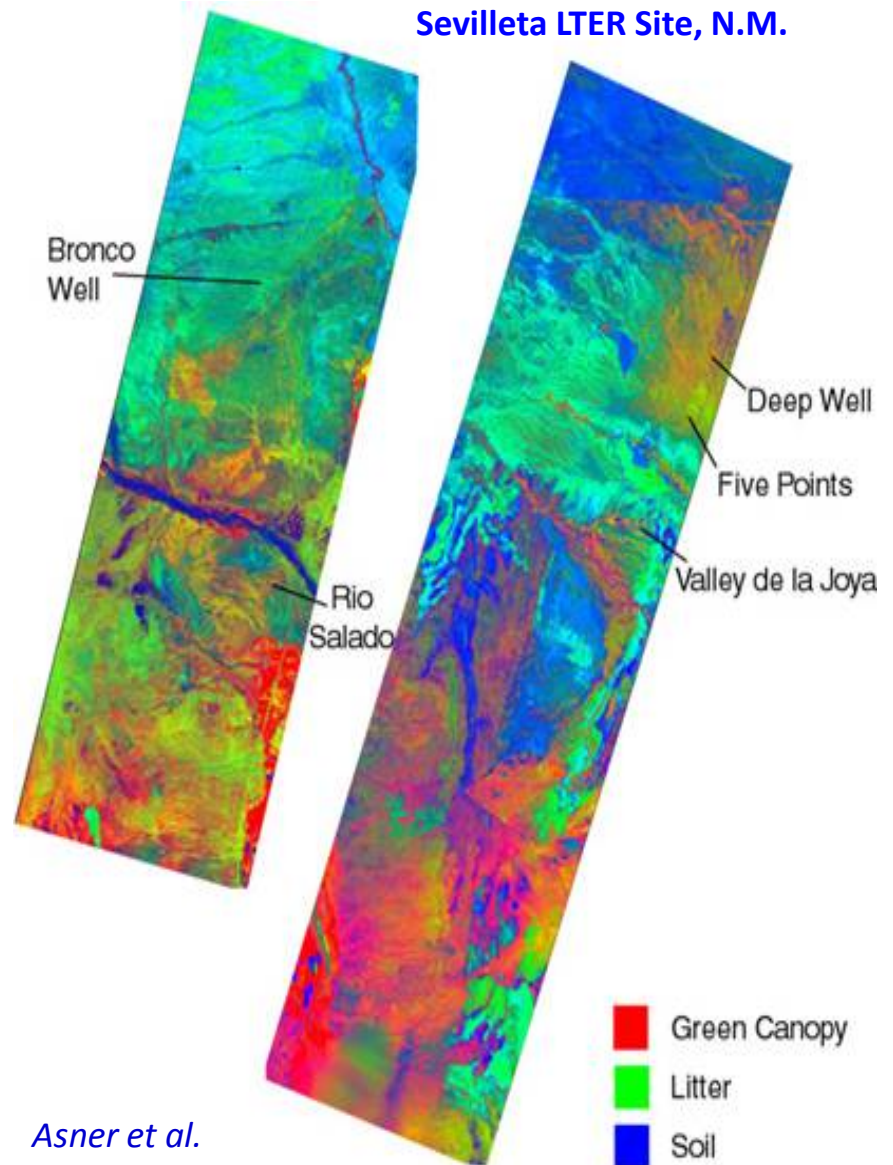
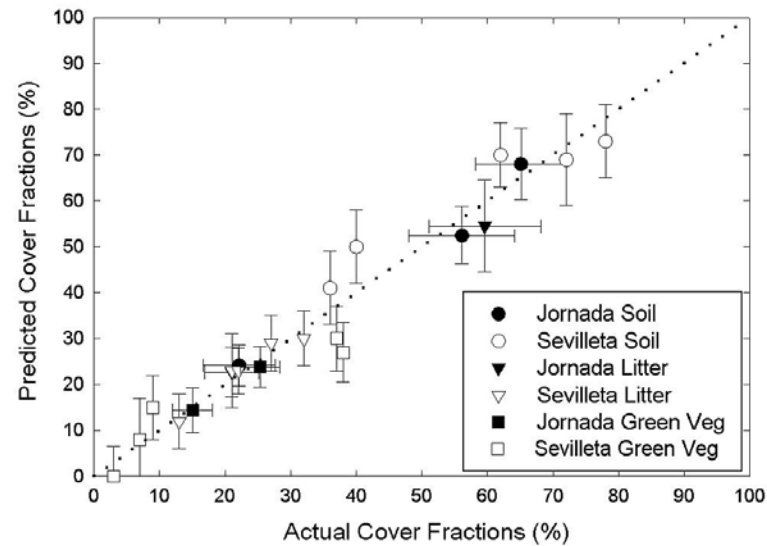
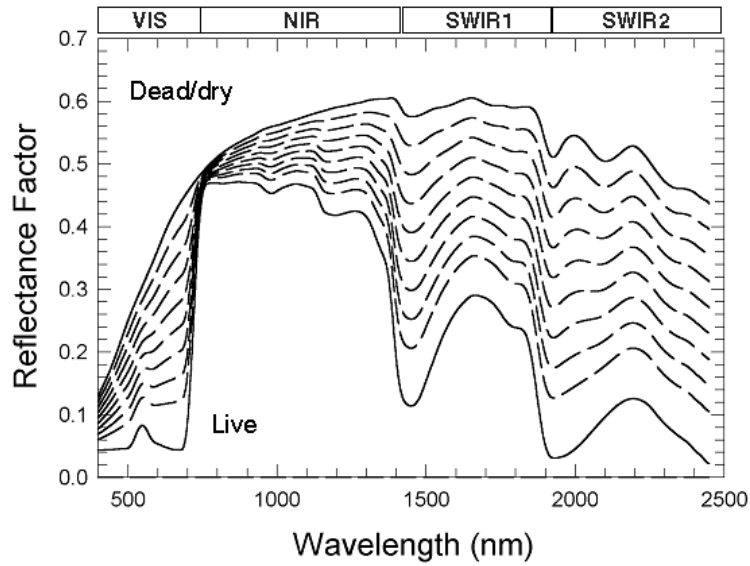


Santa Barbara, CA

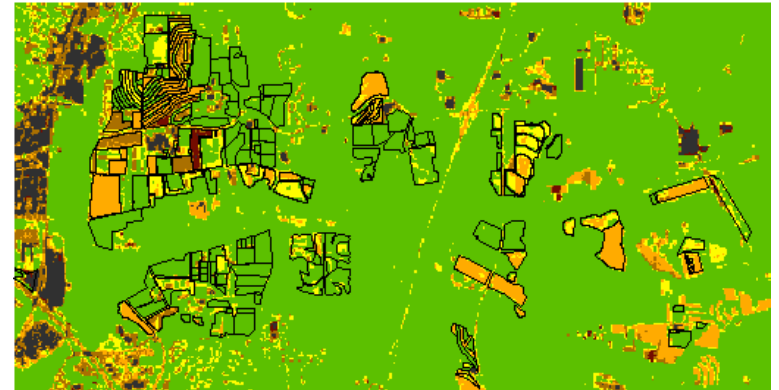
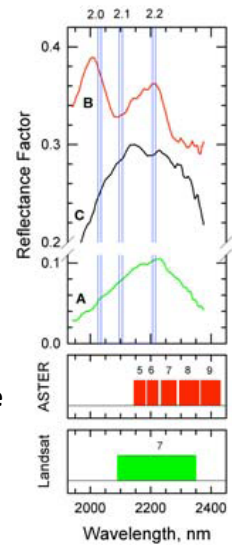
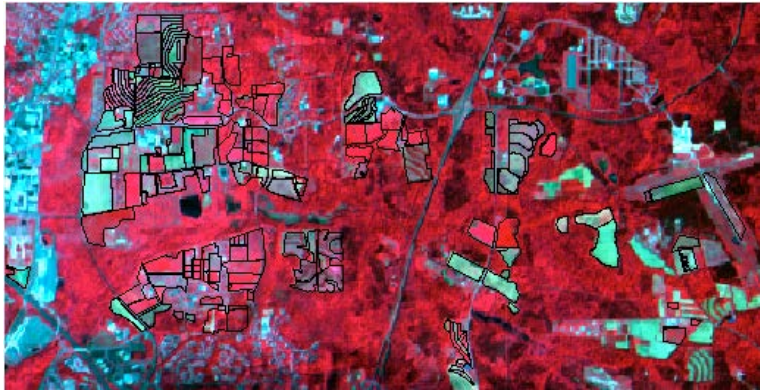


Hawaii, USA





Asner et al.



Tillage intensity classification using CAI and NDVI
(overall classification accuracy = 92%)

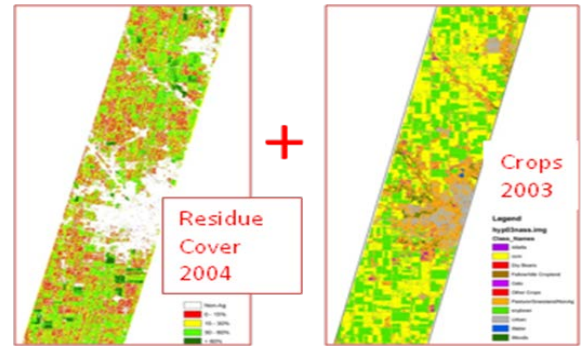
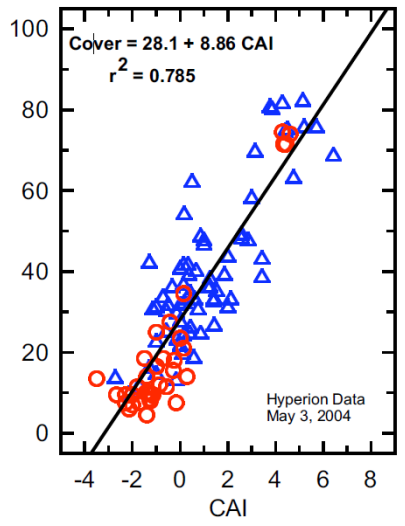
- Classification**
- Non-Agriculture
 - Intensive Tillage
 - Reduced Tillage
 - Conservation Tillage
 - Yellow Vegetation
 - Green Vegetation

Color Infrared composite AVIRIS image with field boundaries, blue (549 nm), green (646 nm), red (827 nm)

$$CAI = 0.5(R_{2000} + R_{2200}) - R_{2100}$$



Crop Residue Cover vs. CAI for Hyperion, Iowa - 5-3-2004



For dry and moist conditions CAI is adequate for assessing crop residue cover.

Hyperspectral Hyperion Images and Spectral Libraries of Agricultural Crops



PE&RS
August 2014 Volume 80, Number 8

Hyperspectral Hyperion Images and Spectral Libraries of Agricultural Crops

Legend
AVHRR NDVI-MVC
High: 1
Low: 0
EO-1 Hyperion

Reflectance (%)
Wavelength (nm)

Corn-late vegetative

Reflectance (%)
Wavelength (nm)

Wheat, early vegetative (56)
Corn, tasselling (64)
Rice, late vegetative (38)
Cotton, late vegetative (52)

80th
1934-2014
asprs

August 2014 1

PE&RS PHOTOGRAMMETRIC ENGINEERING & REMOTE SENSING
The official journal for imaging and geospatial information science and technology
August 2014 Volume 80 Number 8

COLUMNS

Letter from Anatoly A. Gitelson, Technion—Israel Institute of Technology 696
Grids and Datums 712
Republic of Chad
Mapping Matters 715
Book Review 716
Wavelets and Fractals in Earth System Sciences
Behind the Scenes 718

ANNOUNCEMENTS

Pecora 19 & ISPRS Commission I Symposium Call for Papers 693, 724, 744

DEPARTMENTS

Certification 714
Industry News 720
New Members 720
Member Champions 732
Calendar 756
Forthcoming Articles 756
Who's Who in ASPRS 806
Sustaining Members 809
Instructions for Authors 809
Membership Application 812

HIGHLIGHT ARTICLE

697 Hyperspectral Remote Sensing of Vegetation and Agricultural Crops
Prasad S. Thenkabail, Murali Krishna Gumma, Pardhasaradhi Teluguntla, and Irshad A. Mohammed

INTERVIEW

710 John All

SPECIAL ISSUE FOREWORD

721 Research Advances in Hyperspectral Remote Sensing
Prasad S. Thenkabail

PEER-REVIEWED ARTICLES

725 Improved Capability in Stone Pine Forest Mapping and Management in Lebanon Using Hyperspectral CHRIS-Proba Data Relative to Landsat ETM+
Mohamad Awad, Ihab Jomaa, and Fatima Arab
An effective, low cost, and fast method for monitoring the changes in the forest cover, detecting diseases in forests, and mapping different forest species.

733 Combining Hyperspectral and Lidar Data for Vegetation Mapping in the Florida Everglades
Caiyun Zhang
A synergy of hyperspectral and LiDAR systems for automated vegetation mapping in a complex wetland Florida Everglades.

745 Hyperspectral Optical, Thermal, and Microwave L-Band Observations For Soil Moisture Retrieval at Very High Spatial Resolution
Nilda Sánchez, Maria Piles, José Martínez-Fernández, Mercè Vall-Ilossera, Luca Pipia, Adriano Camps, Albert Aguasca, Fernando Pérez-Aragüés, and Carlos M. Herrera-Jiménez
The potential of merging optical and thermal hyperspectral airborne data with microwave observations for estimating surface soil moisture at very high spatial resolution.

757 Biomass Modeling of Four Leading World Crops Using Hyperspectral Narrowbands in Support of HypiPR Mission
NOTE: This paper is open-access and free for all readers
Michael Marshall and Prasad Thenkabail
Ground-based spectroradiometric and aboveground fresh biomass data for four major world crops studied in the Central Valley of California to identify hyperspectral narrowbands sensitive to biomass using empirically-based modeling techniques.

773 Hyperspectral Data Dimensionality Reduction and the Impact of Multi-seasonal Hyperion EO-1 Imagery on Classification Accuracies of Tropical Forest Species
Manjit Saini, Binal Christian, Nikita Joshi, Dhaval Vyas, Prashanth Marpu, and Krishnappa Nadiminti
EO-1 Hyperion data was used to classify three distinct forest species during 3 seasons (monsoon, winter, summer) and the best classification accuracies were achieved using kernel principal component analysis through maximum likelihood classifier (kPCA-ML) for the monsoon season with overall accuracies of 83 to 100 percent for single species, 74 to 81 percent for two species, and 72 percent for three species respectively.

785 Automated Hyperspectral Vegetation Index Retrieval from Multiple Correlation Matrices with HyperCor
Helge Aasen, Martin Leon Gny, Yuxin Miao, and Georg Barth
Introducing the software HyperCor for automated preprocessing and calculation of correlation matrices from hyperspectral field spectrometry and the multi-correlation matrix strategy for the retrieval of hyperspectral vegetation indices to estimate rice biomass in the tillering, stem elongation, heading, and across all growth stages.

797 Automated Class Labeling Of Classified Landsat Tm Imagery Using a Hyperion-Generated Hyperspectral Library
Ilia Parshakov, Craig Coburn, and Karl Staens
A new method for the automatic labeling of classified imagery using Z-Score distance is for class label assignment of Landsat-5 TM imagery using Hyperion hyperspectral data.

PHOTOGRAMMETRIC ENGINEERING & REMOTE SENSING
August 2014 695

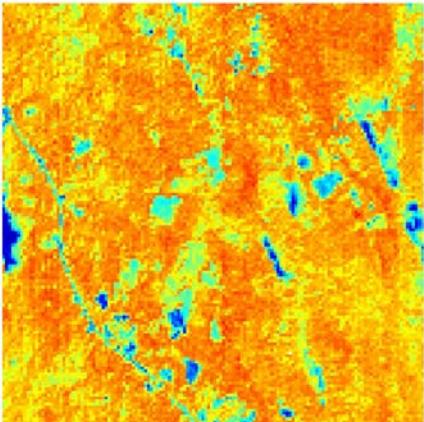
Hyperion → HypsIRI-like Products

fAPAR_{chl} at Harvard & Howland Forests

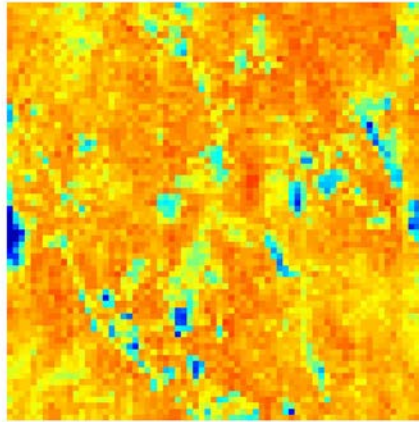


Harvard, June 2008

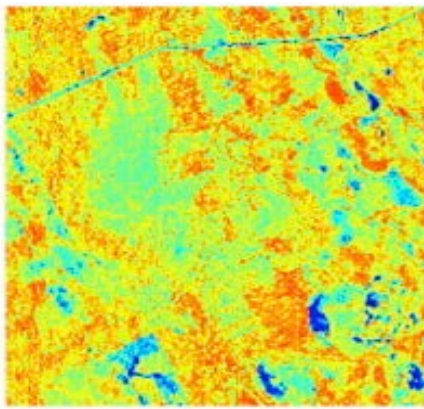
30 m Hyperion



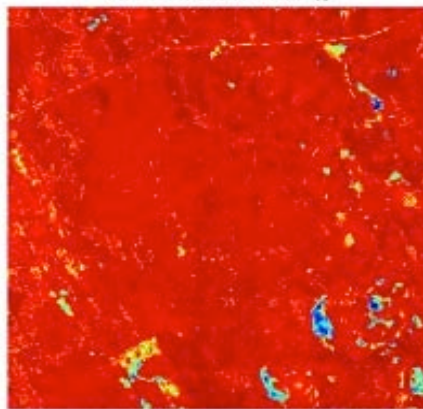
60 m HypsIRI



30 m Hyperion, Howland, June 2015



fAPAR_{chl}

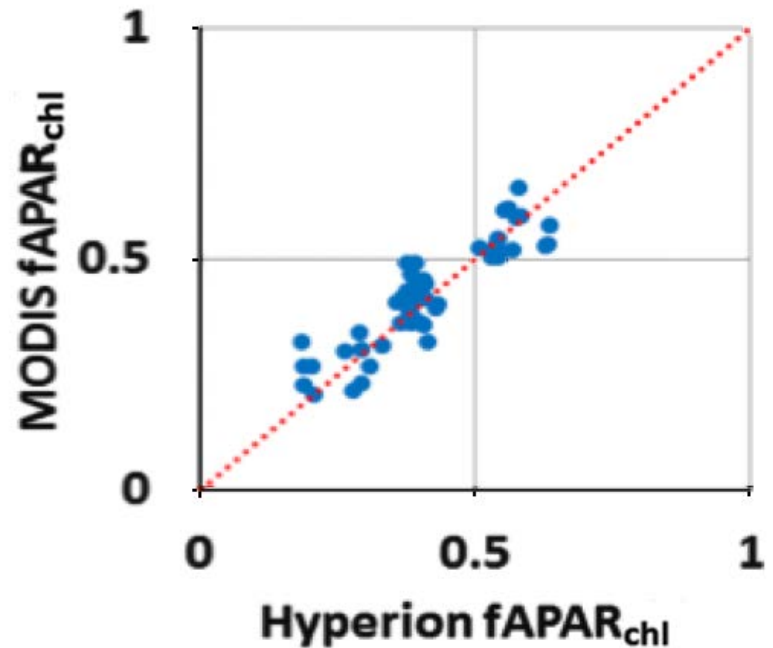


fAPAR_{canopy}

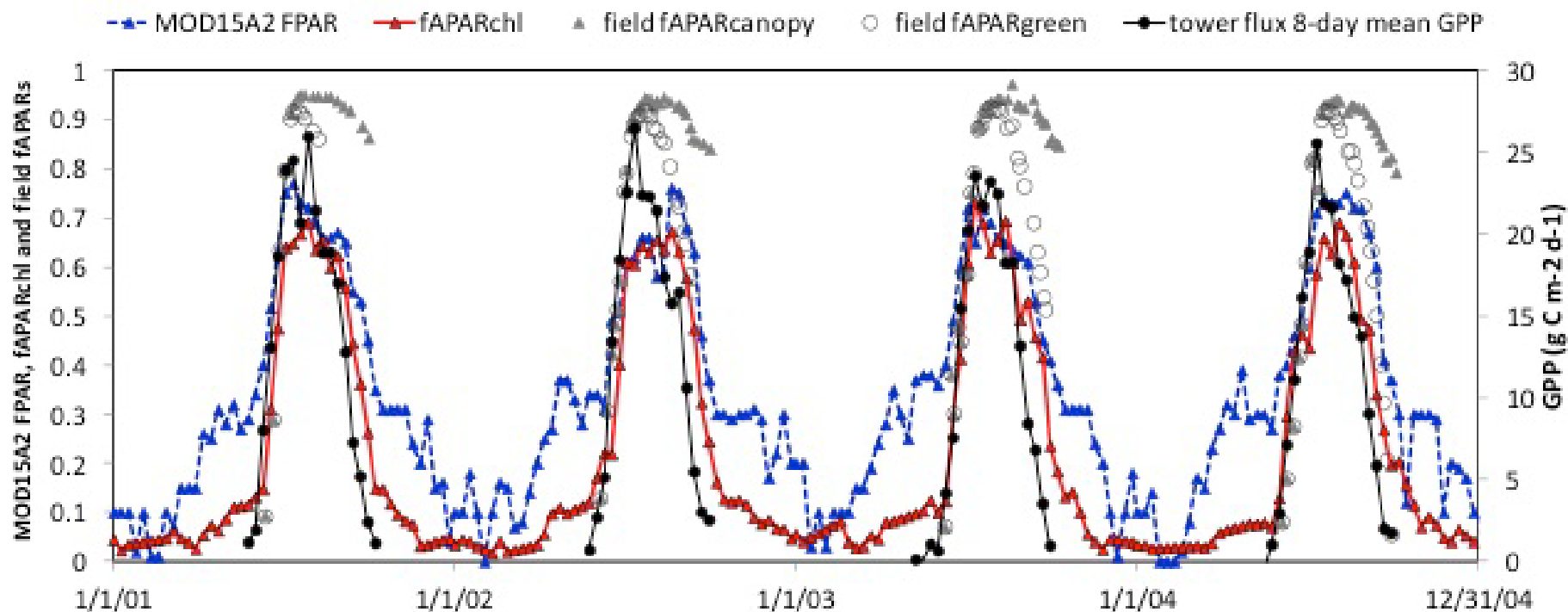


0 0.1 0.2 0.3 0.4 0.5 0.6 0.7 0.8 0.9 1.0

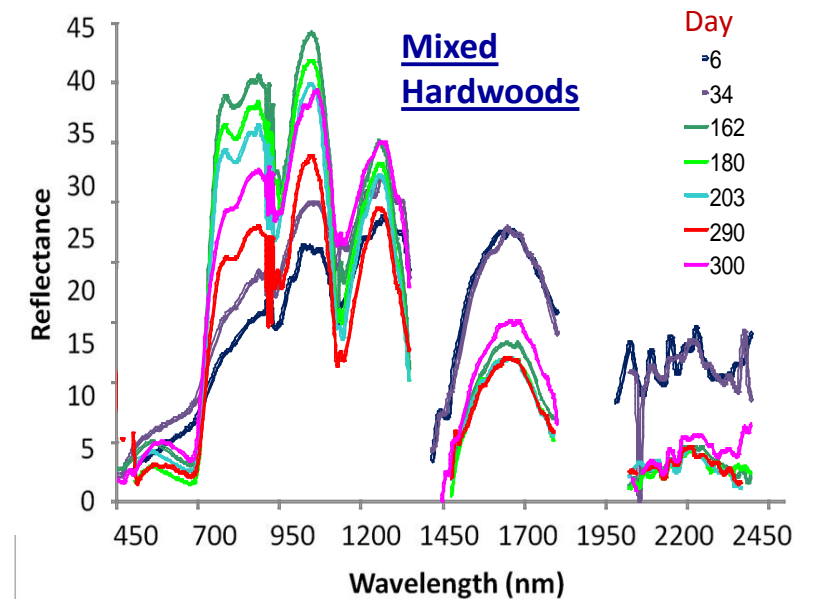
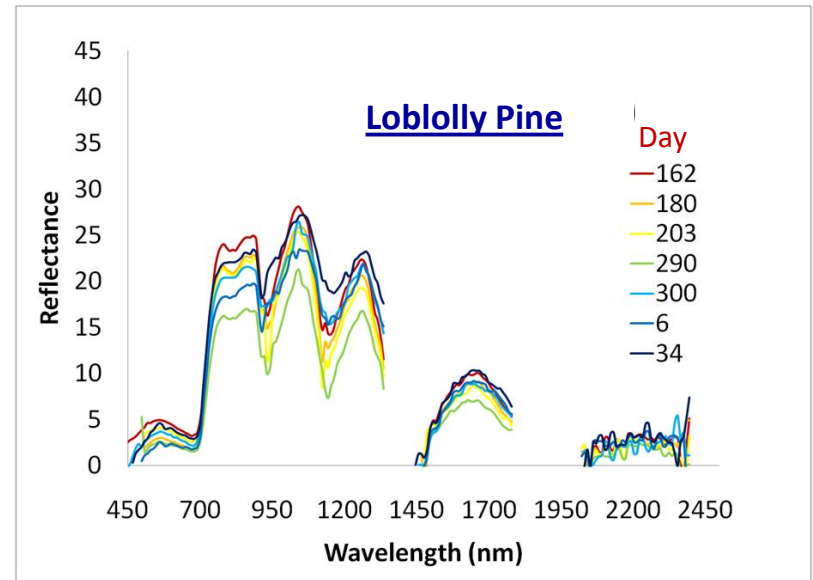
- Hyperion simulates HypsIRI Products
- Hyperion demonstrates accurate fAPAR_{chl} for vegetation (fAPAR_{chl} < fAPAR_{canopy})
- Hyperion fAPAR_{chl} = MODIS fAPAR_{chl}



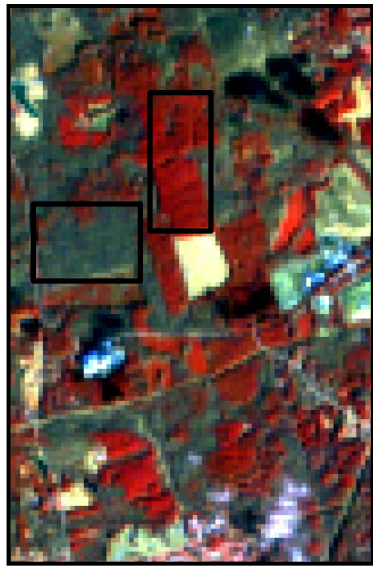
Zhang et al. 2012, 2013, 2014, 2016



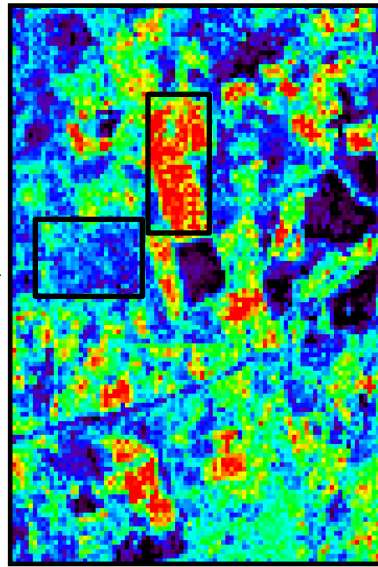
- Retrieved $fAPAR_{chl}$ matches well with tower GPP while MOD15A2 FPAR does not.
- MOD15A2 FPAR does not agree well with field $fAPAR_{canopy}$. It has earlier green-up and later fall-off compared to tower GPP, $fAPAR_{chl}$, and field $fAPAR_{canopy}$. It overestimates $fAPAR_{canopy}$ in spring and fall, but underestimates $fAPAR_{canopy}$ in summer.



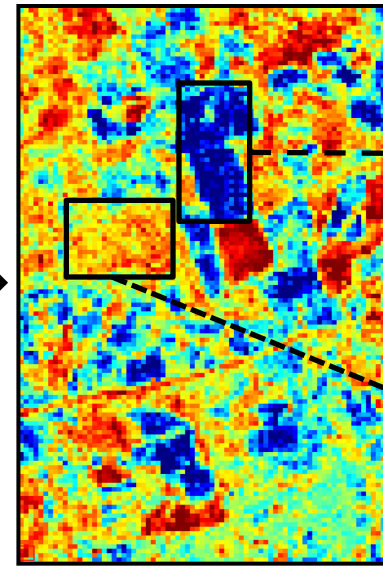
A. Winter (DOY 34)



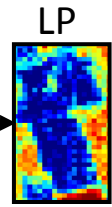
FCC (760, 650, 550 nm)



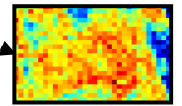
PRI₆₇₀



NEP ($\mu\text{mol m}^{-2} \text{s}^{-1}$)

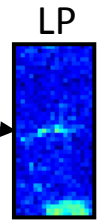
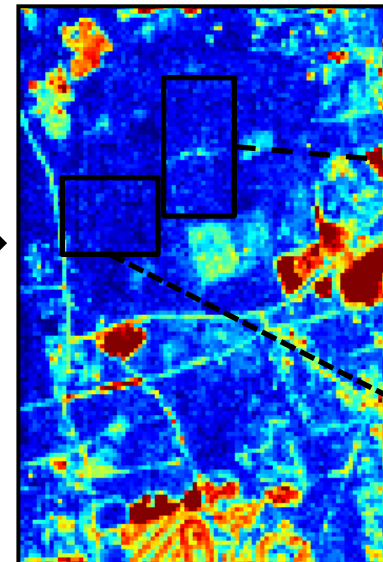
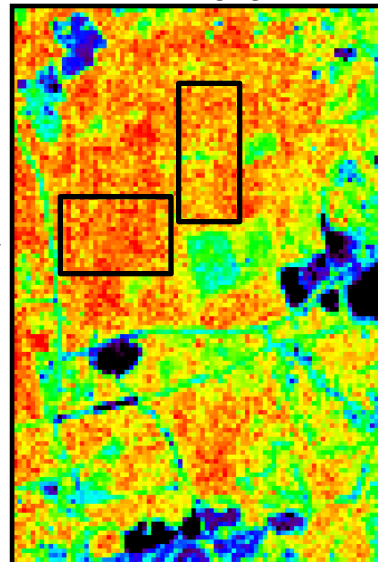
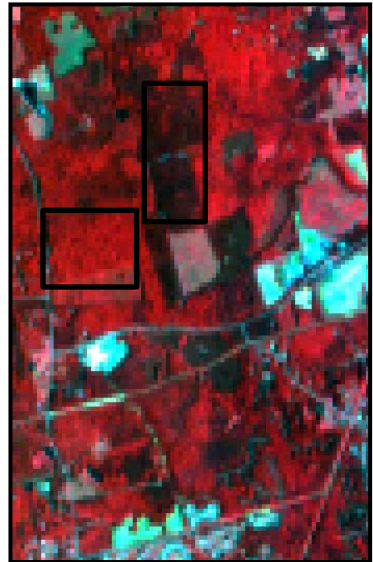


LP

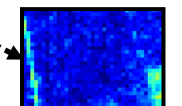


HW

B. Summer (DOY 203)



LP



HW

$y = 92.67x^2 + 44.73x + 7.24, R^2 = 0.70$

Elizabeth Middleton, Qingyuan Zhang, Biospheric Sciences, NASA GSFC

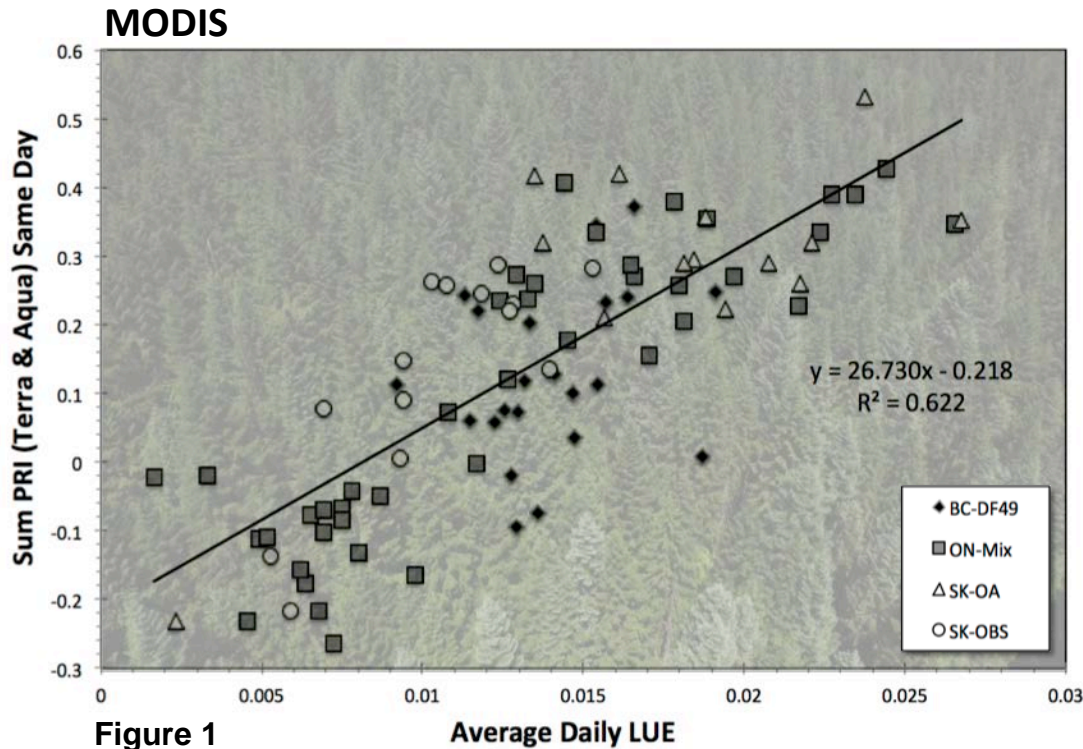


Figure 1

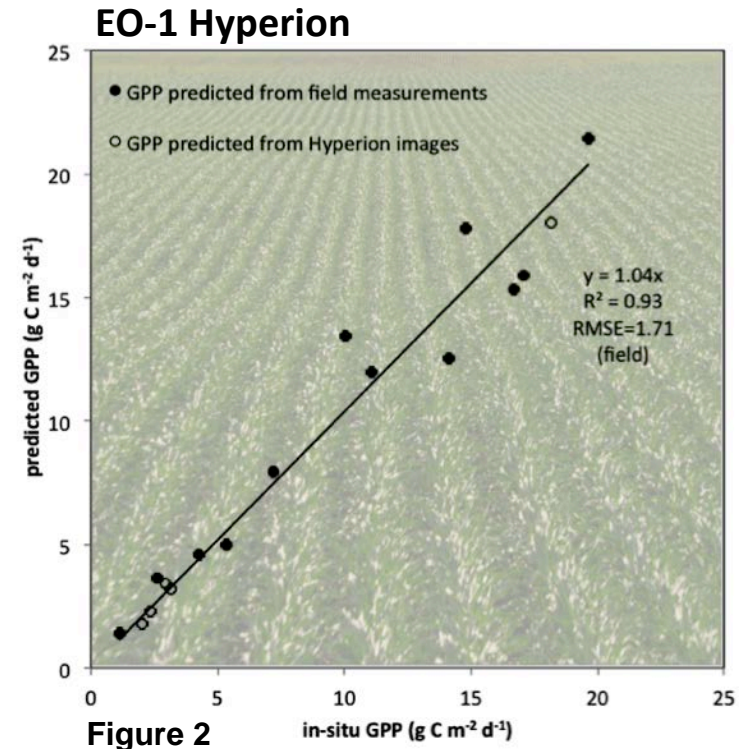


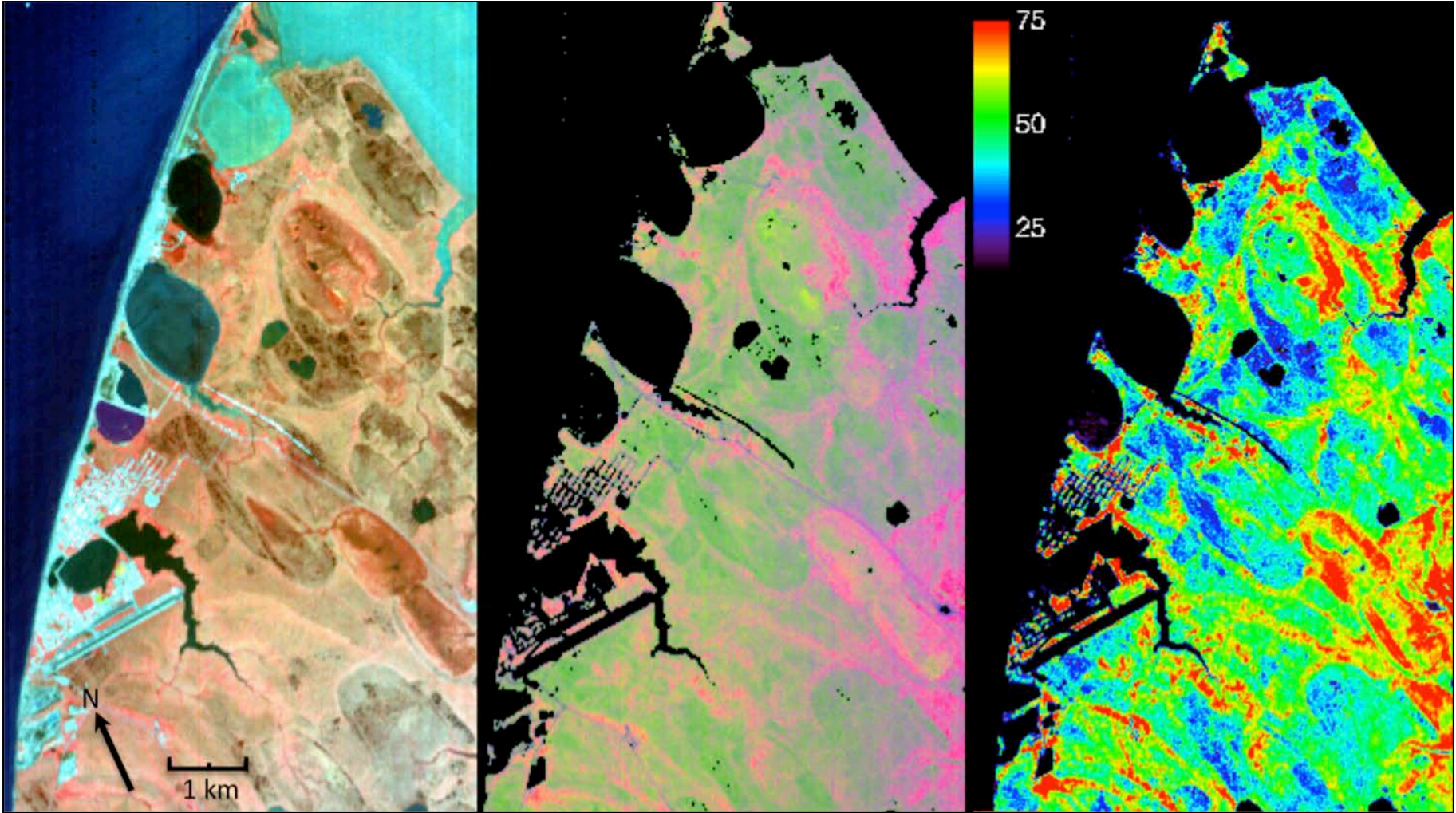
Figure 2

Our study highlights the value of off-nadir directional reflectance observations, and the value of pairing morning and afternoon satellite observations to monitor stress responses that inhibit carbon uptake in Canadian forest ecosystems.

We also demonstrate the potential capacity to monitor GPP with space-based visible through shortwave infrared (VSWIR) imaging spectrometers such as NASA's soon to be decommissioned EO-1/Hyperion and the future Hyperspectral Infrared Imager (HyspIRI) mission.

Hyperion Image of Barrow, Alaska

acquired on July 20, 2009



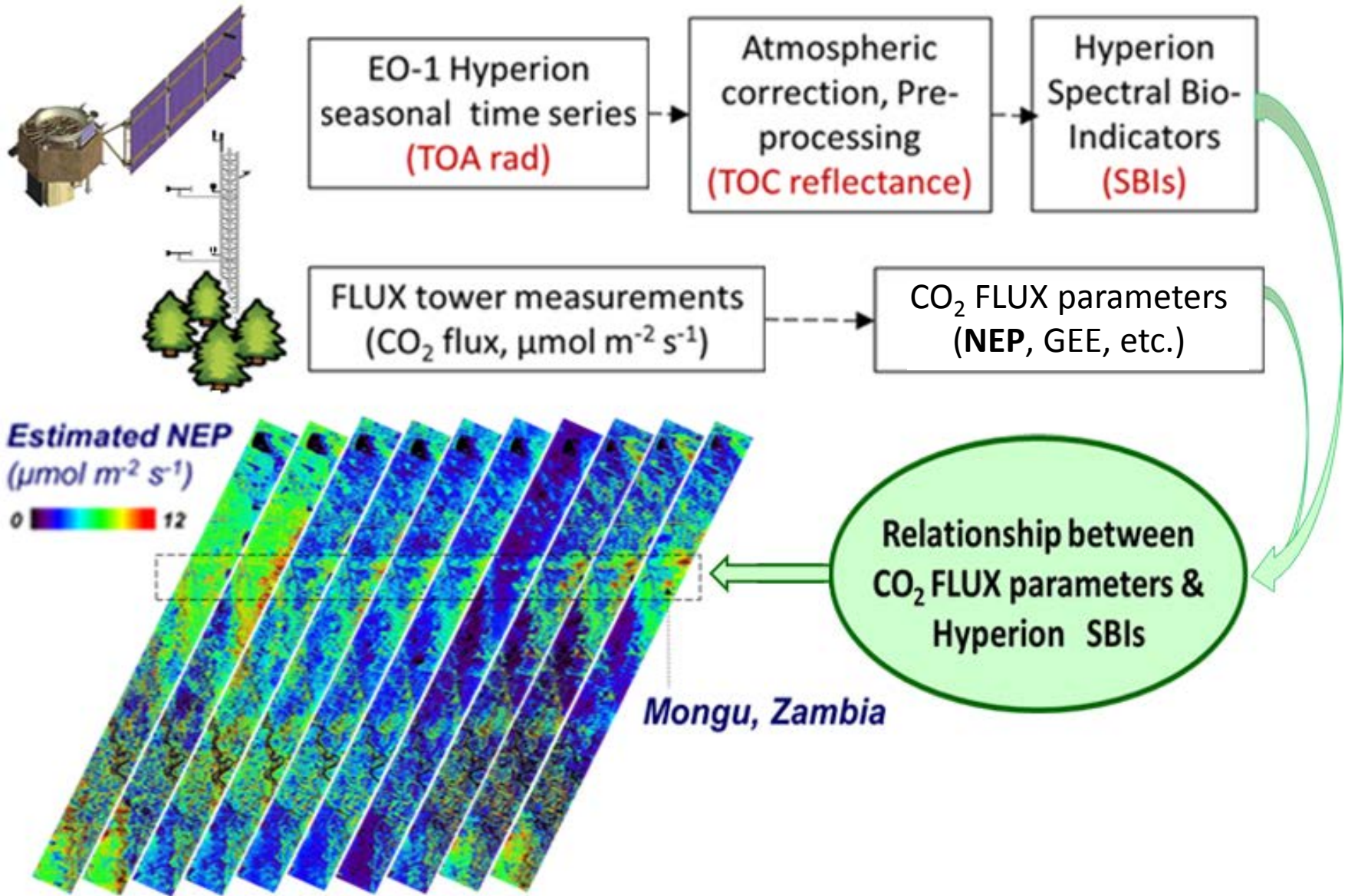
Left: 3-band (RGB=834, 671, and 549 nm) composite image of surface reflectance. The grid of light blue lines on the lower left is the city of Barrow. The straight blue line along the shore near the top of the image is the old airport runway. The oblong features scattered around the region are drained thermokarst lakes and the dark red ones are now marshes.

Middle: Three band RGB continuous fields of estimated coverage of vegetation types derived from spectral unmixing and scaled between 0 and 50% coverage. R = Vascular Plant Cover, G = Moss Cover, B = Lichen Cover

Right: Map of LUE spatial patterns ($\text{mol C mol}^{-1} \text{ quanta} \times 1000$) based on coverage estimates.

Collection	Scenes Total (<10% clouds)	Primary Sensor	Field Earth Observation Networks/Efforts
1 ABoVE	1367 (293)	ALI	Arctic-Boreal Vulnerability Experiment, NASA/TE
2 CEOS/WGCV	1022 (568)	Hyperion	The CEOS Working Group on Calibration & Validation
3 <u>FLUXNET</u>	9680 (3552)	Hyperion	Network of eddy covariance flux measurements of carbon, water vapor, and energy exchange
4 LTER	1181 (412)	ALI	The Long Term Ecological Network
5 NEON	973 (314)	Hyperion	The National Ecological Observation Network
6 SIEGEO	1125 (298)	Hyperion	The Smithsonian Institution Global Earth Observatory, ForestGEO
7 SpecNet	1245 (305)	Hyperion	SpecNet – Linking optical measurements with flux sampling
8 Volcanoes	19155 (3070)	Hyperion	Volcano SensorWeb, NASA/JPL
9 UNESCO-WCH Reserves	992 (172)	ALI & Hyperion	UNESCO World Cultural Heritage, Nature Reserves

A summary of the time series efforts conducted by the EO-1 mission team.



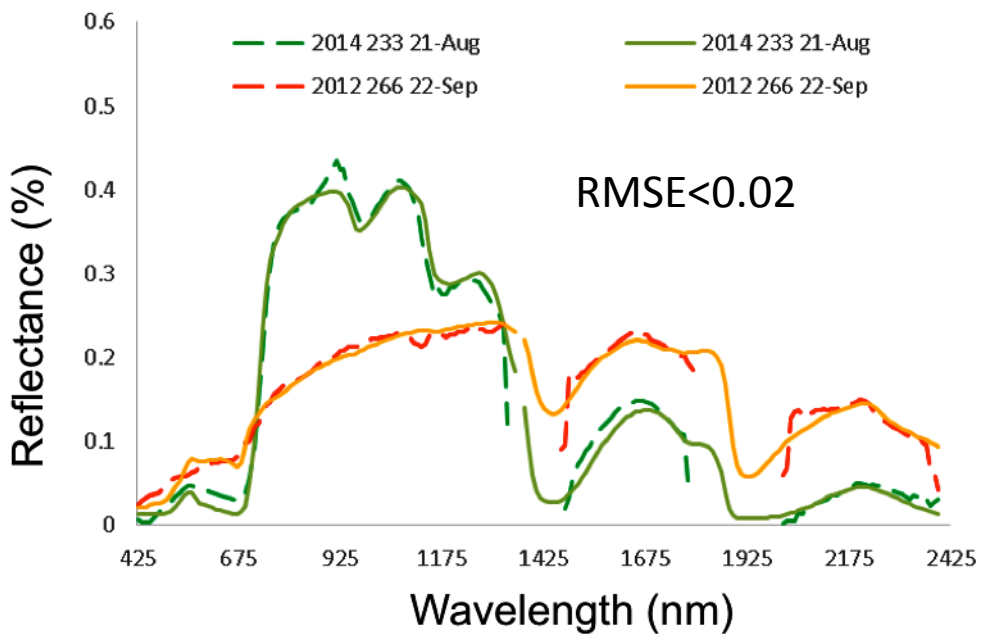
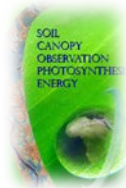
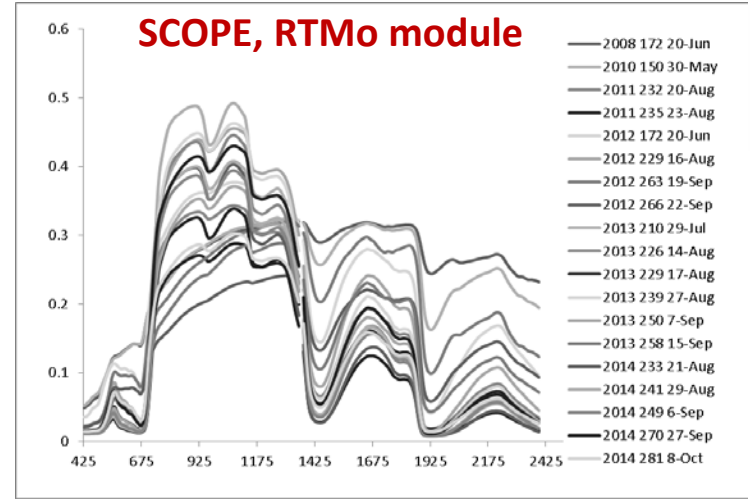
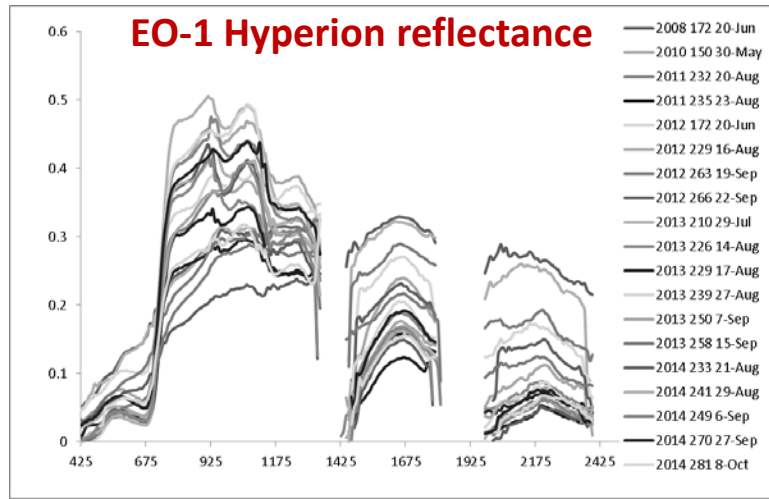
Hyperion data enable retrieval of net ecosystem production (NEP) utilizing spectral time series.



Hyperion's Reflectance Serves for Modeling Canopy Bio-physical Parameters (Traits)

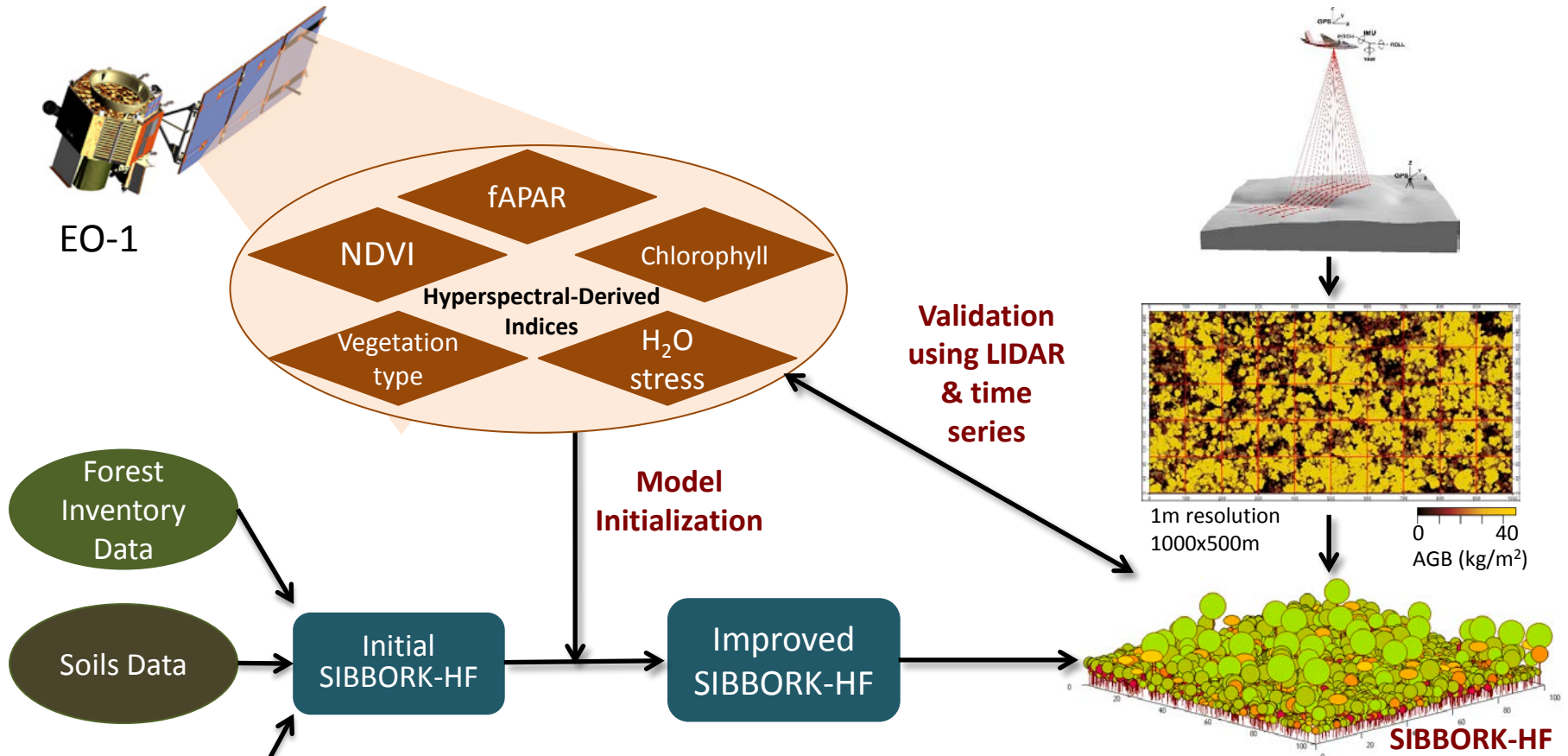


Measured -----> Simulated



RTMo (part of SCOPE) includes:

- 4SAIL - radiative transfer
- Fluspect' - leaf optical
- GSV - soil reflectance

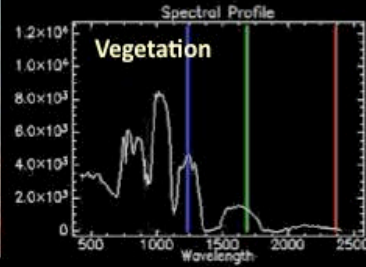
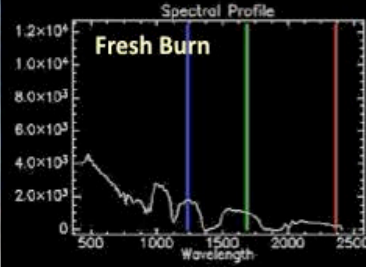
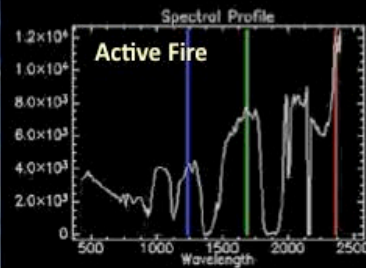
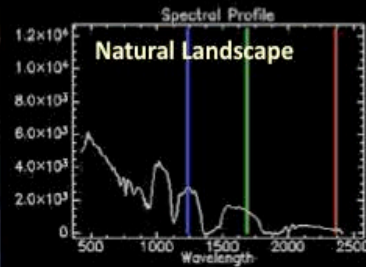


Study Objectives:

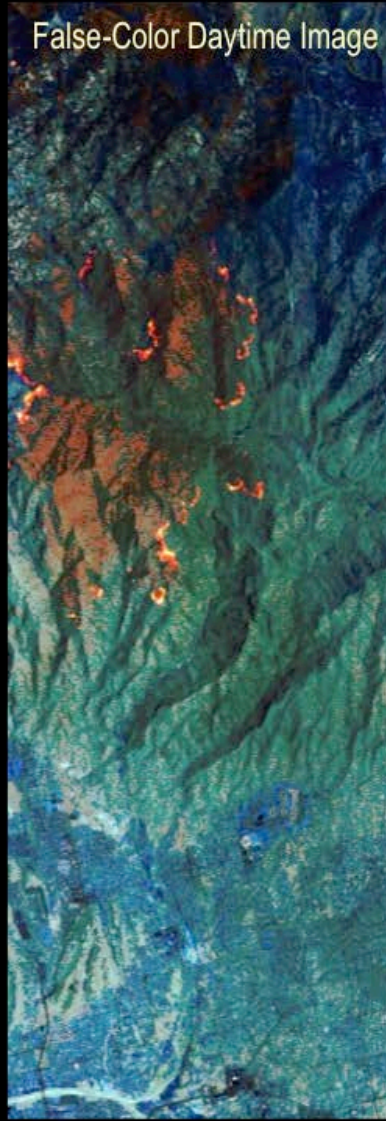
- Parameterize SIBBORK Model for Howland Forest, Maine (SIBBORK-HF)
- Use atmospherically corrected Hyperion data to derive vegetation indices across the Howland Forest (already collected 2001-2015, 56 total images)
- Compare indices (e.g. vegetation type, stress variables) with inventory data (calibrate at plot level, scale to Hyperion tiles)
- Test model parameterization with vegetation indices
- Validate Hyperion indices over time using LIDAR CHMs and modeled forest output raster datasets
- Demonstrate the effectiveness of hyperspectral data indices to initialize and improve models

Hyperion Image of the Tucson Wildfires – July 3, 2003

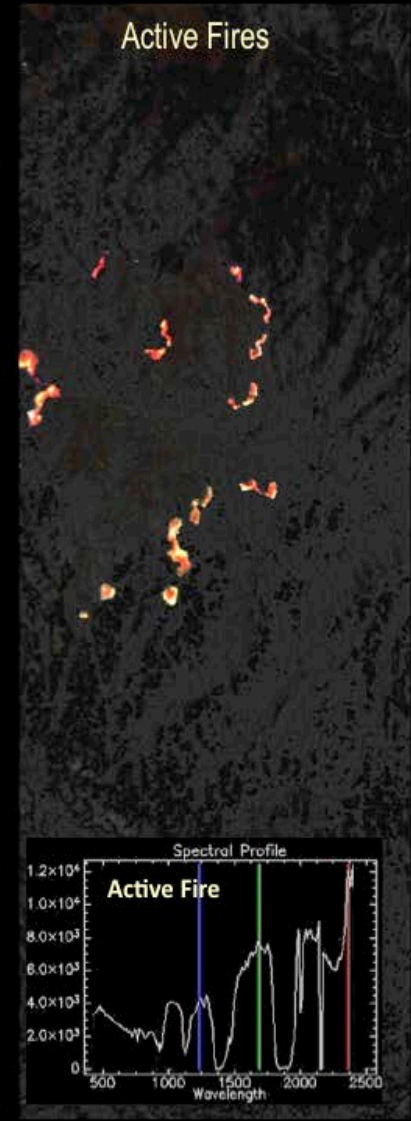
True-Color Daytime Image



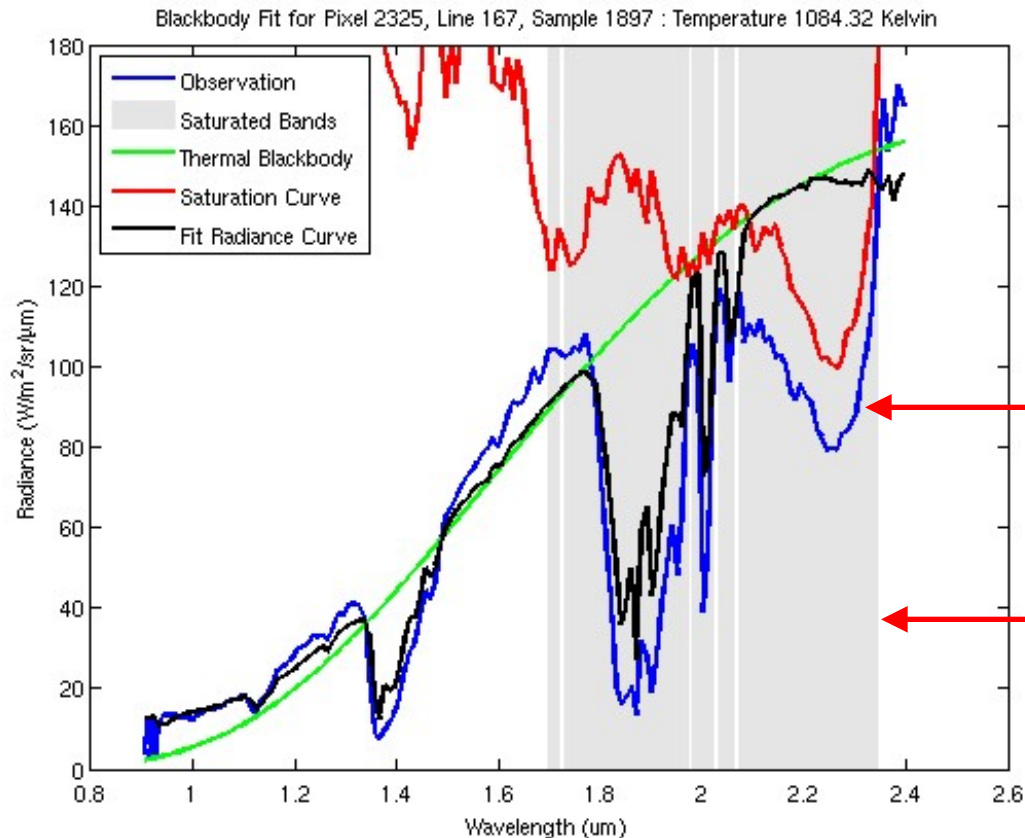
False-Color Daytime Image



Active Fires



- Hyperion is *great* for imaging erupting volcanoes
- Wavelength range is sensitive to pixel brightness temps >450 K

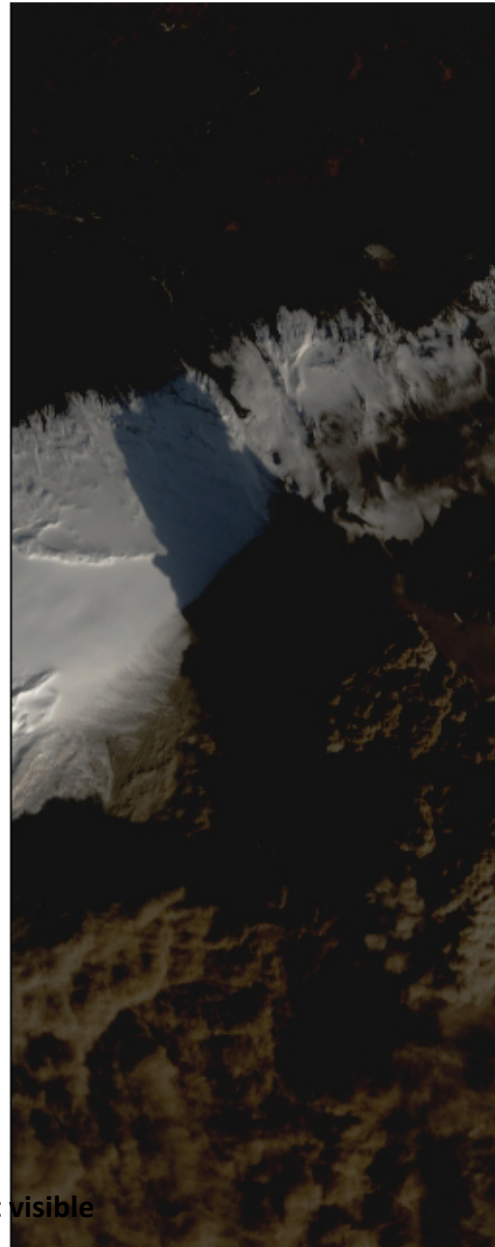
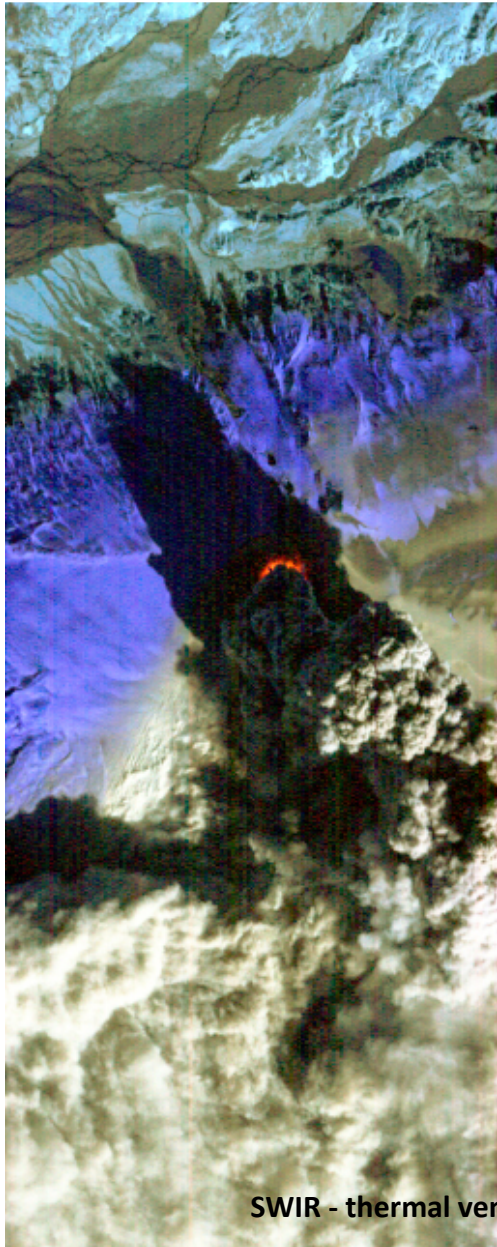


“dip” =
saturation
feature

Grey area
= saturated

If data are saturated at longer wavelengths, shorter wavelengths are usable for fitting black-body curves: see Wright *et al.*, Davies *et al.* pubs.

EO-1 Hyperion Imaging of Eyjafjallajökull Volcano Eruption, April 17, 2010



VIS - plumes coating everything to the South-East making the ice brown/gray

SWIR - components are separated.

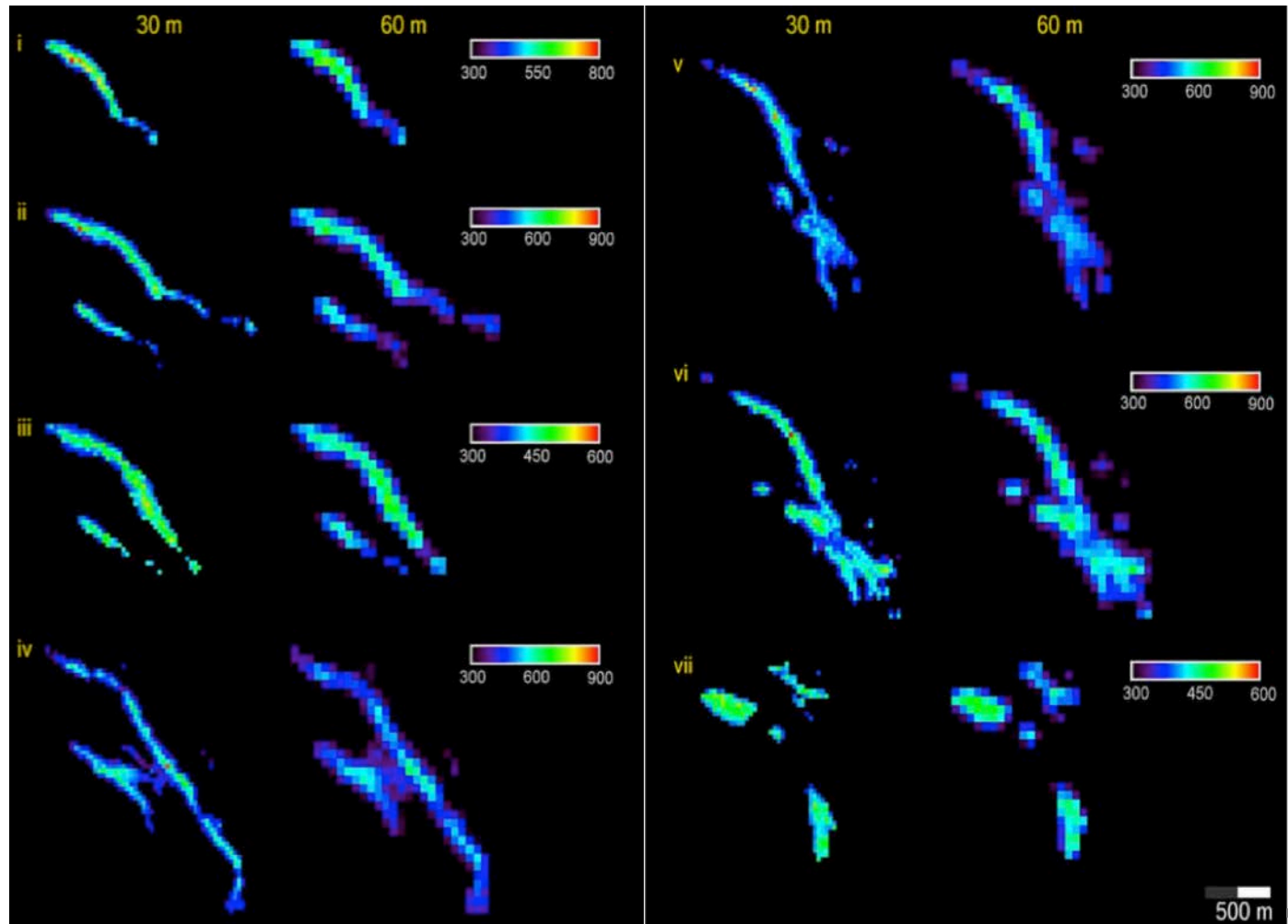
A future **TIR** imager will make daily passes at latitude of Iceland

Using EO-1 Hyperion Data as HypsIRI Preparatory Data Sets for Volcanology Applied to Mt Etna, Italy

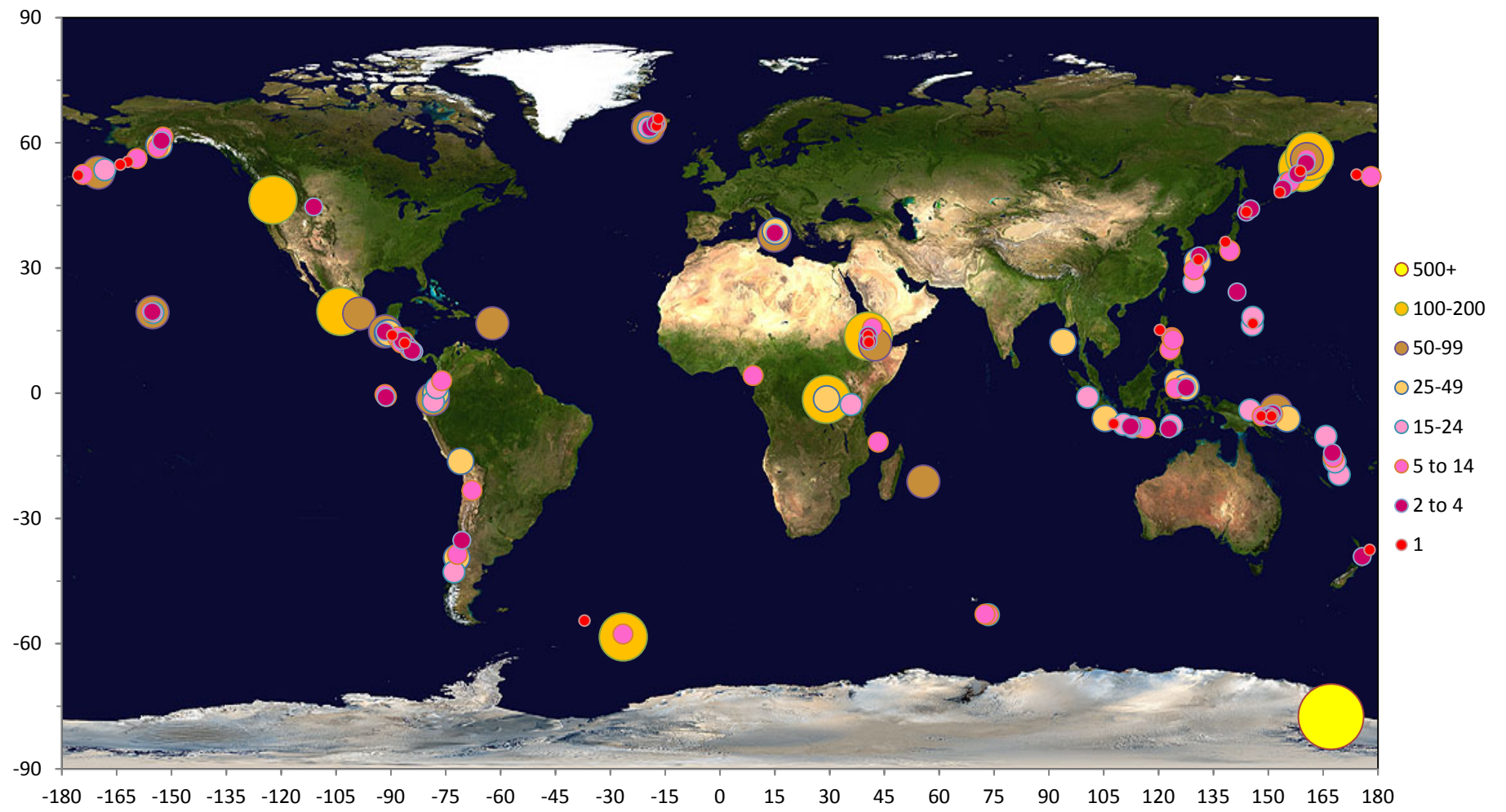
Michael Abrams, Dave Pieri, Vince Realmuto, and Robert Wright

Time Sequence- 7 images:
Lava flows at Mt. Etna, Sicily using the 4- μm band.

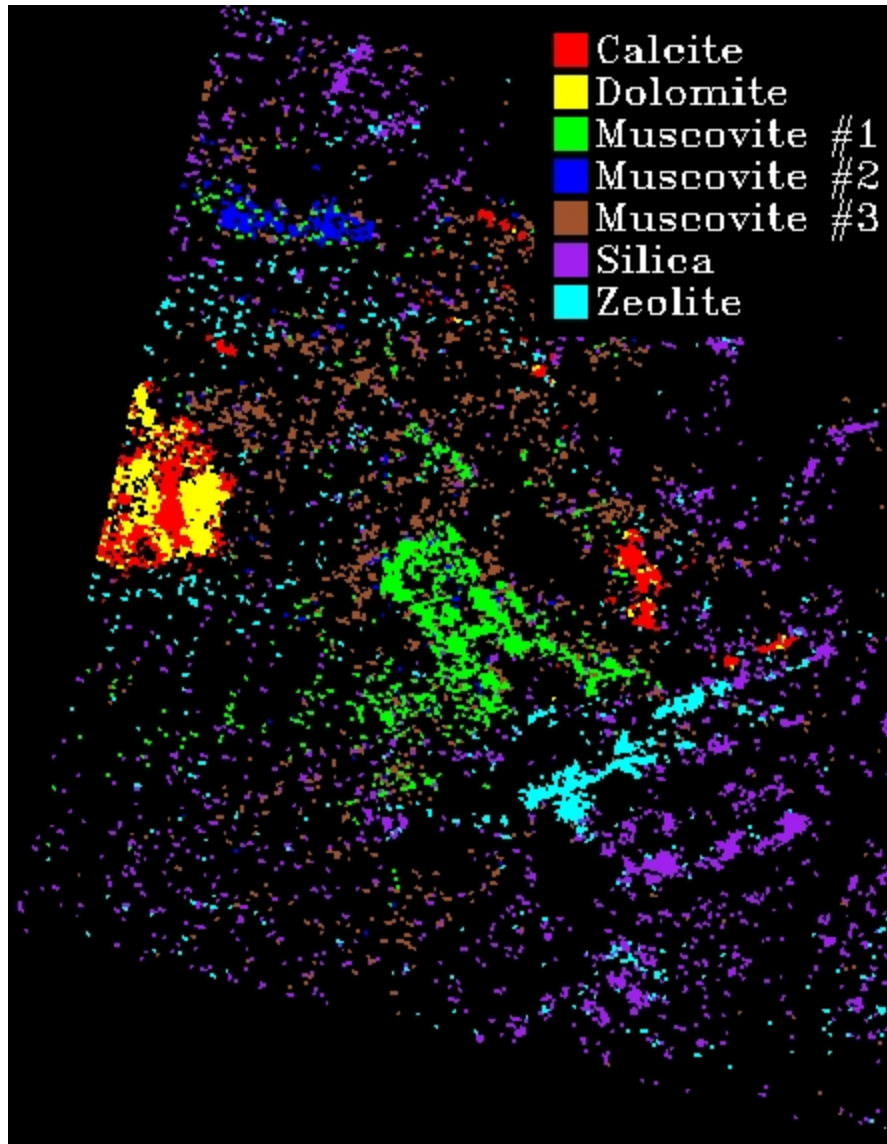
Each native 30-m Hyperion resolution image is paired with a simulated HypsIRI TIR 4- μm image (60 m). Color bar gives the 4- μm brightness temperature for each pixel ($^{\circ}\text{Kelvin}$).



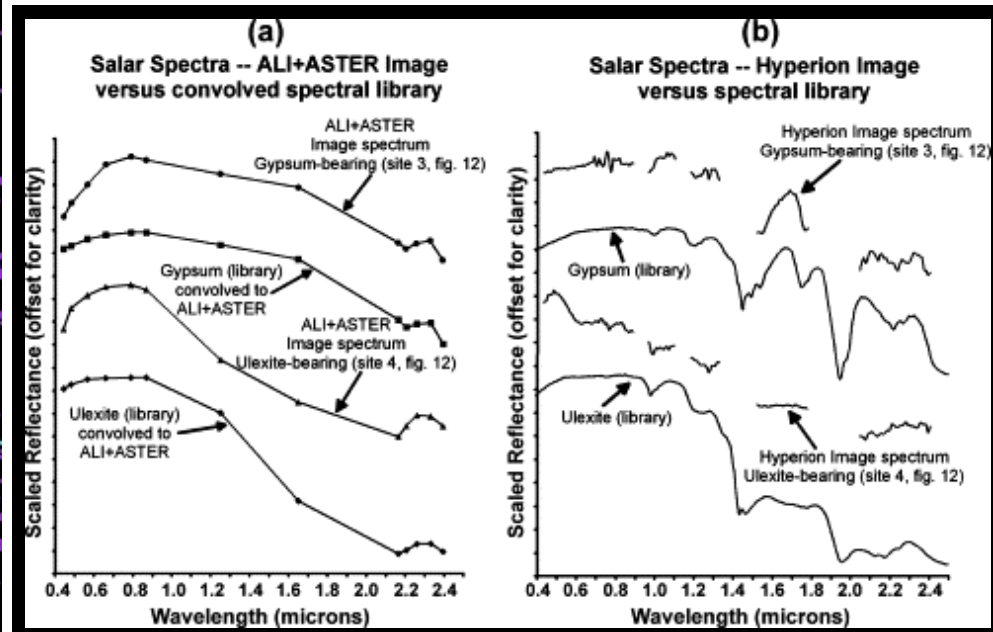
Hyperion images used to generate these results were acquired on (i) 12 Sep 2004, (ii) 14 Sep 2004, (iii) 16 Sep 2004, (iv) 23 Sep 2004, (v) 7 Oct 2004, (vi) 9 Oct 2004, and (vii) 3 Dec 2004.



Total: 4956, including: 576 Erebus; 171 Mt St Helens; 89 Erta 'Ale; 82 Etna



An example of Hyperion's mineral mapping capability relying on full spectrum hyperspectral imaging from 0.4 to 2.45 μm .



- ❑ Hyperion has been useful in developing techniques for future global applications for missions such as HypSIRI, PACE, and GeoCAPE.
- ❑ Hyperion data were collected in Sept 2015 to support research cruises near the the Florida Key to further hyperspectral algorithms (see the next slide).
- ❑ Lunar observations with Hyperion could be valuable in improving consistent calibration techniques across NASA's ocean color climate data record.

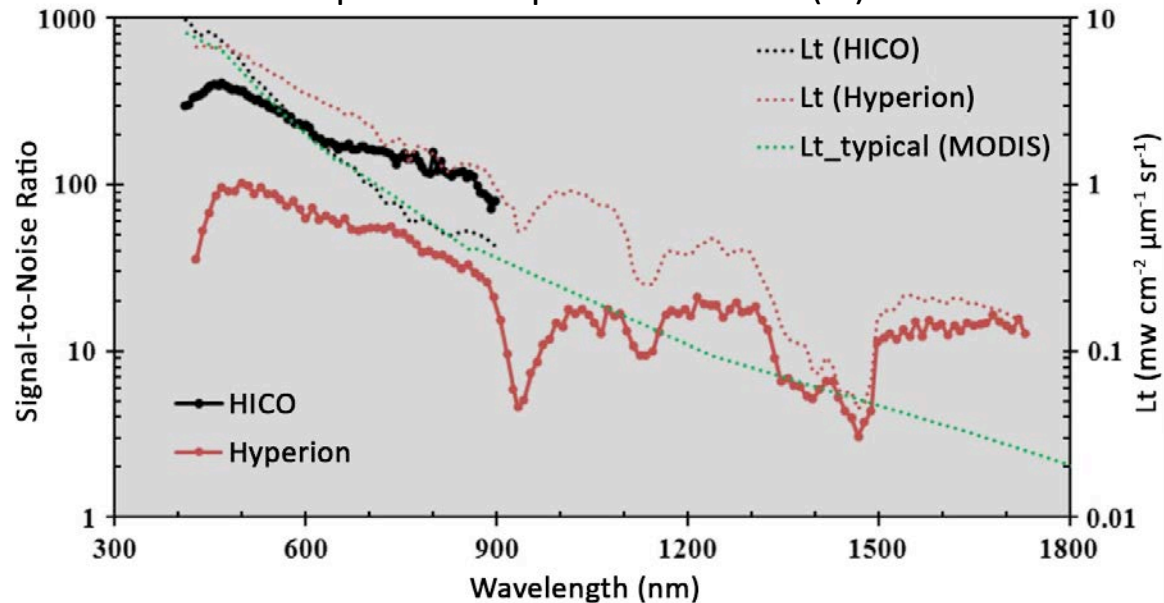
SHALLOW/TURBID WATER FOCUS

Hyperion spatial and spectral resolution is useful for coastal and inland aquatic applications.

Hyperion Signal-to-Noise Ratio (SNR) is lower than the Hyperspectral Imager for the Coastal Ocean (HICO).

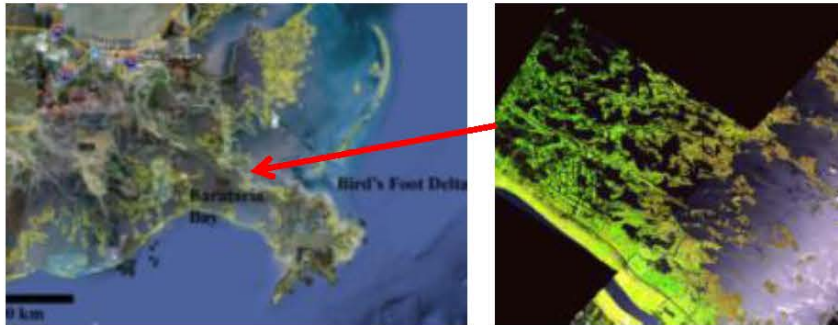
So, spectral (or spatial) aggregation is necessary for the dark water of the open ocean.

Top-of-Atmosphere Radiance (Lt)

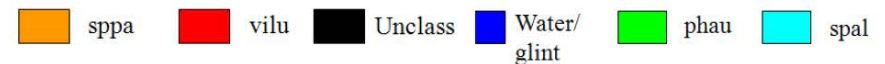
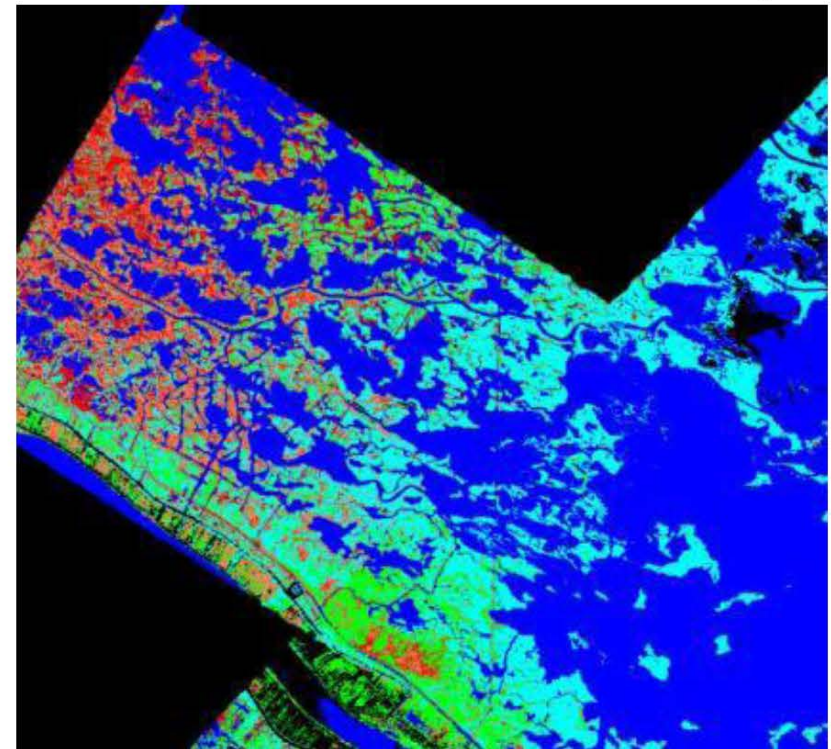
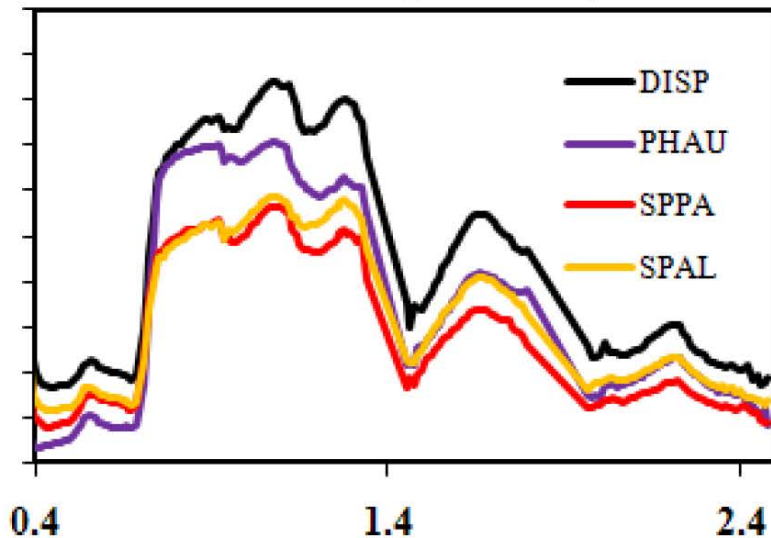


Imaging Spectroscopy Measuring Species Type in Marshlands

D. Roberts, UCSB



AVIRIS Vegetation Spectra

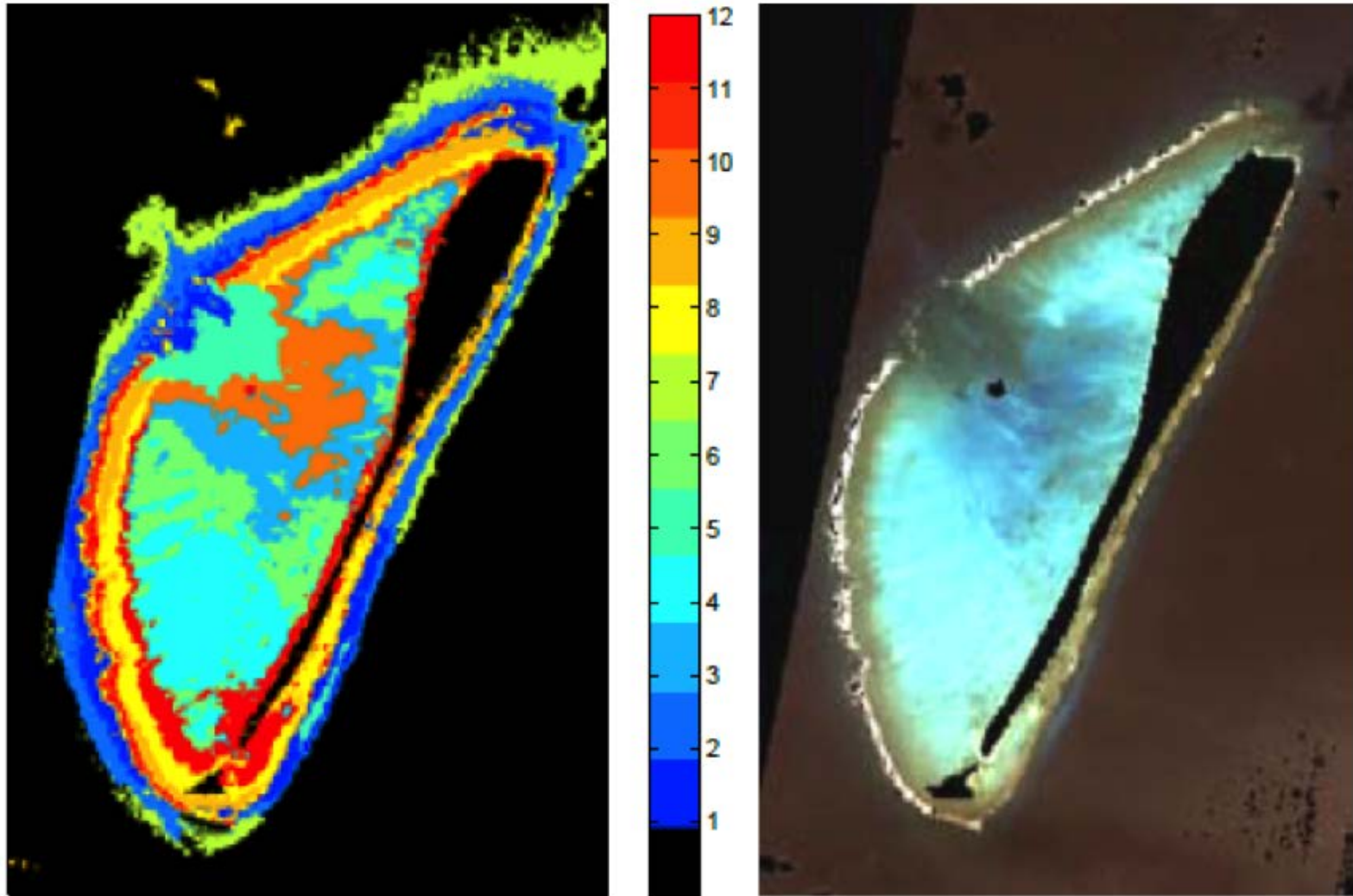


Vegetation mapped cleanly across scene boundaries

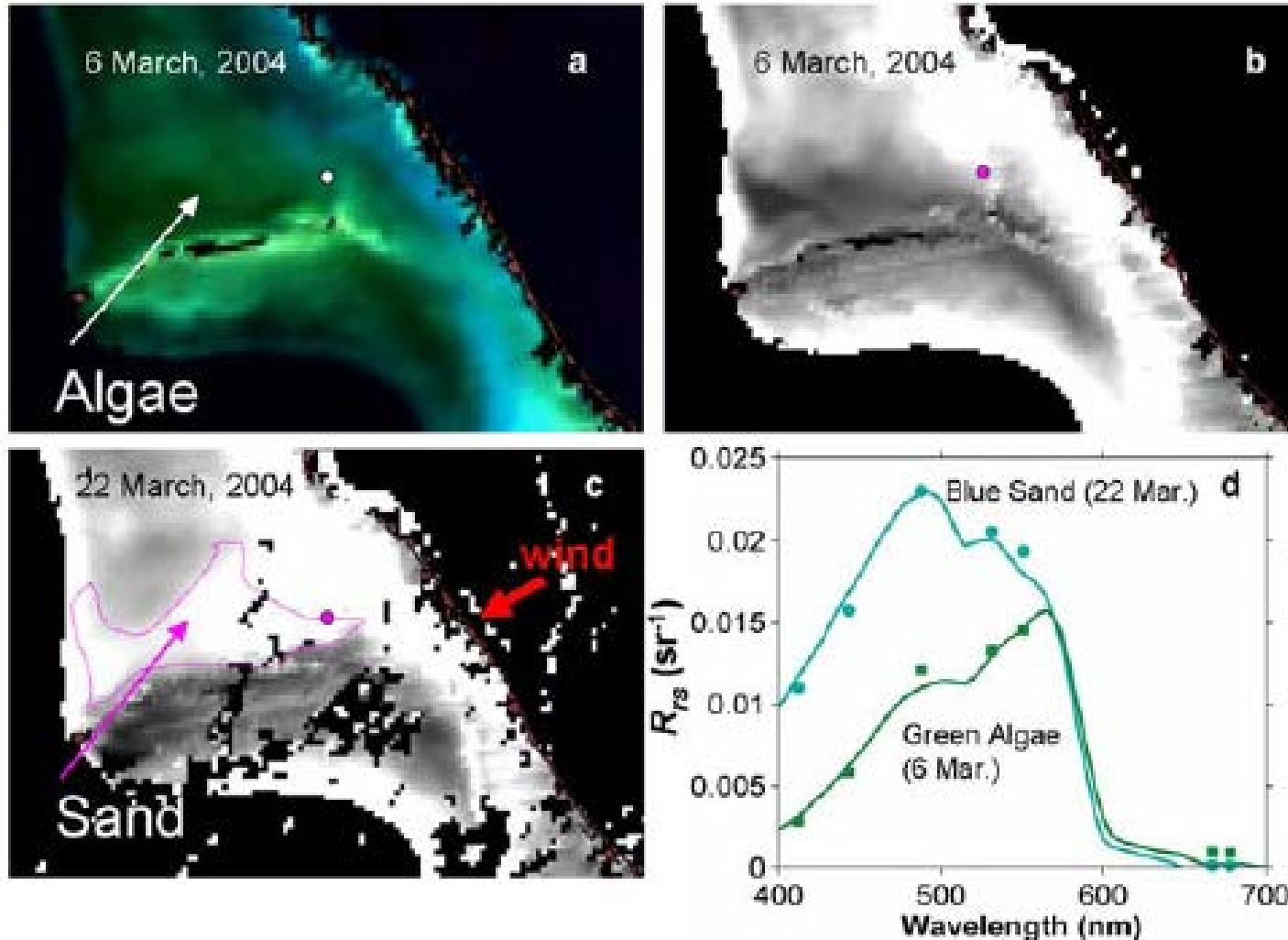
- *Phragmites (phau)*
- *Spartina alterniflora (spal)*
- *Spartina patens (sppa)*
- *Vigna luteola (vilu)*

True "Remote Measurement" with Spectral-Shape [Chemistry]

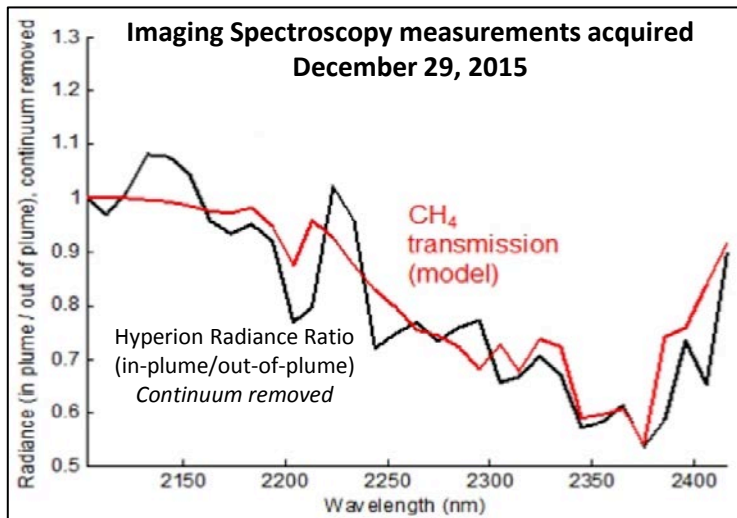
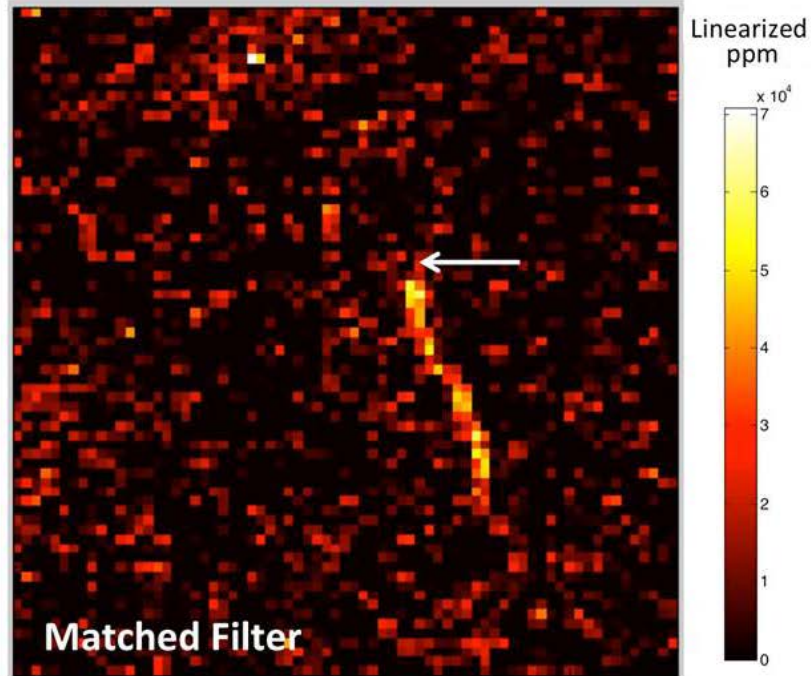
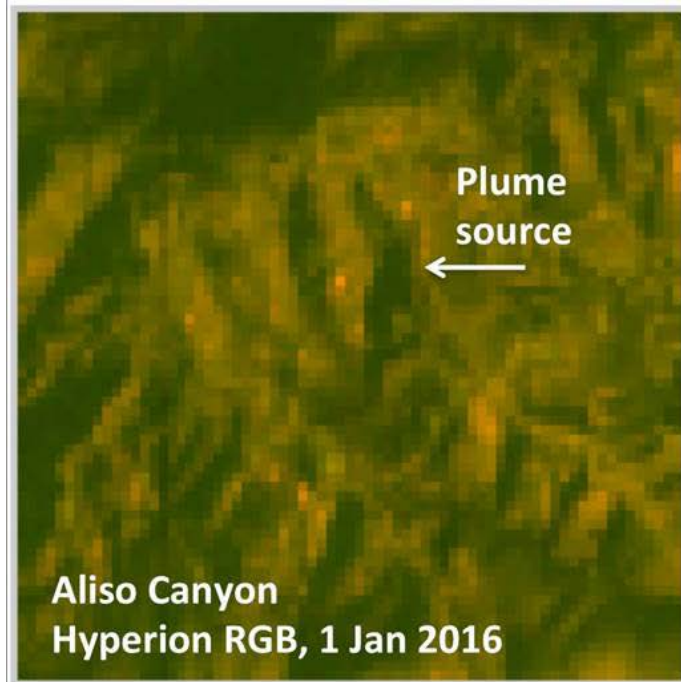
Classification for Agatti Island, India



EO-1 Hyperion k-Means classification for Agatti Island, India, where the classes are represented as 1 and 2: Reef Slope; 3: Intermediate Lagoon; 4: Sand Sheet; 5 and 10: Deep Lagoon; 6 and 12: Shallow Lagoon; 7: Submerged Reef; 8, 9 and 11: Reef Flat.



Pulsed export of $>7 \times 10^{10}$ g of carbon directly to seafloor (negatively buoyant). This is equivalent to the daily carbon flux of phytoplankton biomass in the pelagic tropical North Atlantic and 0.2–0.8% of daily carbon flux from the global ocean.



On January 1, 2016, Hyperion imaged the massive methane leak in the Aliso Canyon region of California. David Thompson's (JPL) algorithm detected the methane leak within the Hyperion data and showed a pronounced plume trending to the south. Since then, six additional acquisitions have been made, thanks to EO-1's ability to rapidly schedule, reorient satellite attitude, and quickly process and distribute the data.



Experimental Intelligent Payload Module Quick Load/Quick Look Ops Con



Web Coverage Processing Service (WCPS)-Client

Uploads to Various Environments

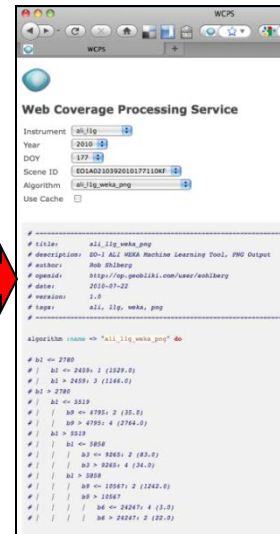
Create Custom Algorithm

SCIENCE USER



Machine Learning
Supervised Classifier
(Regression Tree)
Refined Offline

Custom Algorithm



Quick algorithm upload



GlobalHawk,
Ikhana, ER-2 ...

Lua Scripts

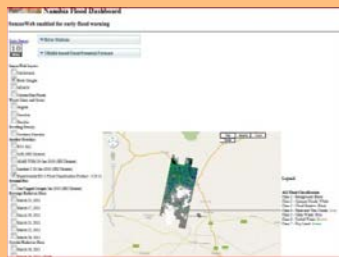


NASA Cloud
Infrastructure As
A Service

WCPS-Runtime

Executes
Algorithm
Against Selected
Sensor Data

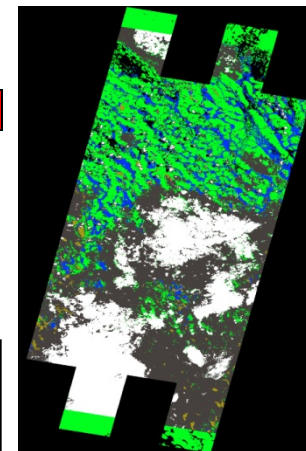
Cloud



Quick look data products



Notification
to user



Custom Data Product
(KMZ, PNG...)



EO-1 Data Products



Standard **EO-1 Level 1** data products are currently distributed **by USGS** (EarthExplorer Website <http://earthexplorer.usgs.gov/>) as 16-bit scaled radiance values. These data are available for free.

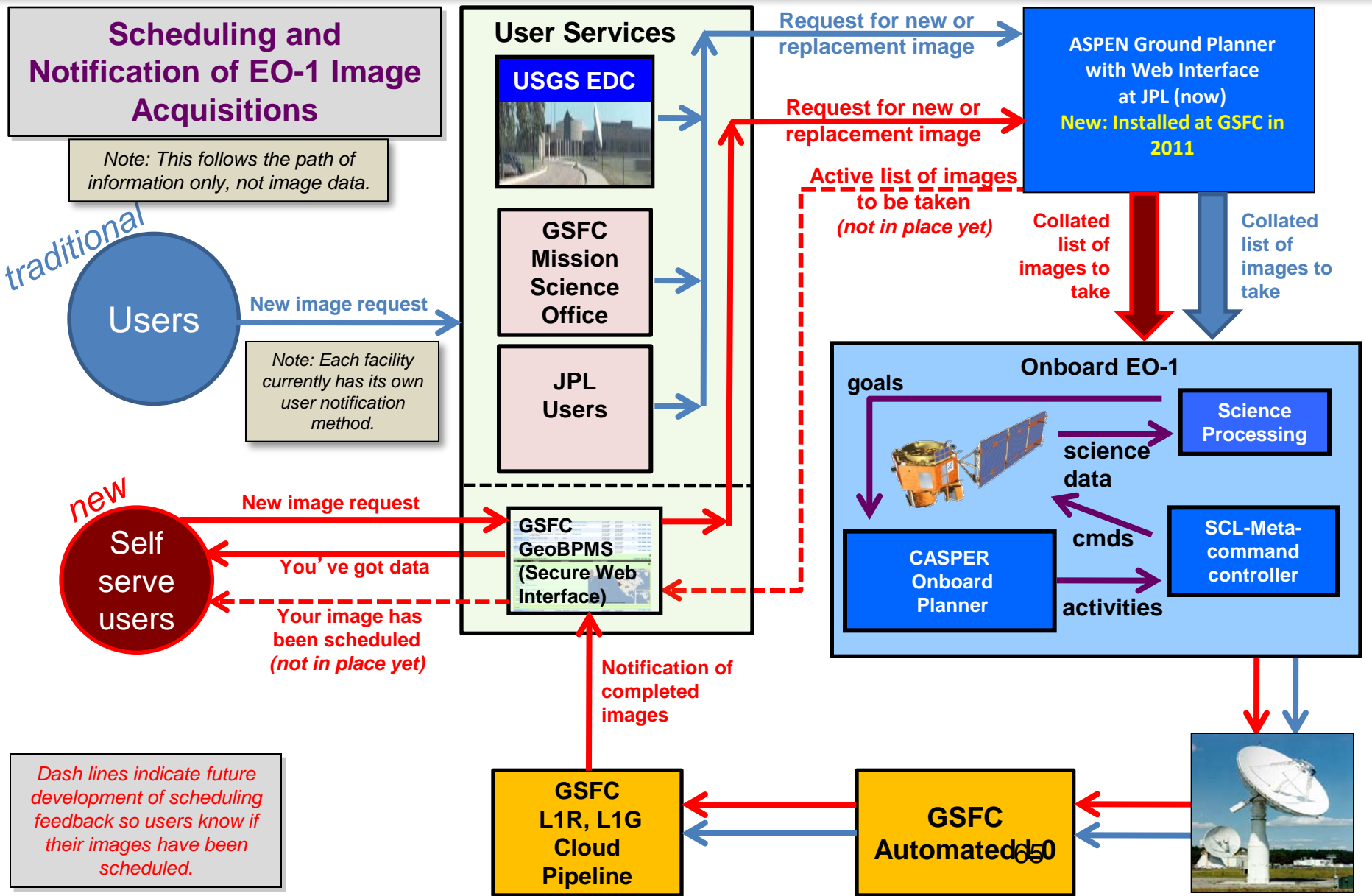
- Level 1R , Hyperion and ALI: *Radiometrically* corrected
- Level 1G, ALI: *Geometrically* corrected to Earth spheroid
- Level 1Gst, Hyperion and ALI: *Geometrically and terrain* corrected through use of a Digital Elevation Model (DEM)
- Level 1T, Hyperion and ALI: Co-registered with Landsat Global Land Survey (Landsat GLS), only available for cloud-free images

New **EO-1 Level 2** data product prototypes (access limited):

- All Hyperion Level 1R images are atmospherically corrected automatically using FLAASH. Products are available for 2014-2016.
- Previous years of data (Level 1 & 2 products) will be added as the Matsu Cloud adds additional storage hardware.
- Fire (detection, severity and temperature); Flood (extent, water quality) for first responders.
- Final archive and access location of these data products: TBD



Ways to Access EO-1 Imagery



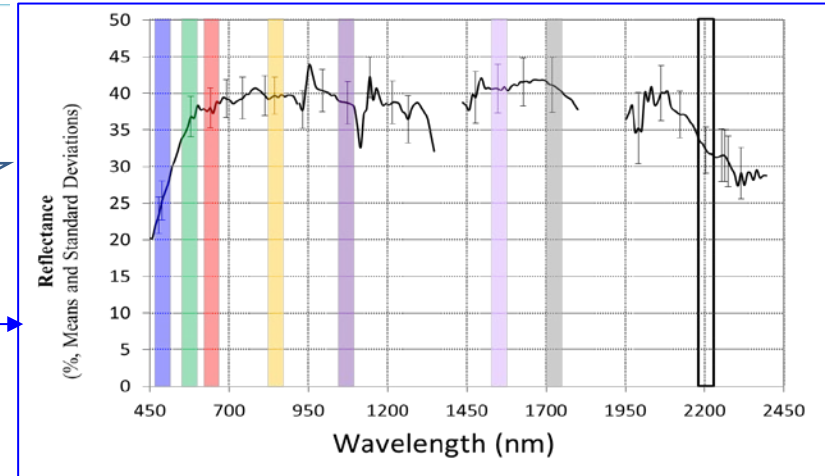
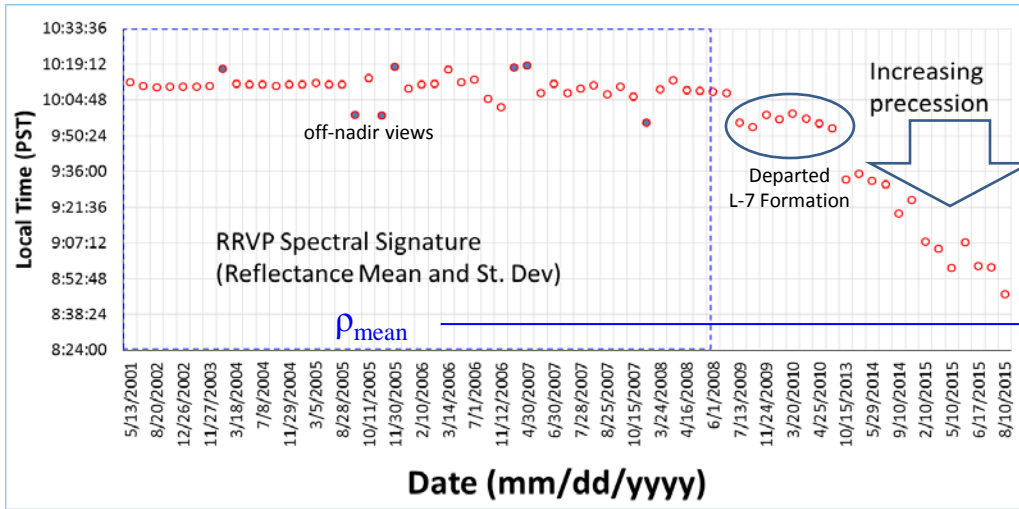


EO-1 Hyperion Reflectance Stability During Increased Precession at Railroad Valley Playa (RRVP)



EO-1 increased precession started in 2011. Acquisition time at RRVP declined from 10:05 to 8:40, approximately.

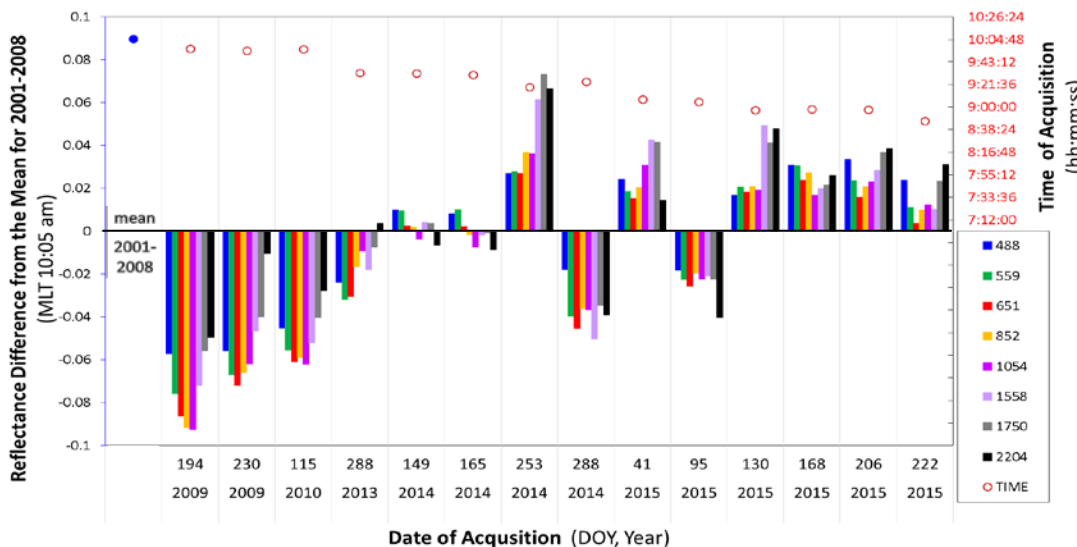
Mean reflectance and standard deviation for RRVP (2001-2008 data, n=15, ~10:05 am MLT acquisition)



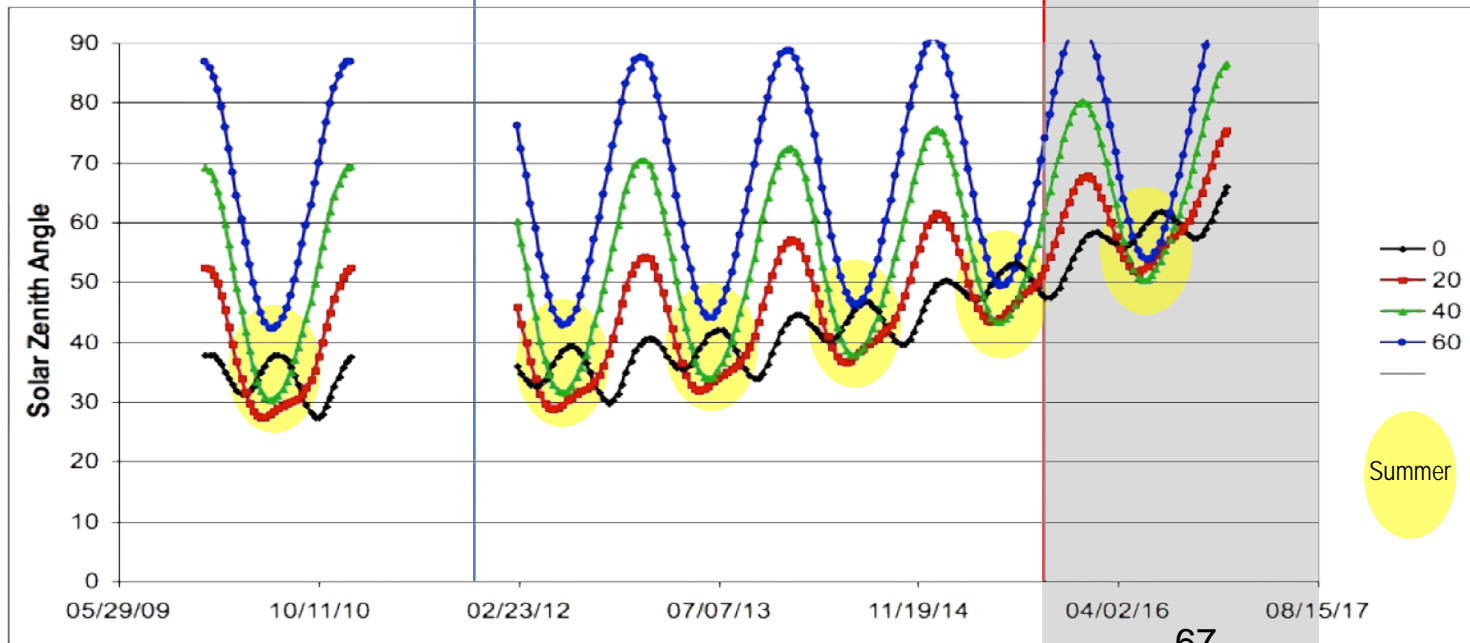
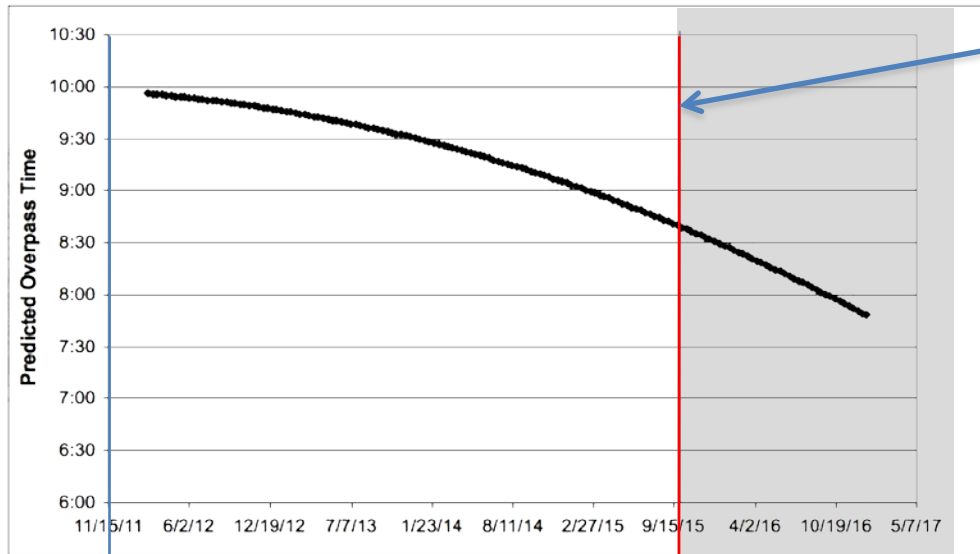
Change in reflectance anomaly ($\Delta\rho$) at select wavelengths at RRVP

The difference in reflectance continues to be within $\pm 5-9\%$ of the mean prior to Δ precession.

The regions of highest spectral stability (e.g. green, red edge, NIR) remain the same.



- Equatorial image data are always usable, even in 2016. And even then, higher-latitude image data could still be acquired in the summer months.
- The seasonal change in SZA is much larger than the change due to EO-1's orbital decay.

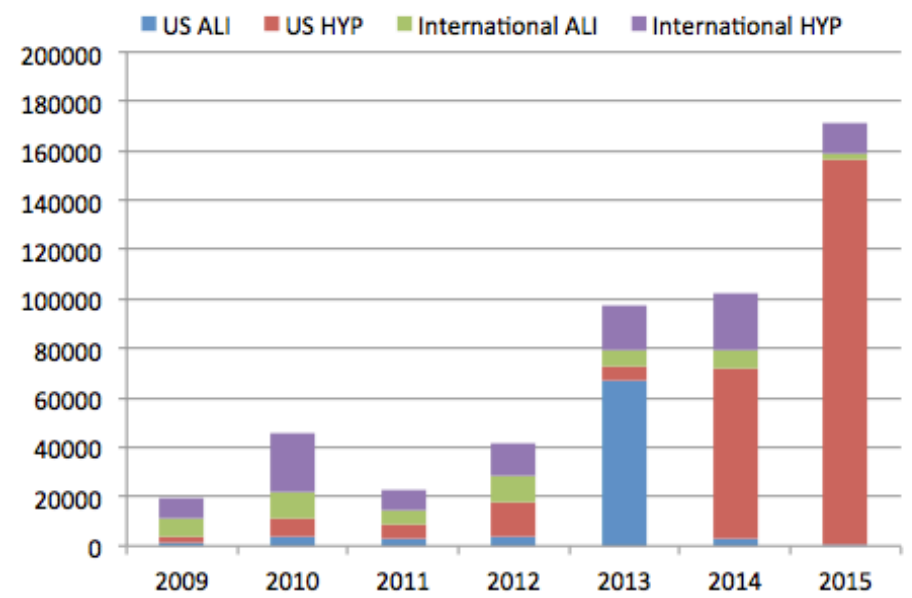
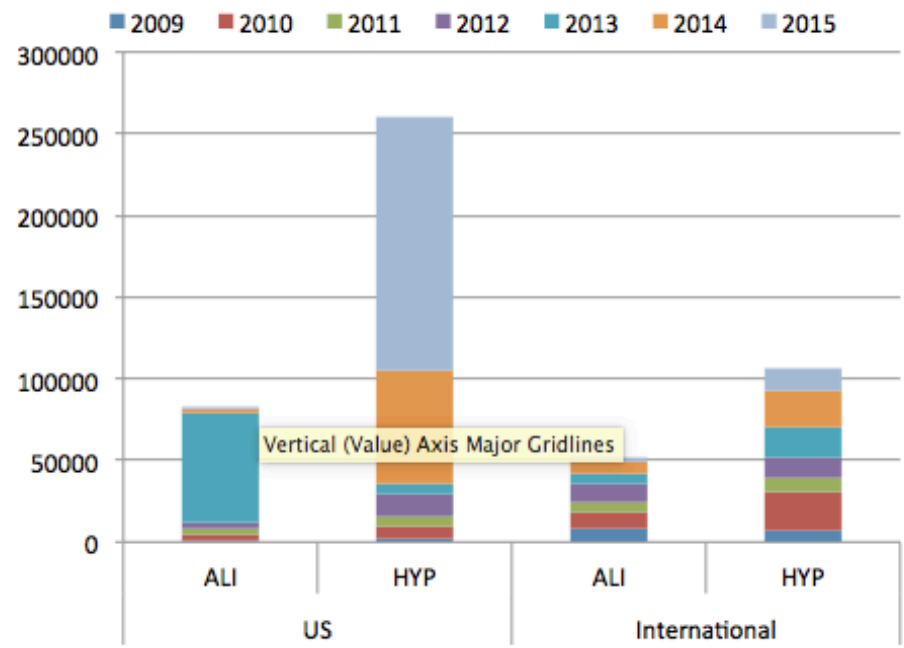




The EO-1 User Community

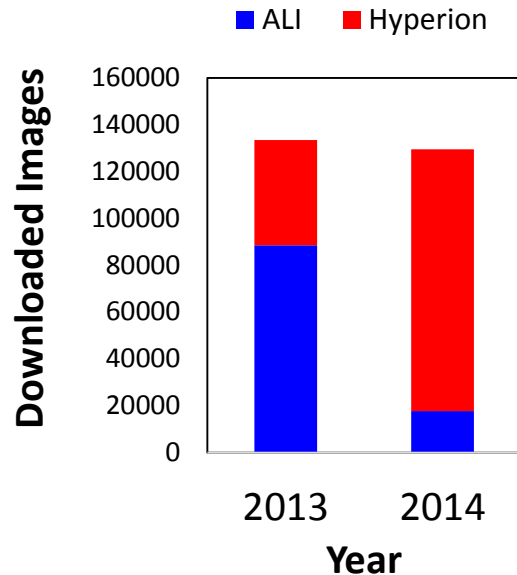


		2009	2010	2011	2012	2013	2014	2015
US	ALI	1276	3818	2980	3737	66704	2854	723
	HYP	2503	7363	5901	13679	6165	69003	155765
International	ALI	7748	11055	5895	10844	6543	7196	2150
	HYP	7572	23156	7984	13339	17792	23276	12807



USGS Accomplishments for EO-1:

- In the 2012 time frame, USGS released the new L1T product along with the "GIS Bundle" allowing for users to download 3-band, GIS-ready JPEG bundles of the imagery.
- In 2013, USGS introduced the Bulk Download Application (BDA) tool which allowed users to download data through a GUI with little to no interaction.
- In 2014, USGS created a Machine-to-Machine (M2M) interface that allowed authorized users the ability to script downloads while still allowing metrics to be captured. In addition to M2M, USGS also saw a larger increase in the demand of bulk media copies, where users sent in hard drives and the entire USGS EO-1 collection was copied and sent back to them.



- There was a large drop in ALI downloads from 2013-2014 after Landsat 8 became available, but there was an equally large increase in Hyperion downloads in 2014.
- For the Global Land Survey 2010, EO-1 collected a large number of islands and shallow water bodies, which are currently of interest for aquatic studies.

Level of effort to support ALI vs. Hyperion – 50/50, the level of acquisition support effort is equal because both instruments are ON during every collect, and different for post-processing, depending on the output product produced.

Larger EO-1 users include: The disaster support, “cloud prediction support” study for GeoCape (Decadal Survey Mission), EnMAP pre-launch support (Hyperion), Landsat 8 support, Sentinel-2, science requests for time series and/or large scale mapping for: mineralogy, tropical spectral diversity, terrestrial ecology, signal processing, and simulations for HypIRI, Sentinel-3, and EnMAP.



Unique Functions of EO-1

now not available for NASA



- Globally distributed hyperspectral Hyperion measurements (@ 10 nm) in the visible through shortwave infrared (VSWIR) at 30 m for Earth surface types (e.g., ice, snow, evergreen & deciduous forest, grasslands).
- Albedo determined across full Hyperion VSWIR spectrum for satellite calibrations, now based on Sentinel-2.
- Time series at vegetated validation sites (especially w/flux towers);
 - Spectral characterization of CEOS LandNet calibration sites (e.g., DOME-C, Libya);
 - High dimension spectral data that enables machine learning & data mining approaches to relate spectra to ecosystem characteristics and processes.
 - Spectral reflectance indices for plant pigments and stress are not available (e.g., the Photochemical Reflectance Index, PRI, which uses narrow wavebands at 531 and 570 nm).
- Temperature estimates from Hyperion based on emitted radiance spectra at 30 m (fires, volcanoes). When “hot” pixels were detected at night, the AI system autonomously scheduled additional collections at the same site.
- EO-1 had pointing ability to increase collections (up to 5 in 16 days) for disaster support. EO-1 led the automated collaborative collections among satellites for disaster monitoring.
- Capability to provide a testbed for flight and sensor-web software from EO-1’s flexible platform. Maneuverability of the whole platform for technology evaluations.

EO-1: Request for Mission Extension

Elizabeth M. Middleton

**EO-1 Mission Scientist 2007- present
Biospheric Sciences Laboratory, NASA GSFC**

Daniel J. Mandl

**EO-1 Mission Manager 2000-present
Software Systems Engineering Branch, NASA GSFC**



**Stuart W. Frye
Lawrence Ong
Stephen G. Ungar
Petya E. Campbell
K. Fred Huemrich
David R. Landis**



March 23, 2015





EO-1 Mission Extension



We request an extension of EO-1 because:

- In spite of orbital changes, EO-1 provides unique and valuable data to the science & applications communities and supports SLI, HypsIRI, & future mission development.
 - Rapid response
 - Hyperspectral imagery
- The risks are low
- The costs are low

EO-1 Celebration

June 7, 2017

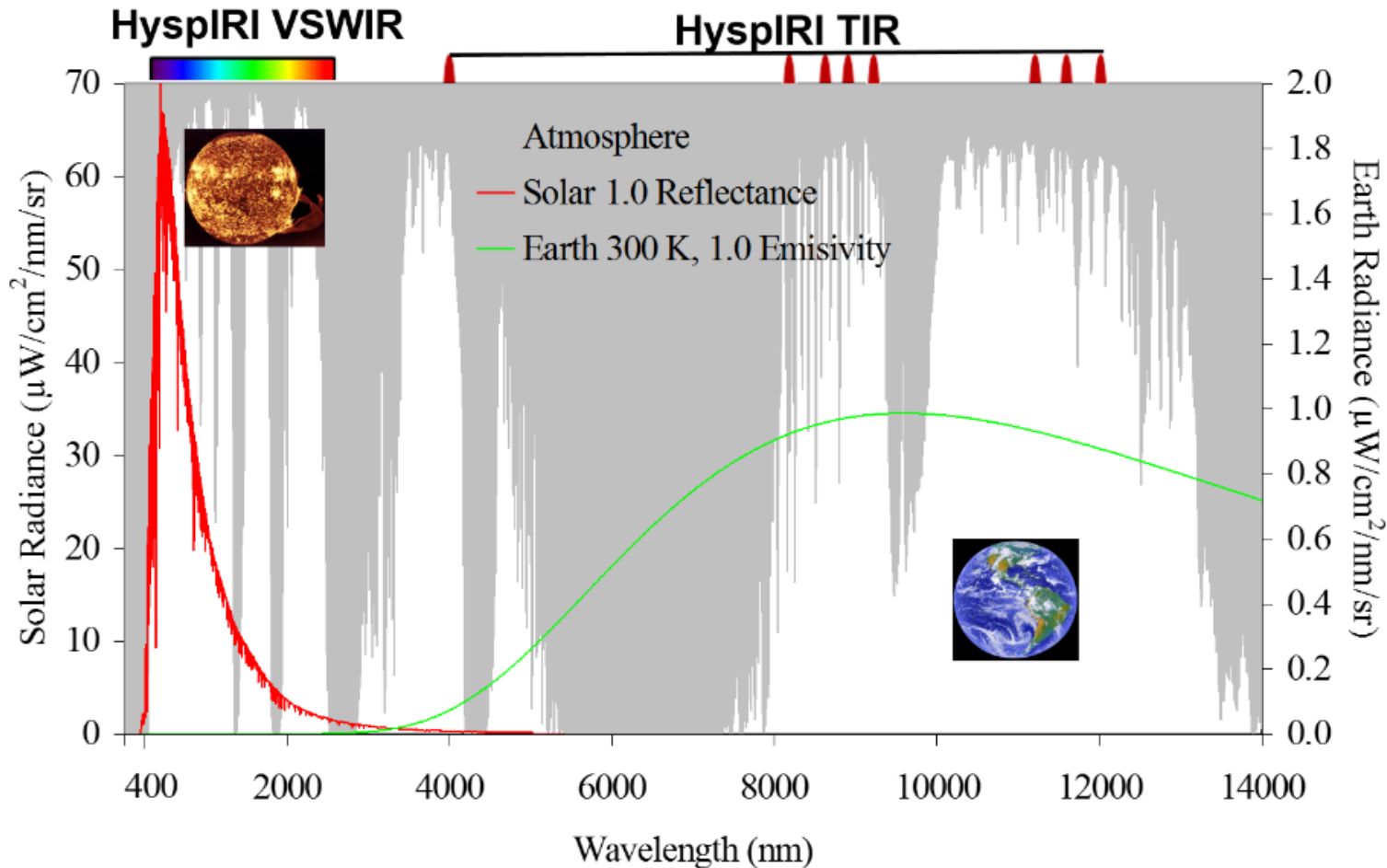
THANK YOU!



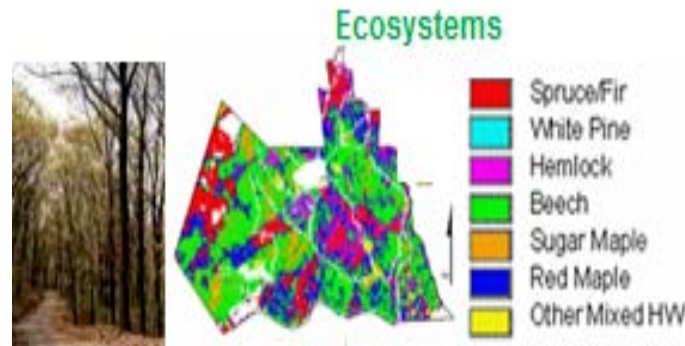
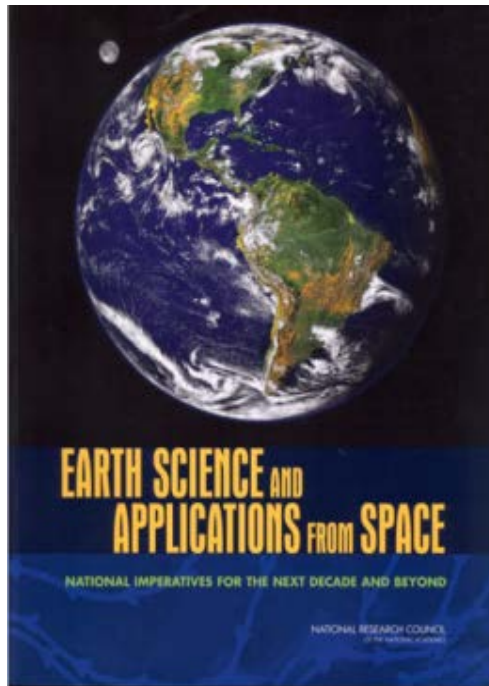
***NASA, SSAI, GST,
and OrbitalATK***

NASA Goddard Space
Flight Center
Rec Center

- Global terrestrial and coastal VSWIR spectroscopy at 30 m, 16 days and multispectral TIR at and 60 m, 4 days with real-time downlink of selected products.



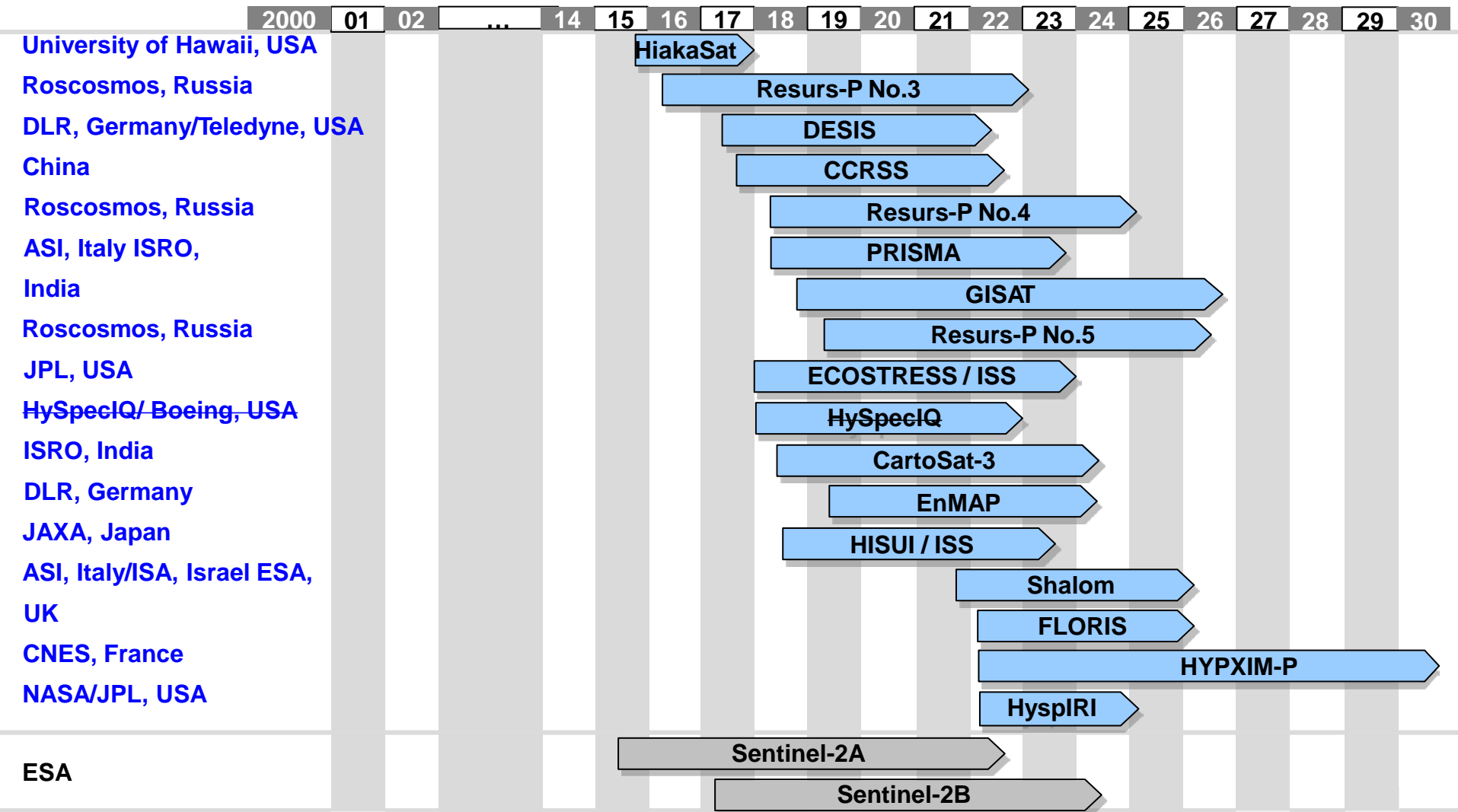
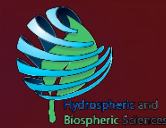
HyspIRI Preparatory Mission Update Science Workshop October 17-19, 2017 Pasadena, California



Robert O. Green and The HyspIRI Team



Future Spaceborne Imaging Spectroscopy EO Missions Launch and Lifetime



Updated July 2017

Thank You

